

11-9-2018

Connectivity Analysis of Electroencephalograms in Epilepsy

Panuwat Janwattanapong

Florida International University, pjanw001@fiu.edu

Follow this and additional works at: <https://digitalcommons.fiu.edu/etd>



Part of the [Bioelectrical and Neuroengineering Commons](#), [Electrical and Electronics Commons](#), and the [Signal Processing Commons](#)

Recommended Citation

Janwattanapong, Panuwat, "Connectivity Analysis of Electroencephalograms in Epilepsy" (2018). *FIU Electronic Theses and Dissertations*. 3906.
<https://digitalcommons.fiu.edu/etd/3906>

This work is brought to you for free and open access by the University Graduate School at FIU Digital Commons. It has been accepted for inclusion in FIU Electronic Theses and Dissertations by an authorized administrator of FIU Digital Commons. For more information, please contact dcc@fiu.edu.

FLORIDA INTERNATIONAL UNIVERSITY
Miami, Florida

CONNECTIVITY ANALYSIS OF ELECTROENCEPHALOGRAMS IN
EPILEPSY

A dissertation submitted in partial fulfillment of the
requirements for the degree of
DOCTOR OF PHILOSOPHY
in
ELECTRICAL ENGINEERING
by
Panuwat Janwattanapong

2018

To: Dean John L. Volakis
College of Engineering and Computing

This dissertation, written by Panuwat Janwattanapong, and entitled Connectivity Analysis of Electroencephalograms in Epilepsy, having been approved in respect to style and intellectual content, is referred to you for judgment.

We have read this dissertation and recommend that it be approved.

Malek Adjouadi

Armando Barreto

Jean Andrian

Naphtali David Rishe

Mercedes Cabrerizo, Major Professor

Date of Defense: November 9, 2018

The dissertation of Panuwat Janwattanapong is approved.

Dean John L. Volakis
College of Engineering and Computing

Andrés G. Gil
Vice President for Research and Economic Development
and Dean of the University Graduate School

Florida International University, 2018

© Copyright 2018 by Panuwat Janwattanapong
All rights reserved.

DEDICATION

This dissertation is dedicated to my parents, sisters and friends.

ACKNOWLEDGMENTS

This dissertation would not have been possible without the strong support and guidance from my advisor, Dr. Mercedes Cabrerizo. I greatly appreciate the time and help provided from my advisor during the entire period of my studies. Dr. Cabrerizo provided amazing insight and encouragement for me to become a better researcher.

I would like to thank my committee that has always been supportive of my studies Dr. Armando Barreto, Dr. Jean Andrian, Dr. Naphtali Rishe, and especially Dr. Malek Adjouadi. Dr. Adjouadi provided me with inspiring classes and motivation to become better every day. I would also like to thank the College of Engineering and Computing and the Department of Electrical and Computer Engineering for giving me a chance to study with world-class professors and work with amazing people. The study was supported by the National Science Foundation under grants CNS 1532061, CNS-0959985, HRD- 0833093, CNS-1042341, CNS-1551221, and IIP-1338922. Support of the Ware Foundation is also greatly appreciated.

It has not been easy on this Ph.D. journey. Thank you to my friends for all of the support and for making this an unforgettable journey. Thank you, Dr. Peeraya Inyim, Nonnarit O-Larnnithipong, Francisco Raul Ortega for enduring this journey together. For my friends in CATE lab, Chen Fang, Hoda Rajaei, Chunfei Li, Harold Martin, and many more, I thank them for their advice and friendship.

Lastly, I would like to thank my family, Pipat, Samorn, Nathinee, and Paranee, for their endless support and understanding. Thank you for believing in me and providing amazing support for me to get through difficult times. Without them, this dissertation would not have been possible. Thank you. Panuwat Janwattanapong
2018

ABSTRACT OF THE DISSERTATION
CONNECTIVITY ANALYSIS OF ELECTROENCEPHALOGRAMS IN
EPILEPSY

by

Panuwat Janwattanapong

Florida International University, 2018

Miami, Florida

Professor Mercedes Cabrerizo, Major Professor

This dissertation introduces a novel approach at gauging patterns of information flow using brain connectivity analysis and partial directed coherence (PDC) in epilepsy. The main objective of this dissertation is to assess the key characteristics that delineate neural activities obtained from patients with epilepsy, considering both focal and generalized seizures. The use of PDC analysis is noteworthy as it estimates the intensity and direction of propagation from neural activities generated in the cerebral cortex, and it ascertains the coefficients as weighted measures in formulating the multivariate autoregressive model (MVAR). The PDC is used here as a feature extraction method for recorded scalp electroencephalograms (EEG) as means to examine the interictal epileptiform discharges (IEDs) and reflect the physiological changes of brain activity during interictal periods. Two experiments were set up to investigate the epileptic data by using the PDC concept.

For the investigation of IEDs data (interictal spike (IS), spike and slow wave complex (SSC), and repetitive spikes and slow wave complex (RSS)), the PDC analysis estimates the intensity and direction of propagation from neural activities generated in the cerebral cortex, and analyzes the coefficients obtained from employing MVAR. Features extracted by using PDC were transformed into adjacency matrices using surrogate data analysis and were classified by using the multilayer Percep-

tron (MLP) neural network. The classification results yielded a high accuracy and precision number.

The second experiment introduces the investigation of intensity (or strength) of information flow. The inflow activity deemed significant and flowing from other regions into a specific region together with the outflow activity emanating from one region and spreading into other regions were calculated based on the PDC results and were quantified by the defined regions of interest. Three groups were considered for this study, the control population, patients with focal epilepsy, and patients with generalized epilepsy. A significant difference in inflow and outflow validated by the nonparametric Kruskal-Wallis test was observed for these groups.

By taking advantage of directionality of brain connectivity and by extracting the intensity of information flow, specific patterns in different brain regions of interest between each data group can be revealed. This is rather important as researchers could then associate such patterns in context to the 3D source localization where seizures are thought to emanate in focal epilepsy. This research endeavor, given its generalized construct, can extend for the study of other neurological and neurodegenerative disorders such as Parkinson, depression, Alzheimers disease, and mental illness.

TABLE OF CONTENTS

| CHAPTER | PAGE |
|--|------|
| 1. INTRODUCTION | 1 |
| 1.1 Problem Statement | 1 |
| 1.2 Objective of Study | 3 |
| 1.3 Significance of Study | 3 |
| 1.4 Literature Review | 4 |
| 1.5 Dissertation Structure | 7 |
| 2. BACKGROUND | 9 |
| 2.1 Complexity of The Human Brain | 9 |
| 2.2 Electroencephalograms | 10 |
| 2.3 Epilepsy | 13 |
| 2.3.1 Focal Epilepsy | 16 |
| 2.3.2 Generalized Epilepsy | 17 |
| 2.4 Brain Connectivity | 17 |
| 2.5 Surrogate Data Analysis | 24 |
| 3. CONNECTIVITY PATTERNS OF INTERICTAL EPILEPTIFORM DIS- CHARGES USING COHERENCE ANALYSIS | 26 |
| 3.1 Introduction | 26 |
| 3.2 Data Acquisition | 28 |
| 3.3 Preprocessing | 28 |
| 3.4 Functional Connectivity with Coherence | 29 |
| 3.5 Quantification of Functional Connectivity | 30 |
| 3.6 Results | 32 |
| 3.6.1 Delta Band Connectivity | 32 |
| 3.6.2 Theta Band Connectivity | 33 |
| 3.6.3 Alpha Band Connectivity | 36 |
| 3.6.4 Beta Band Connectivity | 38 |
| 3.7 Discussion | 38 |
| 3.8 Conclusion | 40 |
| 4. PARTIAL DIRECTED COHERENCE: A MEASURE OF EFFECTIVE CON- NECTIVITY | 42 |
| 4.1 Introduction | 42 |
| 4.2 Computing PDC | 44 |
| 4.3 Overview of PDC using Simulated Data | 47 |
| 4.4 Intensity of Information Flow | 49 |

| | |
|--|-----|
| 5. CLASSIFICATION OF INTERICTAL EPILEPTIFORM DISCHARGES USING PARTIAL DIRECTED COHERENCE | 52 |
| 5.1 Introduction | 52 |
| 5.2 Data Acquisition | 54 |
| 5.3 Preprocessing | 55 |
| 5.4 Feature Extraction | 56 |
| 5.5 Feature Transformation | 57 |
| 5.6 Multilayer Perceptron Neural Network | 61 |
| 5.7 Classification Experiment: Tenfold Cross Validation | 62 |
| 5.8 Results | 64 |
| 5.8.1 Classification between two types of IEDs | 66 |
| 5.8.2 Classification between all types of IEDs | 67 |
| 5.9 Discussion | 68 |
| 5.10 Conclusion | 68 |
| 6. PARTIAL DIRECTED COHERENCE WITH CONCEPT OF INFORMATION FLOW | 70 |
| 6.1 Introduction | 70 |
| 6.2 Data Acquisition | 73 |
| 6.3 Preprocessing and Segmentation | 75 |
| 6.4 Connectivity Extraction | 77 |
| 6.5 Quantification of Information Flow by Cortex Regions | 77 |
| 6.6 Exploratory Statistical Analysis | 82 |
| 6.7 Results | 82 |
| 6.7.1 Information Inflow and Outflow | 84 |
| 6.7.2 Statistical Differences in Information Inflow and Outflow Directions | 87 |
| 6.7.3 Focal Epilepsy and Control Population | 89 |
| 6.8 Discussion | 97 |
| 6.9 Conclusion | 100 |
| 7. CONCLUDING REMARKS AND FUTURE WORK | 101 |
| 7.1 Concluding Remarks | 101 |
| 7.2 Further Research | 103 |
| BIBLIOGRAPHY | 105 |
| APPENDIX | 113 |
| VITA | 117 |

LIST OF TABLES

| TABLE | PAGE |
|-------|---|
| 5.1 | Performance results of binary classification based on neural network classifier with adjacency matrices 67 |
| 5.2 | Performance results of 3-types classification based on neural network classifier with adjacency matrices 67 |
| 6.1 | Patients information 76 |
| 6.2 | Total number of EEG segmentations per group. 77 |
| 6.3 | Kruskal-Wallis test of intensity of information flow with inflow direction. 87 |
| 6.4 | Kruskal-Wallis test of intensity of information flow with outflow direction. 87 |
| 6.5 | Multiple comparison of inflow means within the right hemisphere using Conover-Iman test with level of significance = 0.05 88 |
| 6.6 | Multiple comparison of inflow means within the left hemisphere using Conover-Iman test with level of significance = 0.05 88 |
| 6.7 | Multiple comparison of inflow means within the anterior region using Conover-Iman test with level of significance = 0.05 88 |
| 6.8 | Multiple comparison of inflow means within the posterior region using Conover-Iman test with level of significance = 0.05 88 |
| 6.9 | Multiple comparison of outflow means within the right hemisphere using Conover-Iman test with level of significance = 0.05 90 |
| 6.10 | Multiple comparison of outflow means within the left hemisphere using Conover-Iman test with level of significance = 0.05 90 |
| 6.11 | Multiple comparison of outflow means within the anterior region using Conover-Iman test with level of significance = 0.05 90 |
| 6.12 | Multiple comparison of outflow means within the posterior region using Conover-Iman test with level of significance = 0.05 90 |
| 6.13 | Focal epilepsy patients information 91 |
| 6.14 | Kruskal-Wallis test of intensity of information flow with inflow direction between focal left group and control population. 94 |
| 6.15 | Kruskal-Wallis test of intensity of information flow with outflow direction between focal left group and control population. 94 |
| 6.16 | Kruskal-Wallis test of intensity of information flow with inflow direction between focal right group and control population. 94 |

6.17 Kruskal-Wallis test of intensity of information flow with outflow direction between focal right group and control population. 97

LIST OF FIGURES

| FIGURE | PAGE |
|---|------|
| 2.1 20 seconds of 19-channel EEG with 10-20 montage placement and referential montage. | 12 |
| 2.2 Overall process of brain connectivity analysis | 20 |
| 2.3 Example of a connectivity head map plot | 20 |
| 2.4 Example of a fMRI data | 21 |
| 3.1 Flow diagram of the process | 27 |
| 3.2 Regions of interest, group (a) left-right hemisphere (Left - red, Right - Blue), and (b) anterior-posterior region (Anterior - red, Posterior - blue) | 31 |
| 3.3 Head map average connectivity plots for (a) interictal spike (b) spike with slow wave complex (c) repetitive spikes and slow wave complex from Delta Band | 33 |
| 3.4 Means and standard deviations of number of connections with 80% threshold in the Delta band | 34 |
| 3.5 Head map average connectivity plots for (a) interictal spike (b) spike with slow wave complex (c) repetitive spikes and slow wave complex from Theta Band | 34 |
| 3.6 Means and standard deviations of number of connections with 80% threshold in the Theta band | 35 |
| 3.7 Head map average connectivity plots for (a) interictal spike (b) spike with slow wave complex (c) repetitive spikes and slow wave complex from Alpha Band | 36 |
| 3.8 Means and standard deviations of number of connections with 80% threshold in the Alpha band | 37 |
| 3.9 Head map average connectivity plots for (a) interictal spike (b) spike with slow wave complex (c) repetitive spikes and slow wave complex from Beta Band | 38 |
| 3.10 Means and standard deviations of number of connections with 80% threshold in the Beta band | 39 |
| 4.1 Example of two time series | 43 |
| 4.2 Flow of information based on simulated data | 48 |
| 4.3 Simulated data with 5 channels | 49 |

| | | |
|------|---|----|
| 4.4 | PDC calculation of the simulated data | 50 |
| 5.1 | Types of interictal epileptiform discharges | 55 |
| 5.2 | Random samples of PDC values extracted from interictal spike | 58 |
| 5.3 | Random samples of PDC values extracted from spike and slow wave complex | 59 |
| 5.4 | Random samples of PDC values extracted from repetitive spikes and slow wave complex | 60 |
| 5.5 | Computed partial directed coherence | 61 |
| 5.6 | Adjacency matrix from the computed PDC | 62 |
| 5.7 | Flowchart of the multilayer Perceptron algorithm | 63 |
| 5.8 | Sample of adjacency matrix obtained from interictal spike | 65 |
| 5.9 | Sample of adjacency matrix obtained from spike and slow wave complex | 65 |
| 5.10 | Sample of adjacency matrix obtained from repetitive spike and slow wave complex | 66 |
| 6.1 | Diagram outlining the PDC-based inflow and outflow method of the study | 74 |
| 6.2 | Random samples of PDC values extracted from the EEG segments of control population | 78 |
| 6.3 | Random samples of PDC values extracted from the EEG segments of focal epilepsy group | 79 |
| 6.4 | Random samples of PDC values extracted from the EEG segments of generalized epilepsy group | 80 |
| 6.5 | Regions of interest, group (a) left-right hemisphere (Left - red, Right - Blue), and (b) anterior-posterior region (Anterior - red, Posterior - blue) | 81 |
| 6.6 | Average circular connectivity of (a) control population (b) focal epilepsy (c) generalized epilepsy group. | 83 |
| 6.7 | The medians and interquartile ranges of the intensity of information flow with inflow direction of the three groups with different regions. | 85 |
| 6.8 | The medians and interquartile ranges of the intensity of information flow with outflow direction of the three groups with different regions. | 86 |

| | | |
|------|--|----|
| 6.9 | The medians and interquartile ranges of the intensity of information flow with inflow direction of the focal left group and control population with different regions. | 92 |
| 6.10 | The medians and interquartile ranges of the intensity of information flow with outflow direction of the focal left group and control population with different regions. | 93 |
| 6.11 | The medians and interquartile ranges of the intensity of information flow with inflow direction of the focal right group and control population with different regions. | 95 |
| 6.12 | The medians and interquartile ranges of the intensity of information flow with outflow direction of the focal right group and control population with different regions. | 96 |

CHAPTER 1

INTRODUCTION

1.1 Problem Statement

Epilepsy is a chronic disorder and is one of the most common neurological disorders affecting approximately 0.5 - 1% of the world population [21]. In the United States alone, 1.8% of adults (18 years and older) and 1% of children (aged 0-17), are reported to have epilepsy by the Center for Disease Control and Prevention [21]. The major characteristic which defines the disorder is recurrent and unprovoked seizures. During an episode of seizures, groups of neurons located in the cerebral cortex are being excessively triggered at the same time, resulting in symptoms such as muscle spasms and impaired consciousness [20]. Although the symptoms mentioned above are general symptoms, the location, duration and propagation of the seizure vary depending on the individual. Due to the unpredictable occurrence of seizures, the quality of life of epileptic patients might be greatly impacted by this uncertainty.

Epilepsy is a complex disease with many ambiguous phases. The diagnosis is divided into two major types, focal and generalized epilepsy. In focal or partial epilepsy, seizures are initiated from a specific part of the brain, known as an epileptic focus, while in generalized epilepsy, seizures involve wider areas of the brain propagating from multiple sources [20]. Having seizures is an indication of epilepsy but does not always result in the correct epilepsy diagnosis. In order to provide an accurate and precise result, the process of epilepsy detection and diagnosis is considered to be very subjective and time-consuming.

Among the neurophysiological techniques used to diagnose epilepsy, electroencephalograms (EEG) still remains the most prevalent and reliable modality to examine brain activities, as well as being the main diagnosis assessment tool [70].

EEG recording is simple and inexpensive compared to other neuroimaging techniques. EEG captures the electrical activities produced by the neurons in the brain including the interictal epileptiform discharges (IEDs). Due to its high temporal resolution, EEG is considered a suitable tool for identifying synchronization between a pair of signals [59]. A Substantial amount of epilepsy diagnoses are done by recording and visualizing EEG during seizures and closely monitoring IEDs in long interictal recordings. Extracting epileptic characteristics of EEG in interictal periods plays a key role in the disease detection. Consequently, extracting the hidden patterns of EEG in the interictal phase may be a beneficial tool to alleviate this complex process of epilepsy diagnosis.

With all the available tools and theories, the knowledge of how the human brain functions remains limited. There are different approaches to explore the functionality of the brain, where brain connectivity analysis has received great attention in the field of neuroscience and has yielded promising results in diverse research endeavors [70]. Brain connectivity analysis is defined as a study of the correlation of the events occurring in the different regions of the cortex. The value of connectivity depends on the level of synchronization between groups of neurons. The study of different features, such as brain connectivity features, can be used as a key parameter for classification of patients with epilepsy vs. a healthy control group. Therefore, enhancing epilepsy diagnosis or even predicting the occurrence of seizures through EEG recordings could lead to better planning and therapeutic protocols, which will greatly benefit epileptic patients and society at large.

1.2 Objective of Study

This research aims to utilize brain connectivity analysis to reveal and extract hidden features that could be associated with the neurological disorder under consideration. The study as planned could potentially improve the fundamental understanding of the disease and would consequently enhance the diagnosis significantly. Important connectivity features extracted from epileptic patients will be explored by multiple approaches and compared with the control population to generate distinct patterns that can be used for classification algorithms. By exploring the features extracted from the brain connectivity analysis, a machine learning algorithm, such as the multilayer Perceptron neural network can be used to perform optimal classification of epilepsy patients from healthy controls and to delineate those patients with focal epilepsy from patients who experience generalized epilepsy.

1.3 Significance of Study

Brain connectivity analysis of epileptic patients is a method that could yield more understanding of complex neurological disorders, specifically epilepsy as it pertains to this research endeavor. The analysis would constitute a platform to study common disease attributes as well as highlight hidden characteristics and features of the disease that would add to our understanding of the disease. EEG-based source localization can be integrated with connectivity analysis, resulting in a better performance with high classification accuracy and precision. Patterns extracted from connectivity analysis could be the key to identify types of epilepsy by minimizing the time and the cost for the patients. The study can also provide significant support to the diagnoses of doctors. Using brain connectivity analysis can reveal characteristics of multiple brain disorders.

1.4 Literature Review

Humans have started to explore the structural network of the brain since the nineteenth century to develop the understanding of the complex systems [14]. The studies have led to the increase in popularity of brain network science, including the effort to extract the information from the network structure [58]. In the present time, the increase of availability of high quality data sets of complex systems, such as data from EEG) or intracranial EEG (iEEG), has led to fundamental insight into such complex systems [4]. With the higher computational power and higher amount of data, the results obtained from the analyses are gaining more attention and becoming more reliable [58].

The analysis of EEG signals with the purpose of helping patients suffering from neurological disorders has been one of the most prominent research fields [62]. Various techniques of computational analysis have been performed to enhance the detection of the key characteristics associated with the disease [33, 34, 51]. However, the characteristics of epilepsy still require an extensive exploration and investigation in order to improve our understanding of this challenging disease [62, 20]. The majority of epilepsy diagnostics are based on EEG, where epileptic patients will undergo the procedure of EEG recordings for a period of time while being observed by clinicians and doctors [56]. There have been successful methods utilizing time-domain EEG features for epilepsy detection. Time-domain analyses, such as linear prediction, are utilized for seizure prediction [71]. However, investigating only time-domain features often provides insufficient interpretation of the disease and can be misleading. EEG signals can provide enormous information in the frequency domain. Every EEG frequency band carries specific information that could be analyzed for a purpose of feature extraction purposes [34]. Features extracted from each of these frequency

bands can be interpreted differently and are expected to provide augmented information on the disease.

The study and exploration of EEG lead to an investigation of interaction between brain regions called brain connectivity analysis. The human brain is considered a complex system with over 10 billions of neurons providing a high computational power with complex networks and pathways [27]. Within the cortical grey matter of the human brain, the neurons are processing information simultaneously while their axons comprising the white matter provide networks of communication between subregions of the cortex. The study of brain connectivity aims to understand the structural segregation and functional relationships of the elements in this complex system, where the study of brain connectivity reveals useful information of activities of the brain in both its healthy and disease states [73]. The studies of structural segregation and functional connectivity in the human brain have been explored and well-established for many years [23]. Clusters of neurons distributed throughout the cortex serve different functions and are specialized in processing variety of neuronal computations [65]. To understand the clinical consequences of the brain disorders such as epilepsy, analyzing and quantifying the interactions between distinct clusters of neurons can prove very useful, and can lead to important insights brain activity [26].

Two types of brain connectivity are defined in the context of brain connectivity analysis, structural connectivity and functional connectivity [11], where the process of mapping the human brain networks can also be referred to as *human connectomics* [57]. Several data-driven methods (time and frequency domains) are used to extract the brain attributes as connectivity networks from EEG signals [70]. Even though EEG signals recorded from the brain contain nonlinearity and semi-random features, linear models are the best option to describe and capture the information presented

in the system [9]. Fundamental concepts of connectivity extracted from correlation and coherence have been used widely in the neuroscience fields, where the results are promising [36, 51]. The functional connectivity map of an interictal EEG data is calculated and graph theory features of the network are used for differentiation of epileptic children [33].

In the domain of epilepsy research, applying brain connectivity analysis by using EEG data has become a more preferred approach [18]. By utilizing a high-quality EEG data and appropriated computational power, the newer approaches for epilepsy diagnosis, prediction of seizures, and epileptic focus localization have become more accurate and precise in the modern era [31]. Interesting features and characteristics derived from brain connectivity analysis have shown to improve the accuracy of diagnoses of children with epilepsy significantly [69]. In addition, by analyzing the overall connectivity structure of the brain networks from epileptic patients with temporal lobe epilepsy, the obtained results seem to have significant differences when compared to a control population [49]. For a localization of the epileptic focus, more research is being focused on the behavior of the seizure onset zone. A research from [74] found a high correlation between the seizure onset zone and the increase of information flow within higher brain frequency ranges. The dynamic characteristic of the brain connectivity network during ictal events has also been investigated in the study of partial epilepsy, where patterns of brain connectivity are revealed to be associated with finite brain states where the seizure onset zones are more isolated from the rest of the network during the initial state of seizures [12]. More in-depth reviews of brain connectivity analysis techniques can be found in [70].

1.5 Dissertation Structure

This dissertation is structured and organized in a series of chapters, including background, methodology of connectivity extraction, experiments (two chapters), and conclusion.

Chapter 2 presents the background research, concepts, and terminology related to this dissertation. This chapter includes the introduction of the structure of the human brain, and the common and accepted definition of epilepsy. In order to understand the methodologies used in this dissertation, brain connectivity analysis and surrogate data analysis are introduced.

Chapter 3 introduces a prior experiment implementing coherence analysis to epileptic data. This experiment displays a simple concept of functional connectivity that leads to the study of effective connectivity in this dissertation.

Chapter 4 describes the concept of partial directed coherence (PDC) including the steps to compute PDC and an overview of PDC concept using simulated data. The mathematical framework, aspects of modeling and empirical evaluations using simulated data are presented in this chapter. The intent in this chapter is in gauging the merits of PDC as a measure of effective connectivity.

Chapter 5 introduces an initial experiment deploying the PDC method of Partial Directed Coherence (experiments using the concept of PDC with electroencephalogram data. To the best of our knowledge, this is perhaps the first experimental study to incorporate the propagation of information flow for classifying the common types of IEDs by utilizing machine learning on the propagation patterns extracted from the EEG data segments and using the PDC methodology.

Chapter 6 introduces an approach for quantifying information flow using brain connectivity analysis and partial directed coherence (PDC). The thrust of this chap-

ter is in determining key characteristics that delineate normal controls from patients with epilepsy considering both types of seizures: focal and generalized seizures. The PDC is used in this case as a feature extraction method for scalp electroencephalograms (EEG) recordings as means to reflect the physiological changes of brain activity during interictal periods (these are periods in between seizures). The intensity (or strength) of information flow, including (a) inflow or information from distant region reaching a specific region, and (b) outflow or the flow of information spreading from a specific region of interest into other regions.

Finally, Chapter 7 provides the conclusion with a retrospective on the main findings of this dissertation. This chapter also outlines the advantages such a research endeavor provides the research community and also highlights limitations that still need to be overcome as we inch forward towards a more enhanced understanding of such complex neurological disorder.

CHAPTER 2

BACKGROUND

2.1 Complexity of The Human Brain

The human brain is one of the largest and most complex organs in the human body. It is considered to be the “controller unit” of the human body, where the brain is involved in producing our every thought, memory, feeling, and experience of the world. This approximately 1.4 kilograms mass of tissue contains enormous amount of neurons, which it is approximated to be around 86 to 100 billion neurons [5]. Each neuron is interconnected and communicates with other neurons by using synapses, where a single neuron can have numerous connections with thousands of synapses that are connected to other neurons. Even by a low estimation of thousand connections per neuron, this would mean that a single human brain is consisted of at least 100 trillions synaptic connections resulting in 100 trillions different pathways that brain signals can travel through [75]. To mimic this processing power of a human brain, more than 82,000 processors are required to perform a 1-second of a normal brain activity. Furthermore, the synapses are not static but dynamic, creating a high levels of plasticity, an elusive concept in the realm of computing. This allows the brain to learn, process, and memorize stimuli and information and use such stimuli and information as context and help for understanding future events and for resolving future tasks.

Though there are about 20 different types of neurons, their structures are basically the same. A neuron is composed of its cell body called soma, its dendrites with a treelike structure and its axon. Information produced in other neurons are transferred to the neuron by the synapses that are located on the dendrites and also on the cell body. Electrical charges produced at the synapses propagate to

the soma and produce a net postsynaptic potential. If the postsynaptic potential is large enough to exceed the threshold (a depolarization of $10 - 15mV$), the neuron will trigger a spike of electrical pulse or action potential at the axon hillock, where the axon hillock is the point of connection between the soma and the axon. The produced action potential will be propagated through the axon and reach the synapses resulting in transferring the information to another neuron.

2.2 Electroencephalograms

With 100 billions of neurons communicating via action potential, these electrical activities can be captured by using an electrophysiology technique called Electroencephalograms (EEG). The first known neurophysiology was recorded on animals was performed by Richard Caton in 1875 and later was done on human beings in 1924 performed by Hans Berger [10]. Given its high temporal sensitivity, EEG is a great instrument to capture the dynamic cerebral functional. Thus, EEG is particularly useful for evaluating patients with suspected epilepsy.

EEG is one of the methods used to record electrical activity generated by the brain with the utilization of specific sensors called electrodes. EEG captures the internal field potential differences created by ionic currents generated from the communication between neurons. Before the action potential is generated, the differences of ions concentrations between inside and outside of the cell produce a membrane potential. When the potential is depolarized, the rapid movement of ions between inside and outside of the neuron generates the action potential. EEG captures this phenomena in a large scale and records the electrical activity across the cortex with millions of neurons communicating simultaneously. Though EEG seems to be a perfect instrument, an unfortunate reality of EEG is that the cerebral activities

generated by neurons may be contaminated by the electrical activities generated by the body or the environment. Given that for the electrodes to capture the electrical activities, the signals generated by neurons have to pass through multiple biological filters including cerebrospinal fluid (CSF), meninges, the skull and the skin, which in different ways attenuate the signals' amplitudes prior to reaching the electrodes. Additionally, other bio-generated electrical activities such as eye movement, muscle movement, or even pulses from the heart can create a high voltage potential which could interfere with the desired signals. Fortunately, there are methods of removing artifacts making EEG data more reliable and useful for interpretation.

The EEG signals are recorded by measuring the difference of voltage potential between a pair of electrodes. Figure 2.1 provides an example of a multichannel scalp EEG recording. A typical EEG display multiple channels with voltages on the y -axis and the time on the x -axis providing an ongoing cerebral activity. The data shown in figure 2.1 covers a period of 20 seconds with 19 channels and 10-20 montage placement. The "10-20" represents the intervals of measurement in percentage of positioning electrodes over the anterior-posterior between the nasion andinion. Each of the electrodes is labeled with a letter and a number. The letter represents the location of the brain where the electrode site is located and the number represents the side of the cortex. Odd-numbered electrode sites are located on the left side of the cortex and the even-numbered ones are on the right side.

The letters used for the different brain areas are as follows:

- F: Frontal lobe
- T: Temporal lobe
- P: Parietal lobe
- O: Occipital lobe

- A: Auricular sites are on the mastoid processes/ears

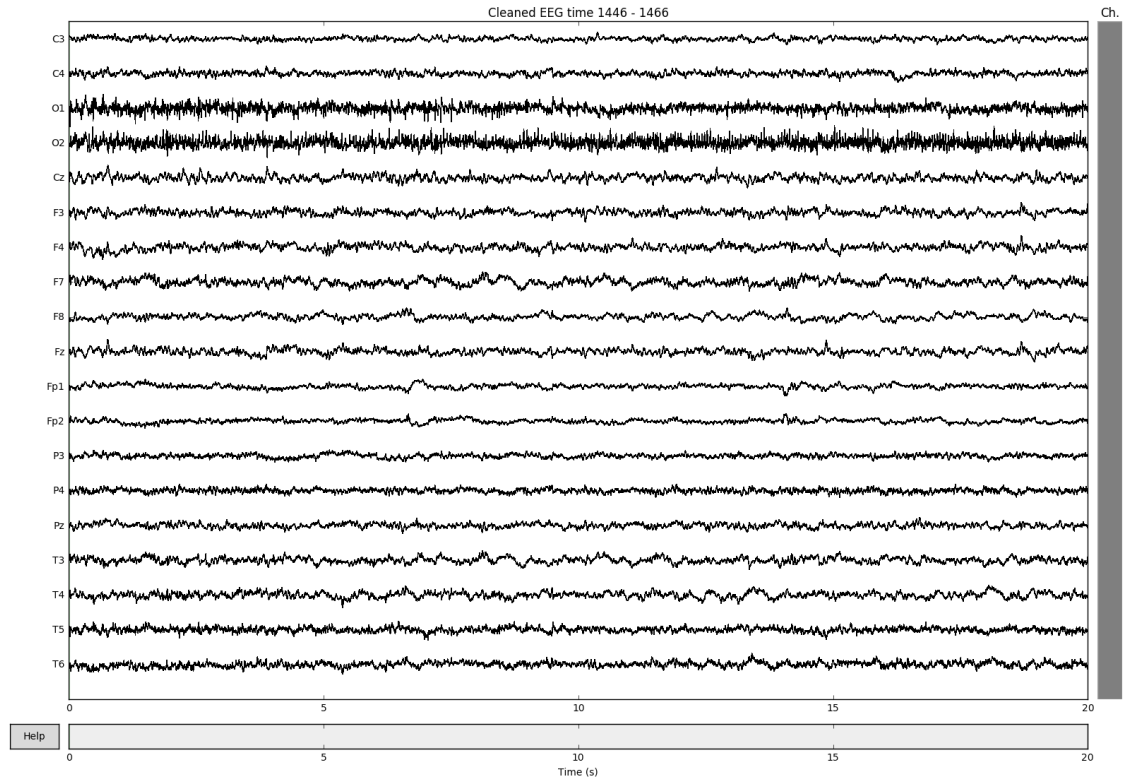


Figure 2.1: 20 seconds of 19-channel EEG with 10-20 montage placement and referential montage.

Among the neurophysiological techniques, EEG still remains the most prevalent modality used for examining brain activities as well as for carrying out the main diagnosis assessment. EEG captures the electrical activities produced by the neurons in the brain including important biomarkers. Due to its high temporal resolution, EEG is considered a suitable tool for identifying synchronization between a pair of signals, which makes EEG an important tool to extract specific activity patterns in relation to the brain dysfunction.

2.3 Epilepsy

Epilepsy is a class of neurological disorders characterized by the recurrent unprovoked interruption of brain function, called epileptic seizures. The definition of epileptic seizure is defined by the international league against epilepsy (ILAE) as “a transient occurrence of signs and/or symptoms due to abnormal excessive or synchronous neuronal activity in the brain” [19]. During epileptic seizures, groups of neurons in the cerebral cortex are being excessively triggered simultaneously resulting in symptoms such as muscle stiffness, muscle spasms and impaired consciousness. Clinical symptoms can vary widely as well, ranging from a brief loss of awareness (absence seizures) to a complete loss of consciousness with loss of bodily control (tonic-clonic seizures). Furthermore, epilepsy can be classified into different clinical manifestations depending on the behavior of the seizures. If the seizures initiate in a particular location of the brain, epilepsy is deemed as partial or focal epilepsy. On the hand, if the seizures initiate from multiple sites across the cortex simultaneously, the type of epilepsy is diagnosed as generalized epilepsy.

In the United States alone, 1.8% of adults (18 years and older) and 1% of children (aged 0-17), are reported to have epilepsy by the Center for Disease Control and Prevention [21]. Approximately 2.2 million Americans have been diagnosed with epilepsy and the number of new cases are still increasing [29]. With an estimation of 1% of the global population suffering from epilepsy, this makes epilepsy the fourth most common neurological disorder [29]. The recurrence of epileptic seizure events has great impact on the cognitive, psychological, and social aspects of the patients suffering from epilepsy.

Epilepsy affects persons of various ages and can develop at any stage of life, but the highest incidence of epilepsy is found to be in the first year of life and after the

age of 65 [53]. In many cases, the precise causes are still unknown. Nonetheless, many factors including genetic factors, head trauma, tumors, and many more can cause epilepsy. Therefore, the study of epilepsy will help reveal the cause of the disorder and provide more precise results.

Diagnosing a person with the condition of epilepsy requires experienced doctors and physicians to observe the electrophysiology of the brain during ictal periods. This is the most common test to diagnose epilepsy, where the aforementioned utilization of EEG is used as the main tool. During the test, doctors or physicians will attach electrodes to the scalp of a patient and record the electrical activity of the brain. If the patient is diagnosed with epilepsy, it is common to observe changes in the normal pattern of brain waves, even when the patient is not currently having a seizure. Currently epilepsy is not curable and patients with epilepsy are treated with antiepileptic drugs (AEDs). However, the occurrence of seizures of approximately 70% of people diagnosed with epilepsy can be controlled by using AEDs , unfortunately the remaining of patients do not benefit from such AEDs [54]. Among the subset of these patients where AEDs have no effect, if the patients are diagnosed with focal epilepsy, a viable option may be surgical intervention.

As previously mentioned, the types of epilepsy can be determined through classification of seizures. Seizure classification is a way of naming the many different types of epileptic seizures and classifying these types of seizures into predefined groups. In 2017, the ILAE redefined the classification of seizures to improve the process of diagnosing epilepsy to be more efficient. In the long run, researchers are hoping that this way of classifying epilepsy will be easier. Three important factors are required to be observed by the doctors when classifying the types of epilepsy:

1. The location of the cortex where the seizure initially propagates, referred to as the seizure onset zone.

2. During the period of seizure, determine the state of awareness of the person.
3. Movements of the body involved during the seizure period.

All types of epilepsy have symptoms related to seizures. If a person has seizures which is suspected to be caused by epilepsy, the diagnosis from the doctors will follow three general steps in order to provide a correct assessment.

1. Identify the type of seizure a person is having.
2. Based on the identified type of seizure, identify the type of epilepsy.
3. Decide on specific treatments based on the type of epilepsy.

To be able to identify the type of epilepsy, tests involve EEG recordings are required. Experts now divide the types of epilepsy into four basic types depending on the types of seizures patients are having:

- Focal epilepsy
- Generalized epilepsy
- Generalized and focal Epilepsy
- Unknown

For patients in the generalized and focal epilepsy group, as the name of the group suggests, this is the type where patients are having both generalized and focal seizures. For the unknown group, doctors are not able to identify the types of seizures that patients experience. This can happen for various reasons, including the case where a person might have an episode of seizure alone where no one can observe the characteristics displayed. Generalized epilepsy and focal epilepsy groups will be further explained in the next sections.

2.3.1 Focal Epilepsy

People with focal epilepsy type, the seizures initiate in a particular location of the cortex in one of the hemispheres of the brain. Previously, this type of seizure is called “partial seizures”. Focal epilepsy seizures can be further classified into four different categories.

- **Focal aware seizures**

During an episode of epileptic seizure, if a person has an awareness of the surrounding, then it is classified to be focal aware seizures. This type of seizure used to be called “simple partial seizures”.

- **Focal impaired awareness seizures**

Contrary to the focal aware seizures, a person with this type of seizure will be confused and will not able to remember anything during an episode of seizure. This type of seizure used to be called “complex partial seizures”.

- **Focal motor seizures**

In this type of seizure, during an episode of seizure, a person will experience body movement to some extent from anything between twitching, muscle spasms to rubbing hands and walking around.

- **Focal non-motor seizures**

For this type of seizure, having a seizure does not lead to any movement, but rather changes in feeling and thinking abilities of a person. Symptoms such as racing heart, intense emotions, or waves of heat or cold spells will be observed.

2.3.2 Generalized Epilepsy

For this type of epilepsy, seizures are initiated on both hemispheres of the brain simultaneously and could quickly affect networks of the brain on both side. Typically, this type of epilepsy has two different kind of seizures.

- **Generalized motor seizures**

Generalized motor seizures or once used to be called “grand mal” seizures, cause a body to move in an uncontrollable manner. An example of this type of seizure is tonic (stiffness)-clonic (muscle twitch) seizure, also called a convulsion. When such an episode of epilepsy is presented, a person might lose consciousness and control of the entire body.

- **Generalized non-motor (or absence) seizures**

This type of seizures used to be called “petit mal” seizure. More specific types associated with generalized non-motor seizures are typical, atypical, and myoclonic seizures. During an episode of such a seizure, a person may stop any activity and stare into space. Other repetitive activities might occur such as repetitive movement or smacking lips.

2.4 Brain Connectivity

Brain connectivity analysis has been a fast-growing field that has received great attention in the field of neuroscience. Brain connectivity analysis has yielded promising results in diverse brain research endeavors. The study is focused on studying the complex network structure of a human brain where it is characterized by segregation and integration in the processing of information. Brain connectivity analysis can be divided into three different but related forms of connectivity [57].

- **Structural Connectivity:**

Structural connectivity provides an insight into the physical pathways or connections within brain regions. The connection is formed through synaptic contacts between neighboring neurons linked by the axonal pathways connecting different brain regions. The characterization of the links can be determined by statistical measures of pathways or cross-correlation in gray matter thickness, volume, and surface area [11]. The structural connectivity can be obtained by examining neuroimaging data such as magnetic resonance imaging (MRI), Computed Tomography (CT) and diffusion tensor imaging (DTI) [28], where the different determined structural measurements are assessed in context to the brain connectivity networks that define them.

- **Functional Connectivity:**

Functional connectivity is defined as a temporal or biomarker dependency of the neuronal communication patterns between predefined brain regions, these include functional MRI and positron emission tomography (PET). Functional connectivity can be estimated by using statistical approaches, which reflects statistical dependencies between the neuronal populations at the different brain regions. By applying simple statistic concepts such as cross-correlation, spectral coherence or phase locking, functional connectivity can be extracted from the EEG recordings as well.

- **Effective Connectivity:**

Effective connectivity shares a similar concept to that of functional connectivity. However, it describes the information flow or the influence of a neuronal system exerts upon another reflecting causal interactions between brain regions. The connectivity is combined with a structural connectivity into a

“wiring diagram” reflecting directional effects between neuronal populations. This research will focus only on the concept of effective connectivity where Partial Directed Coherence as described in Chapter 4 will be used to extract these effective connectivity networks or patterns.

Thus, only the concept of effective connectivity will be explored further in this research. Effective connectivity estimates a cause and effect relationship between neuronal systems. By using time dependent data, we can infer the causal relationship between neural systems by exploring the temporal structure in the time series data expressed through the EEG recordings.

Figure 2.2 describes an overall process of performing a brain connectivity analysis. First of all, the data in the form of time series are collected from EEG recordings, which capture the neuronal characteristic or behavior of interest. The obtained data are preprocessed by performing artifact rejection techniques such as filtering, principle component analysis (PCA), and independent component analysis (ICA). The cleaned data are then processed to extract the relationships between brain regions and modeled into networks. Figure 2.3 shows an example of a network of connection displayed as a connectivity head map plot. The vertices of the plots represent the positions of the EEG electrodes where the edges represent the connection between each brain region. Then at the last step, interesting features such as intensity of information flow and graph theory features are extracted and analyzed in order to obtain meaningful results.

For both functional connectivity and effective connectivity, multiple techniques of electrophysiology and neuroimaging have been widely used by many researchers, where each the technique by itself has different pros and cons in terms of acquiring and processing data. On the spectrum of high spatial resolution, functional magnetic resonance imaging (fMRI) uses the blood oxygen level dependent (BOLD) signals to

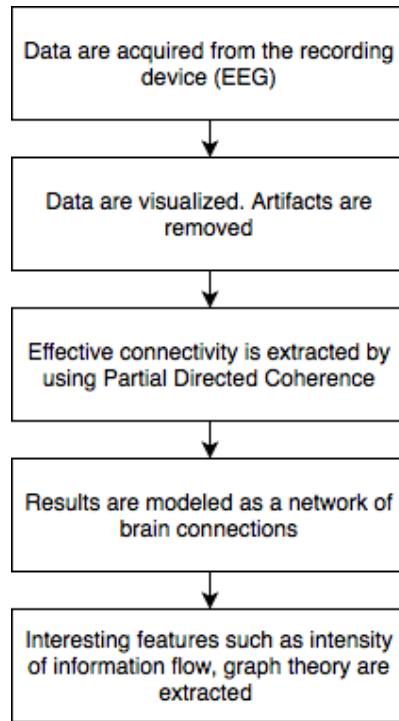


Figure 2.2: Overall process of brain connectivity analysis

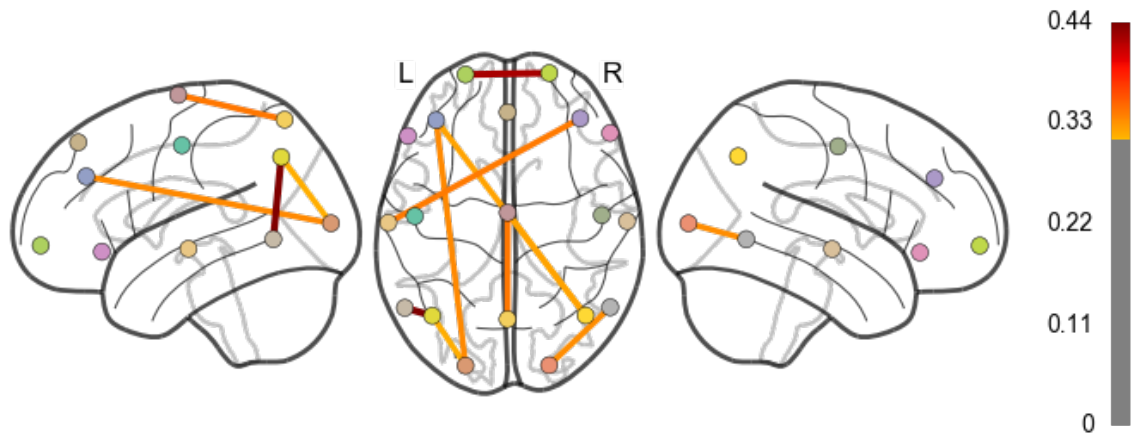


Figure 2.3: Example of a connectivity head map plot

estimate the connectivity between voxels of brain tissues. Figure 2.4 Though we can see that fMRI data provides a high spatial resolution, fMRI can only perform with a low sampling frequency resulting in a low temporal resolution. To compensate for the low temporal resolution, advanced analytical techniques are required to extract connectivity from the fMRI data. On the other hand, techniques such as EEG can collect data with a high sampling frequency. Furthermore, The high temporal resolution from EEG recording allows researchers to study the dynamics of brain function in both its healthy and disease states. In contrast to magnetic resonance imaging, EEG recordings lack the high spatial resolution offered through MRI and fMRI modalities.

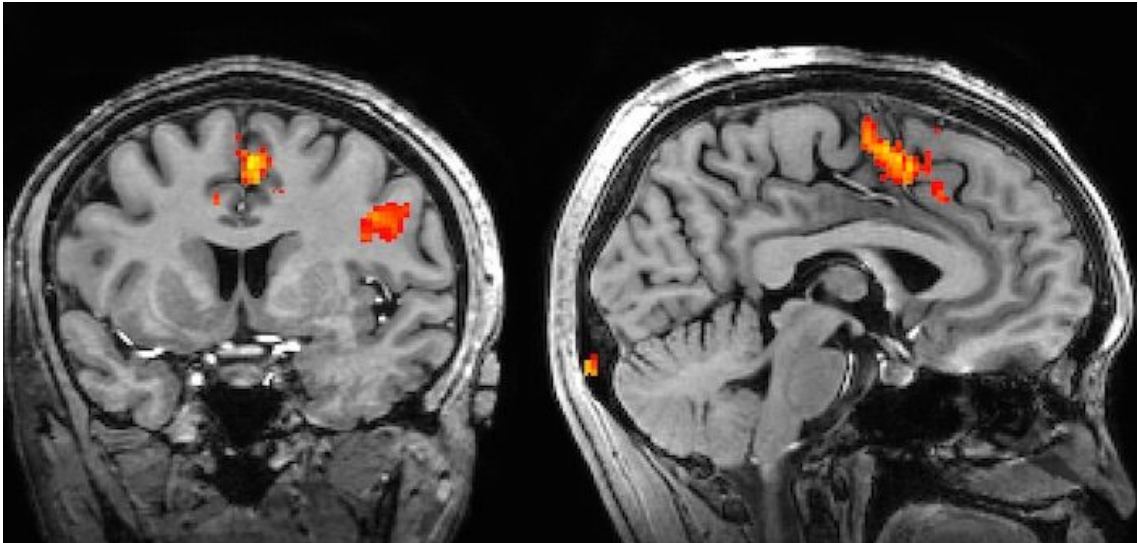


Figure 2.4: Example of a fMRI data

The ultimate recourse is to consolidate the individual strengths each modality brings in order to accomplish both high temporal resolution and high spatial resolution. These multiple datatypes and imaging modalities can be used in concert for brain connectivity to quantify the activation of the different cortex regions. Typically for the extraction of connectivity from the EEG data, the pairwise relationship between neuronal elements is defined by the measurement generated by

signal processing techniques such as cross-correlation and coherence, among others. The definition of pairwise relationship is that, given an EEG recording with 19 channels of electrodes, each pair of the channel is being compared one at a time. For cross-correlation, the extraction is performed by calculating the cross-correlation of every pairwise electrodes creating what we term in this dissertation as connectivity matrices. If 19 electrodes are used, then a 19×19 connectivity matrix will be obtained where the eye of the matrix is the autocorrelation of the individual montage itself. The cross-correlation is performed accordingly to the following equations:

$$\begin{aligned}
 C_{xy} &= \frac{1}{N} \sum_{t=0}^{N-\tau} (x_t - \bar{x})(y_{t+\tau} - \bar{y}) \\
 C_{xx} &= \frac{1}{N} \sum_{t=0}^{N-\tau} (x_t - \bar{x})(x_{t+\tau} - \bar{x}) \\
 C_{yy} &= \frac{1}{N} \sum_{t=0}^{N-\tau} (y_t - \bar{y})(y_{t+\tau} - \bar{y})
 \end{aligned} \tag{2.1}$$

The cross-correlation coefficient is as defined below:

$$r_{xy} = \frac{C_{xy}}{\sqrt{C_{xx}C_{yy}}} \tag{2.2}$$

The value of the cross-correlation coefficient ranges from -1 to 1 where 0 is an indication that there is no connection between the pair of signals and where a value of 1 indicates the strongest connection. In the negative range, a value of -1 also indicates the strongest connection when the one of the signal is completely inverted in the opposite direction. Therefore in terms of connectivity, the absolute value of cross-correlation coefficients are taken into considered. The cross-correlation is the simplest algorithm that can be used to extract the connectivity. patterns It measures the similarity between the signals point by point where the amplitude of the signal

is taken into account. The drawback of the algorithm is that, cross-correlation could introduce some errors and non-precise connectivity values due to various problems due to such things such as volume conduction.

To determine brain connectivity by using coherence, interactions between neural activities in different frequencies across brain regions are extracted using the coherence equation rather than using cross-correlation. Coherence between two signals $x(t)$ and $y(t)$, which represent a vector of the data from the EEG measurements, is defined as the magnitude squared of the cross-spectral density between 2 designated signals divided by the product of power spectral densities (PSD) of each of the signals as shown in equation 2.3, where f is the selected frequency.

$$C_{xy}(f) = \frac{|G_{xy}(f)|^2}{\sqrt{G_{xx}(f)G_{yy}(f)}} \quad (2.3)$$

$G_{xx}(f)$ and $G_{yy}(f)$ denote the calculated PSD of signal x and y respectively. $G_{xy}(f)$ represents the cross-spectral density of signals x and y . To improve the estimation, Welch's average periodogram can be implemented to calculate the coherence [16]. The method computes the modified periodogram for the segments and averages the output to estimate the PSD of the time series. The computed coherence coefficient varies in the range between 0 and 1, where 0 indicates that there is no connection between the pair of electrodes and where 1 indicates that there is a strong connection similar to the interpretation for the cross-correlation coefficient.

However, more advanced connectivity measurements such as Directed Transfer Function (DTF) [37] and Partial Directed Coherence (PDC) [7] can be used to observe the interaction between brain regions while avoiding the volume conduction problem. These measurements also account for the effect of contributions from all other region by using a multivariate analysis. The difference between a multivariate

analysis and a pair-wise analysis is that, all of the interested signals, in this case are the 19 EEG channels, are compared simultaneously resulting in more a more accurate representation of a human brain. Both DTF and PDC measures can provide directional information, where we can infer the causal relationship between brain regions.

These techniques for connectivity extraction can restrict the type of network that can be constructed. For both cross-correlation and coherence measures, these types of estimation can only provide undirected networks, where DTF and PDC methods can provide directed networks. Another parameter to consider is the edge weights of the network. If edge weights are required to construct a network, direct coefficients computed from these extraction techniques can be used. On the other hand, to create unweighted networks, thresholds can be applied on the coefficients, where the coefficients under the specified threshold are considered insignificant, and will not be included in the connectivity networks.

2.5 Surrogate Data Analysis

This section introduces the concept of surrogate data analysis. Surrogate data analysis is one of the statistical approaches used to determine whether the connectivity extracted from the given data using partial directed coherence (PDC) is considered statistically significant or not. The concept of surrogate data analysis is to measure the difference between measured PDC values and simulated PDC values. In order to simulate the PDC values with the same distribution of the real values, Monte Carlo simulation method will be used on the time series data to generate M surrogate time series for each of the PDC values [40].

The formal application of the method of surrogate data testing can be explained by using statistical hypothesis testing. The test is conducted with the null hypothesis H_0 and alternative hypotheses H_a shown in equation 2.4.

$$\begin{aligned}
 H_0 : PDC_{j \rightarrow i} &= 0 \\
 H_a : PDC_{j \rightarrow i} &\neq 0
 \end{aligned}
 \tag{2.4}$$

The notation PDC represents the value of PDC ranging from 0 to 1, where $j \rightarrow i$ represents the information flow from channel j to channel i . To generate M surrogate time series data, the improved amplitude-adjusted Fourier Transform (iAAFT) algorithm is used [64]. The iAAFT algorithm provides a randomized data of a time series that still maintain the same distribution of amplitude and power spectrum of the original time series data. By using iAAFT algorithm, each time series is being performed iteratively and individually in a multivariate process. Because the estimation is done independently, no causal relationship between the time series should remain since the phase relationship should be attenuated by the randomized process. Thus, the computed PDC values of the surrogate time series data will be estimated corresponding to the unrelated parts of the signals.

CONNECTIVITY PATTERNS OF INTERICTAL EPILEPTIFORM DISCHARGES USING COHERENCE ANALYSIS

3.1 Introduction

This chapter introduces an analysis of functional connectivity patterns extracted from the EEG data containing interictal epileptiform discharges (IEDs) by using coherence method mentioned in section 2.4. Prior to exploring the effective connectivity, functional connectivity was used to obtain the preliminary results. The analysis was done in each of the frequency bands (Delta, Theta, Alpha, and Beta). EEG contains a specific clinical and physiological range of frequency components of interest, which is between 0.5 - 30 Hz, where frequency components higher than 30 Hz (Gamma) are usually found not to be related to IEDs [2]. In this chapter, we want to limit the search to this frequency range since scalp EEG data is usually manually screened using a band pass filter with cut-off frequencies from 0.5 to 30Hz. Coherence of all the pair-wise electrodes are calculated creating connectivity matrices based on the placement of the electrodes. High value of coherence indicates the strong connection between the selected pair of electrodes and low values infer otherwise. After thresholds are applied, the connectivity matrices are quantified and validated by performing analysis of variance (ANOVA) to generate patterns of each type of IEDs.

The overall structure of the algorithm, together with its main steps, is shown as a flow diagram in figure 3.1. After the functional connectivity extraction, the number of connections in the regions of interest (ROI) was collected. A statistical analysis was applied to analyze the pattern of different type of IEDs.

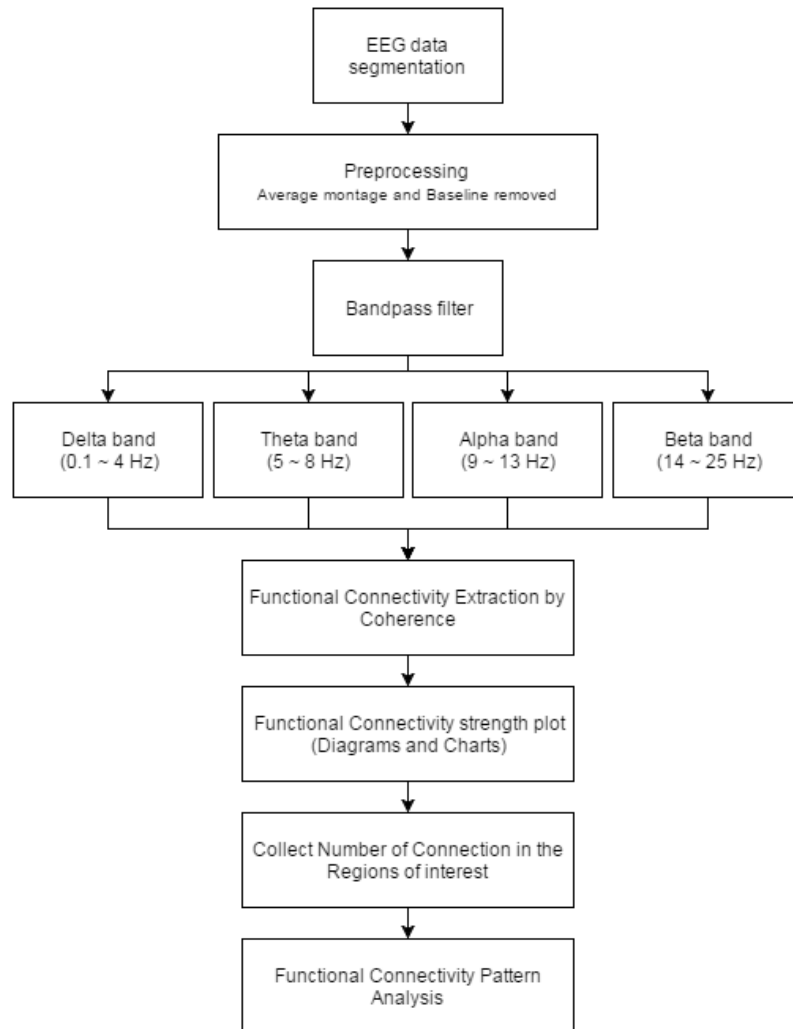


Figure 3.1: Flow diagram of the process

3.2 Data Acquisition

In this study, only interictal epileptiform discharges were used to extract the different characteristics of the 3 types of epileptic biomarkers, which are: interictal spike (IS), spike with slow wave complex (SSC), and repetitive spikes and slow wave complex (RSS). In order to explore synchronization between brain regions in focal and generalized cases, a total of 30 EEG segments from a male patient diagnosed with generalized epilepsy and a female patient diagnosed with focal epilepsy having partial complex seizures were obtained. The data were recorded with the 10-20 electrode placement protocol containing 3 types of IEDs. Recordings are performed containing 19 electrodes (Fp1, F7, T3, T5, O1, F3, C3, P3, Fz, Cz, Pz, Fp2, F8, T4, T6, O2, F4, C4, and P4) using referential montage. The data was collected with a sampling rate of 200 Hz.

3.3 Preprocessing

The EEG data was divided into 3 separated groups according to the types of IEDs. They were segmented into 1-second window containing a single occurrence of IED in the center of the segment. IEDs of IS type were arranged at the 0.5 s of the segment, where SSC and RSS were arranged at the 0.2 s of the segment due to its longer extent. In total, 10 segments of each type of IEDs were extracted from the original EEG data.

The data were converted from a referential montage to an average montage in order to reduce the effect of volume conduction [47]. A zero-phase finite impulse response (FIR) bandpass filter (0.5 - 30 Hz) from EEGLAB [16] was implemented to filter the frequency bands of interest and to remove the artifacts. The focus was

placed on the four following frequency bands, Delta band [0.1 - 4 Hz], Theta band [5 - 8 Hz], Alpha band [9 - 13 Hz], and Beta band [14 - 25 Hz].

3.4 Functional Connectivity with Coherence

Functional connectivity was extracted by performing a computation of coherence between all pairwise 19 multichannel EEG electrodes. Coherence between two signals $x(t)$ and $y(t)$, where $x(t)$ and $y(t)$ each represents a vector of the data of an electrode measurement with each containing 200 data points. Coherence is defined as the magnitude squared of the cross-spectral density between 2 designated signals divided by the product of power spectral densities (PSD) of each of the signals as shown in equation 3.1 where f is the selected frequency.

$$C_{xy}(f) = \frac{|G_{xy}(f)|^2}{\sqrt{G_{xx}(f)G_{yy}(f)}} \quad (3.1)$$

$G_{xx}(f)$ and $G_{yy}(f)$ denote the calculated PSD of signal x and y respectively. $G_{xy}(f)$ represents the cross-spectral density of signal x and y . In this experiment, Welch's average periodogram [72] has been implemented to calculate the coherence. The method computes the modified periodogram for the segments and averages the output to estimate the PSD of the time series. In this research, 0.5s hamming windows with 50% overlap had been used to calculate the PSD of the 1s epoch, where the overlap protects the loss of information caused by windowing. The results obtained from this method provided a better performance compared to other estimation algorithm [36] in terms of signal to noise ratio. The computed coherences were then examined within the frequency bands of interest by obtaining the average coherence value for each of the 4 frequency bands as shown in equation 3.2.

$$A_{xy}(f) = \frac{\int_L^U C_{xy}(f)df}{U - L} \quad (3.2)$$

U is the upper bound and L is the lower bound of the selected frequency. For example, if the Delta band is selected, the lower bound and the upper bound that will be used are [0.1, 4 Hz] respectively. The computed average coherence coefficients vary in a range of 0 to 1, where 0 indicates that there is no connection between the pair of electrodes where 1 indicates that there is a strong connection. The values of average coherence extracted from each pair of electrodes together form a matrix called connectivity matrix. After the connectivity matrices for every frequency band of interest and each type of IEDs were obtained, the connectivity matrices were then applied with different thresholds (50%, 70%, 80%, 90%, and 95%). The head map connectivity plots, which are shown in the results section, were analyzed and validated by statistical tests.

3.5 Quantification of Functional Connectivity

The brain cortex was subdivided into different regions based on two specific cases. The subdivision of the first case was done by dividing the cortex based on the left and right hemispheres (LR region). The activities on the left hemispheric region included Fp1, F7, T3, T5, O1, F3, C3, and P3 electrodes and the right hemispheric region contained Fp2, F8, T4, T6, O2, F4, C4, and P4 electrodes. The LR region was separated by the central line, which is a longitudinal fissure that contains Fz, Cz, and Pz electrodes. Connections between a pair of electrodes occurring within the right hemispheric region were labeled as the right “intra-connection”. The same concept was applied to the left hemispheric region as well, where the labeled connection

was identified as “left intra-connection”. If the connection occurs between the two hemispheres, the connection was labeled as “LR interconnection”.

The subdivision of the second case was done base on the anterior-posterior regions (AP region), where the anterior region contained Fp1, Fp2, F7, F3, Fz, F4, and F8 electrodes and the posterior region contained T5, P3, Pz, P4, T6, O1, and O2 electrodes. These regions were separated by the electrodes located along the central sulcus line, which contains T3, C3, Cz, C4, and T4 electrodes. The same principle of identifying these connections were applied to this case with the labels anterior “intra-connection”, “posterior-intra-connection”, and “AP interconnection”.

Figure 3.2 illustrates the specified regions of interest that was used in the quantification process. The number of connections obtained was used as one of the features to be analyzed using variance (ANOVA) statistical test. Each type of IEDs are expected to carry different characteristics which varies in different frequency bands and thresholds used.

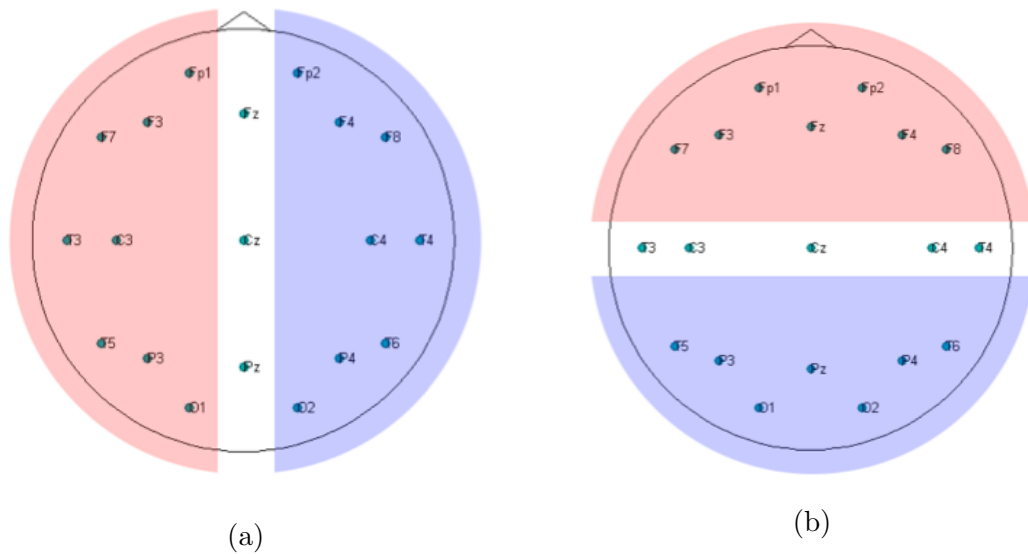


Figure 3.2: Regions of interest, group (a) left-right hemisphere (Left - red, Right - Blue), and (b) anterior-posterior region (Anterior - red, Posterior - blue)

3.6 Results

The connectivity results from the feature extraction are displayed separately by the specific frequency bands. The head map average connectivity plots were obtained by taking an average of the connectivity matrices from the extracted 10 segments. The color indicates the strength of the connection, where dark red indicates strong connections and dark blue indicates weaker connections.

3.6.1 Delta Band Connectivity

The results of the head map average connectivity plots of the Delta frequency band shown in figure 3.3 reveal some differences in the number and strength of connections between each type of IEDs. The connectivity map of IS shows a significantly less propagation between AP and LR regions and the strong connection is displayed only in the temporal lobe region between F7 and T3 electrodes. The observation obtained infers that these characteristic are related to focal epilepsy. On the contrary, the connections of SSC and RSS propagate throughout the entire cortex including AP and LR regions with very strong connections, inferring that these features fall into a generalized type of epilepsy.

Figure 3.4 shows the means and standard deviations of the strongest connections (Average coherence value greater than 0.80) for each type of IEDs in the different ROIs within the Delta band. The ANOVA was calculated for each type of IEDs with the null hypothesis that, the number of strong connections of the different ROIs is the same within each type of IEDs. The analysis for IS type is not significant with ($F(5, 54) = 1.2142, p - value > 0.31$), resulting in accepting the null hypothesis; whereas the analyses for SSC and RSS are significant with ($F(5, 54) = 114.98, p - value < 0.00$) and ($F(5, 54) = 5.6458, p - value < 0.00$) respectively. By analyzing 3

different types of IED, it was noted that the number of stronger connections of SSC and RSS differed from IS significantly with ($F(2,177) = 175.13, p\text{-value} < 0.00$), whereas the post-hoc analysis indicated that the IED types with the highest number of stronger connections are SSC and RSS respectively.

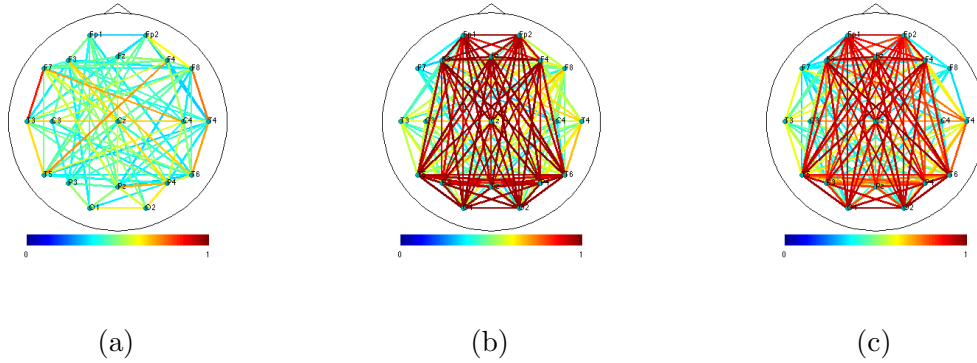


Figure 3.3: Head map average connectivity plots for (a) interictal spike (b) spike with slow wave complex (c) repetitive spikes and slow wave complex from Delta Band

3.6.2 Theta Band Connectivity

The obtained average connectivity head map plots in Theta band shown in figure 3.5 illustrate similar result as Delta band. The IS stronger connections between LR region increased when compared to the previous frequency band, but in general, the pattern of IS still shows characteristics presented in a focal epileptic behavior.

The null hypotheses have not been rejected. The IS type provides ($F(5, 54) = 0.453, p\text{-value} > 0.80$), SSC type provides ($F(5, 54) = 1.739, p\text{-value} > 0.14$) and RSS type provides ($F(5, 54) = 1.985, p\text{-value} > 0.09$). In general, the analysis showed that the number of connections in every type of IED is not different across the ROIs.

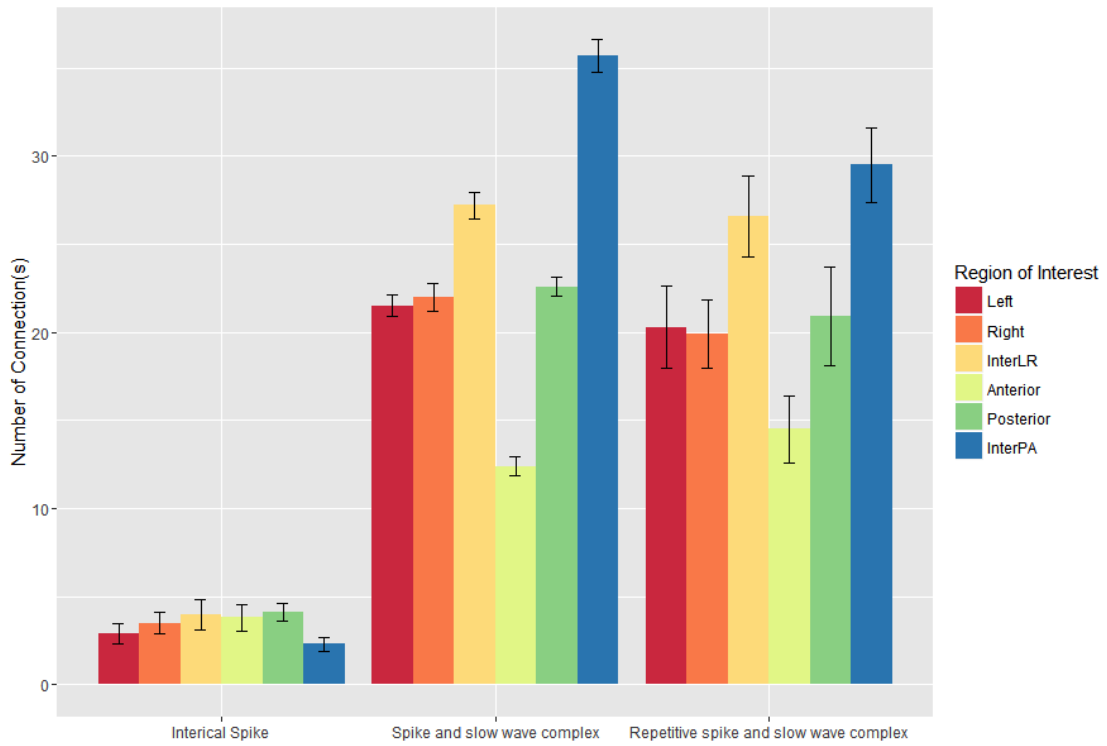


Figure 3.4: Means and standard deviations of number of connections with 80% threshold in the Delta band

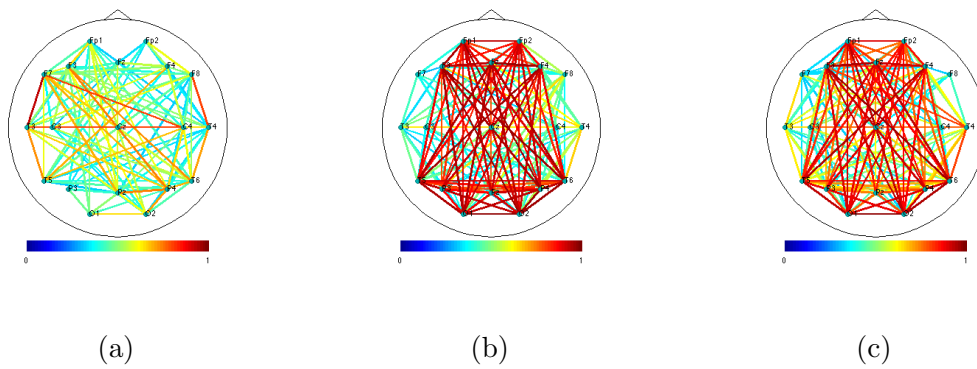


Figure 3.5: Head map average connectivity plots for (a) interictal spike (b) spike with slow wave complex (c) repetitive spikes and slow wave complex from Theta Band

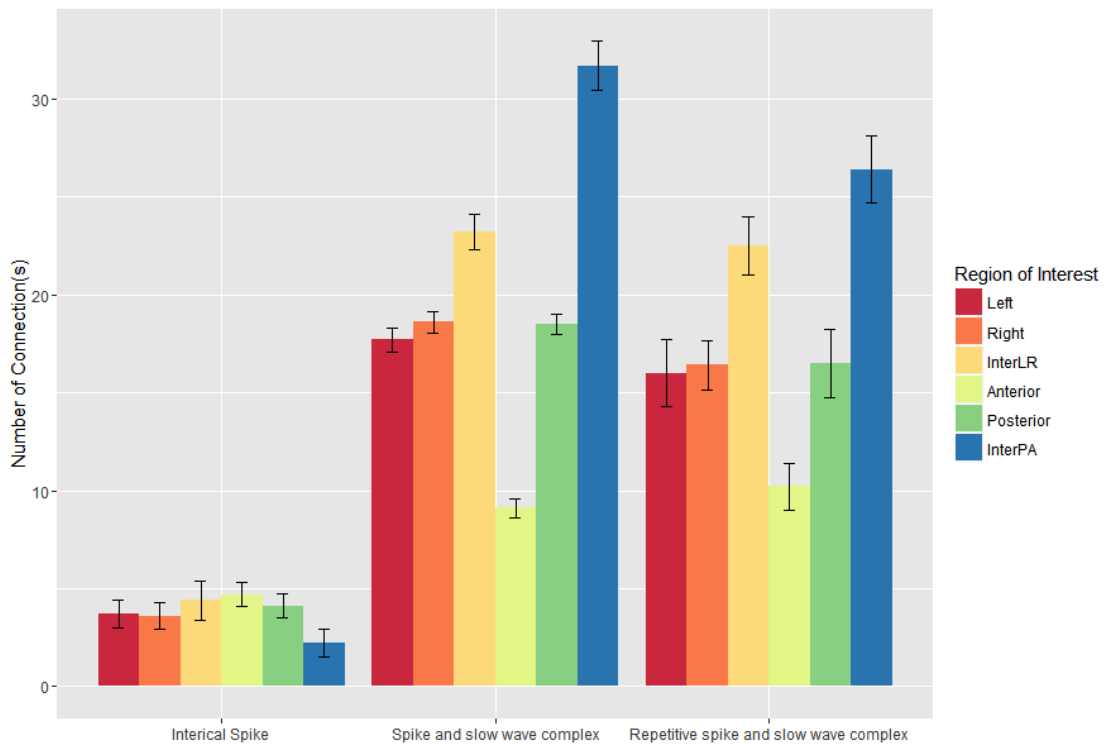


Figure 3.6: Means and standard deviations of number of connections with 80% threshold in the Theta band

3.6.3 Alpha Band Connectivity

The strongest connections obtained in Alpha band from SSC and RSS showed a decrease in the propagation when compared to Delta and Theta band results, whereas the activities obtained for IS are not significantly different from the previous frequency bands outcome. By comparing within Alpha band, SSC and RSS still provide a higher propagation, which indicate the generalized type of epilepsy.

Same statistical analysis has been applied to the mean and standard deviation of the Alpha band results shown in figure 3.8. Similar results were obtained from the calculations. The difference is not significant, whereas the null hypothesis for IS type was accepted with ($F(5, 54) = 0.897, p\text{-value} > 0.48$). The analyses for SSC and RSS still exhibited similar results with the rejection of the null hypotheses, ($F(5, 54) = 3.561, p\text{-value} < 0.00$) and ($F(5, 54) = 8.9211, p\text{-value} < 0.00$). SSC and RSS also contained a significant amount of stronger connections when compared to IS.

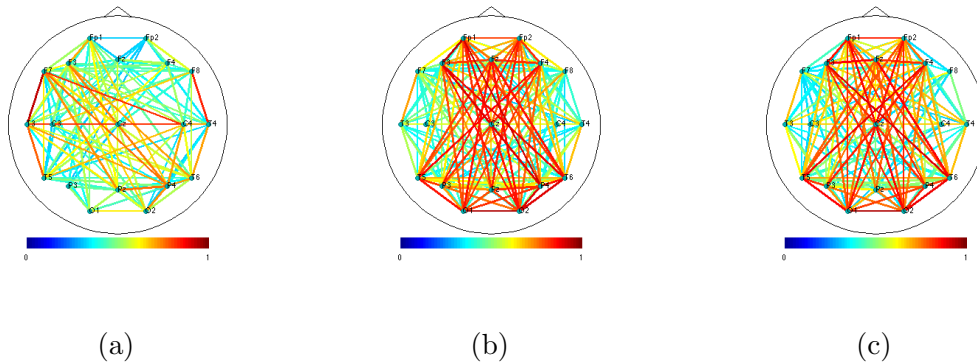


Figure 3.7: Head map average connectivity plots for (a) interictal spike (b) spike with slow wave complex (c) repetitive spikes and slow wave complex from Alpha Band

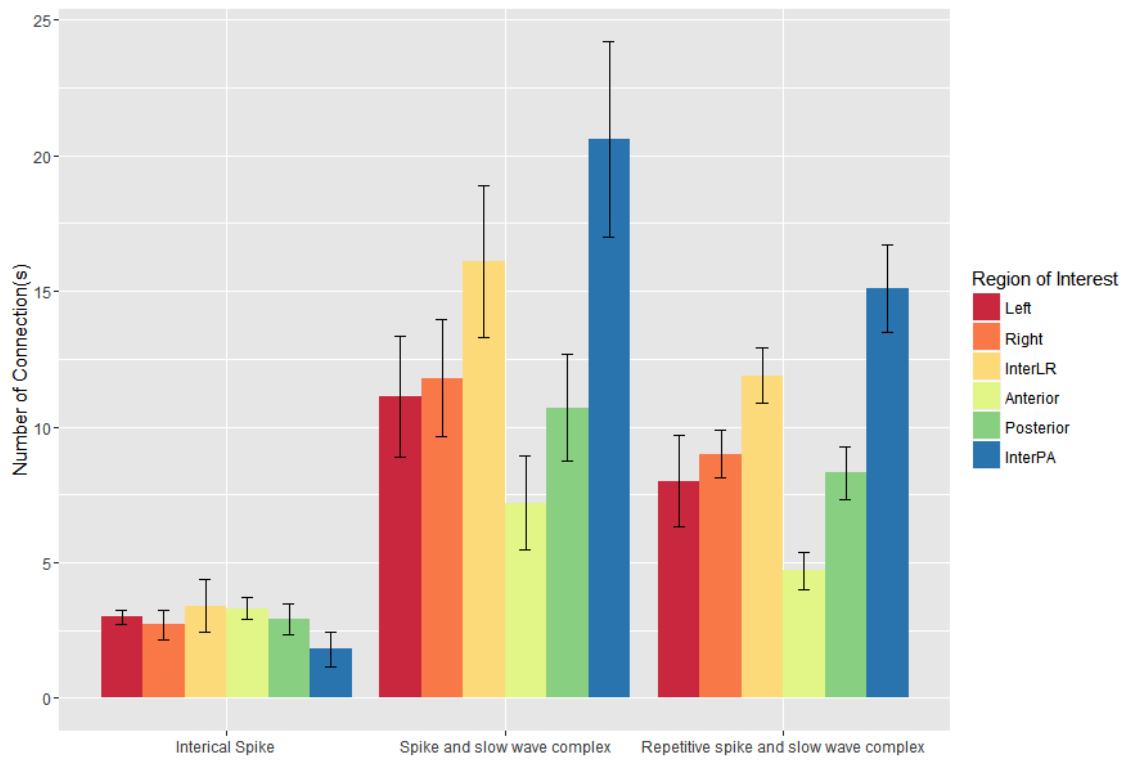


Figure 3.8: Means and standard deviations of number of connections with 80% threshold in the Alpha band

3.6.4 Beta Band Connectivity

The patterns extracted from Beta band as shown in figure 3.9 delineated different structures for SSC and RSS from other frequency bands. The average connectivity head map plots show less stronger connections including a weaker propagation. For IS type, the same area of cortex between (F7T3) and (F8T4) electrodes still contain the strongest connection indicating a focalized type of epilepsy.

The null hypotheses have not been rejected. The IS type provides ($F(5, 54) = 0.453, p - value > 0.80$), SSC type provides ($F(5, 54) = 1.739, p - value > 0.14$) and RSS type provides ($F(5, 54) = 1.985, p - value > 0.09$). In general, the analysis showed that the number of connections in every type of is not different across the ROIs.

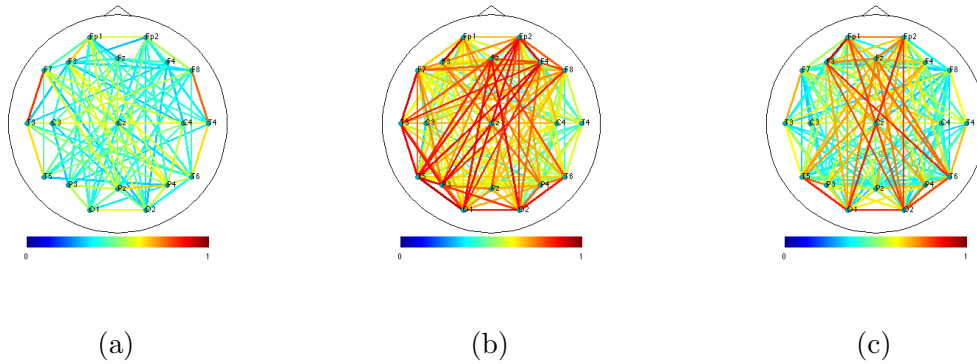


Figure 3.9: Head map average connectivity plots for (a) interictal spike (b) spike with slow wave complex (c) repetitive spikes and slow wave complex from Beta Band

3.7 Discussion

The presented chapter focused on examining the patterns generated from the extraction of EEG functional connectivity patterns during the occurrence of IEDs. With the quantification of the strongest connections presented in each of the frequency

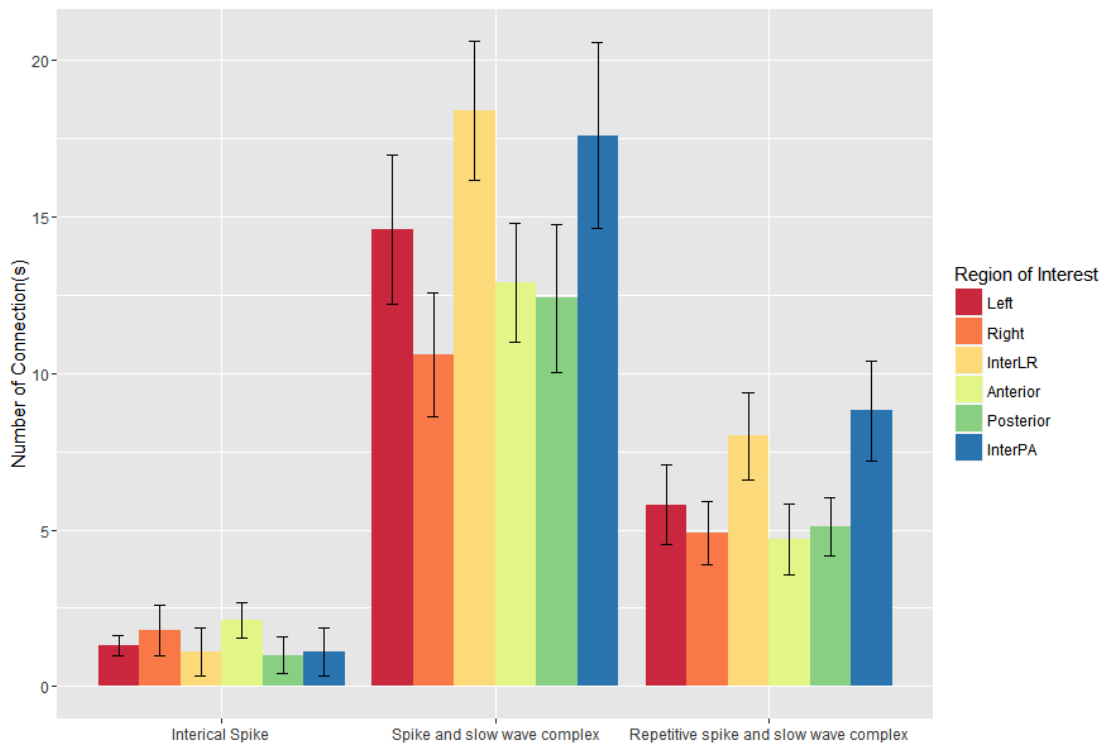


Figure 3.10: Means and standard deviations of number of connections with 80% threshold in the Beta band

bands and in the different ROIs, the characteristics of each type of IED show significance differences that can be used for a classification approved method. A similar approach to the previous analysis [36] was performed on the data, but the functional connectivity extraction was done by using cross-correlation method, which is prone to the error induced by volume conduction. The same work was performed in [55] and [17] using similar approaches, but without examining the occurrence of IEDs in the different frequency bands. It is interesting to apply different generative and discriminative classification approaches to the information selected frequency bands and compare the results for practical applications [60, 46, 43].

3.8 Conclusion

The quantification and extraction of functional connectivity patterns using scalp EEG can generate important features that can be used to classify the type of epilepsy. The patterns extracted by performing coherence analysis revealed different characteristics of each type of IEDs exhibited in different frequency bands. Specific patterns of connectivity along the cortex are obtained as a function of the neurological disorder (epilepsy) using coherence analysis. This method measures the consistency of the relative amplitude and phase between a pair of signals, which defines the strength of the connectivity between all pair-wise electrodes. Whether the seizure event will be focalized or generalized type of epilepsy, these distinct features and characteristics of the connectivity maps in each frequency band can be used for classification, which in turn will lead to enhanced diagnosis of the disorder.

However, the outcome of the connectivity analysis by using coherence has to be interpreted with care. This method does not provide causality assessment, where the flow of information cannot be determined. The aforementioned case leads to

the limitation of the interpretation of the results. Even though the origin of certain synchronizations cannot be determined, the actual connections between and within brain regions will help in the assessment and diagnosis of epileptic patients. The study presented in this chapter has led to the study of effective connectivity by exploring the direction of information flow, which will be explored further in this dissertation.

PARTIAL DIRECTED COHERENCE: A MEASURE OF EFFECTIVE CONNECTIVITY

4.1 Introduction

After Clive Granger proposed his theory of causality in 1969 [25], it had a great impact on the idea of causal relationship between time series analysis. The theory of causality was first applied in economics. The concept of “*Granger Causality*” is rather simple. As shown in figure 4.1, an example of two time series are introduced as X_1 and X_2 signals. This concept is based on whether the knowledge of the past of a signal allows for a better prediction of the behavior of another signal. In this, if the knowledge of the past of signal X_1 provides a better understanding of the future behavior of X_2 , one can assume that signal X_1 *Granger causes* signal X_2 , where signal X_2 does not necessarily *Granger cause* signal X_1 . Although the concept of Granger causality was formulated to solve economics problems, the theory was widely accepted by the engineering and computing community in the field of signal processing.

Granger causality can be formulated into an equation as shown in 4.1. With the assumption that signal X_1 Granger causes signal X_2 , a model can be constructed with annotations of X_1^- and X_2^- represent the past information of signal X_1 and X_2 respectively, with the signal X_2 represented as $X_2 = f(X_2^-, X_1^-)$. By adequately estimating the parameters of the model $f(X_2^-, X_1^-)$, the causality can be estimated by the prediction of signal X_2 based on X_2^- alone versus the prediction based on X_2^- and X_1^- .

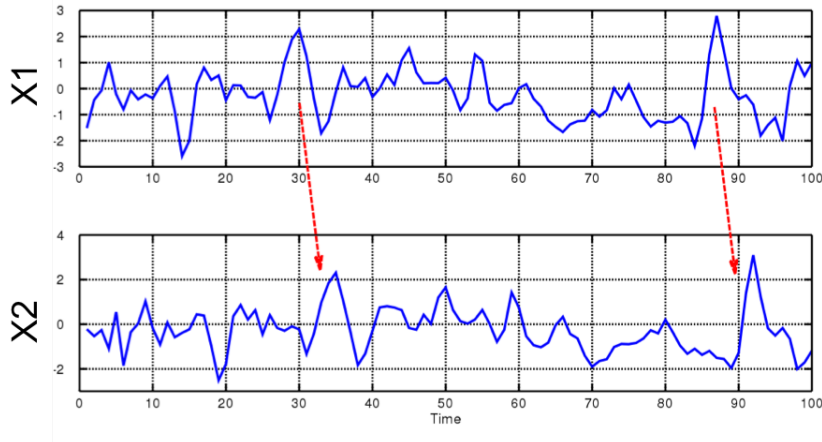


Figure 4.1: Example of two time series

$$G_{X_1 \rightarrow X_2} = \ln \frac{\text{var}(X_2 | X_2^-)}{\text{var}(X_2 | X_2^-, X_1^-)} \quad (4.1)$$

Also, to simply calculate the Granger causality of signal X_2 to X_1 , the variables are interchanged in equation 4.1. Thus, the values of $G_{X_1 \rightarrow X_2}$ and $G_{X_2 \rightarrow X_1}$ are different resulting in a bi-directional causality between two signals. However, the performance of the model depends heavily on the parameters estimation accuracy.

Among these bivariate and time domain approaches, the contributions of Caines and Chan in 1975 [13] and Geweke in 1982 [24] focused at multivariate time series generalization. Although methods of computing Granger causality was mentioned earlier, a more robust method would be more ideal to deal with the dynamical properties of electrophysiology. A research study conducted by Saito et al. was implemented using the concept of Granger causality to the EEG data [52]. The method as introduced was known as Directed Coherence (DC) with a decomposition of coherence function into bi-directional coherences. The limitation of the algorithm is that the results would be unstable as the number of EEG channels

is increased beyond two channels. In the work of Kaminski and Blinowska [37], Directed Transfer Function (DTF) was formulated in an attempt to measure the effective connectivity of the brain structure with decent results obtained. However, the DTF would rank the interaction among the EEG channels with respect to the total inflow of information only.

After the tests for DC and Granger causality as performed by Baccal et al. in [6], one could see the need for using Partial Directed Coherence (PDC) as formulated. PDC calculation offers the representation of connectivity as a matrix of information flow between every connection and between all EEG channels [7]. The use of PDC would thus provide a useful tool for estimating the effective connectivity and extract the underlying features of epilepsy from EEG recordings.

4.2 Computing PDC

Partial directed coherence (PDC) is a well-established method that calculates the effective connectivity from the estimated coefficients of the multivariate autoregressive (MVAR) model. PDC provides an approximation of causality between a pair of EEG channels creating a directed graph, which reflects the inter-dependence and information flow between distinct EEG channels. The segmented scalp EEG data was fitted into the MVAR model as expressed in 4.2.

$$\begin{bmatrix} x_1(t) \\ x_2(t) \\ \vdots \\ x_k(t) \end{bmatrix} = \sum_{i=1}^p \mathbf{A}(i) \begin{bmatrix} x_1(t-i) \\ x_2(t-i) \\ \vdots \\ x_k(t-i) \end{bmatrix} + \begin{bmatrix} e_1(t) \\ e_2(t) \\ \vdots \\ e_k(t) \end{bmatrix} \quad (4.2)$$

$$\mathbf{X}(t) = \sum_{i=1}^p \mathbf{A}(i)\mathbf{X}(t-i) + \mathbf{E}(t)$$

In terms of the model, a k -channel process can be represented as a vector X of k EEG signals recorded in time, where the signal matrix can be expressed as $\mathbf{X}(t) = [\mathbf{x}_1(t)\mathbf{x}_2(t)\dots\mathbf{x}_k(t)]^T$, and the matrix containing the uncorrelated white noise at time t can be expressed as $\mathbf{E}(t) = [\mathbf{e}_1(t)\mathbf{e}_2(t)\dots\mathbf{e}_k(t)]^T$, where the p term in the summation is the model order, and $\mathbf{A}(i)$ is the $k \times k$ coefficient matrix of the model. The MVAR coefficients are estimated by using the method of Vierra-Morf [44]. The model order defines the number of past data points that are included in the estimation of a current MVAR model. The estimation of an element A_{ij} from the coefficient matrix describes the influence of the data from channel $\mathbf{x}_j(t-i)$ on the selected channel \mathbf{x}_i , thus providing knowledge of the directed information flow between all signals. In this case, 19 scalp EEG channels were used, therefore, the value of k is 19. The model order p of the MVAR model was determined by using Akaike Information Criterion (AIC) [3], which can be calculated as shown in equation 4.3.

$$AIC(p) = \ln|\sum_e(p)| + \frac{2pK^2}{N} \quad (4.3)$$

Element $\sum_e(p)$ represents the covariance matrix of the residuals, N is the total number of time points, p is the model order, and K is the number of signals considered, which in this case is the number of EEG recordings. The fitting results of the MVAR model is related to the model order p . However, the previous work from Franaszczuk has found that small changes to the model order did not influence the results significantly [22].

Then, to obtain the coefficient of MVAR model in the frequency domain $\mathbf{A}(f)$, the Fourier transformation is applied to the MVAR coefficient as shown in equation

4.4.

$$\mathbf{A}(f) = \sum_{r=0}^p \mathbf{A}(i) e^{-2\pi i r f} \quad (4.4)$$

where the transfer function of the EEG signals can be quantified by the equation:

$$\bar{\mathbf{A}}(f) = \mathbf{I} - \mathbf{A}(f) = \begin{bmatrix} \bar{a}_1(f) & \bar{a}_2(f) & \dots & \bar{a}_k(f) \end{bmatrix} \quad (4.5)$$

and where the elements contained in $\bar{\mathbf{A}}(f)$ are defined as:

$$\bar{\mathbf{A}}_{ij}(f) = \begin{cases} 1 - \sum_{i=1}^p a_{ij}(r) e^{-2\pi i r f} & \text{if } i = j \\ - \sum_{i=1}^p a_{ij}(r) e^{-2\pi i r f} & \text{otherwise} \end{cases} \quad (4.6)$$

The PDC value $\pi_{ij}(f)$ can be calculated as in equation 4.7.

$$\pi_{ij}(f) = \frac{\bar{\mathbf{A}}_{ij}(f)}{\sqrt{\bar{a}_j^H(f) \bar{a}_j(f)}} \quad (4.7)$$

$\bar{a}_j(f)$ is the j^{th} column $j = 1, 2, \dots, k$ of the matrix $\bar{\mathbf{A}}(f)$ and the value of $\pi_{ij}(f)$, ranging from 0 to 1, represents the intensity and direction of information flow from channel i to channel j at frequency f .

PDC thus measures the strength of the relative signal exerting from one structure to another, where the measurement is considered as a spectral aspect of the Granger causality. Comparing to other connectivity extraction techniques, PDC has an advantage of providing partialized coupling strengths between neuronal populations, where it measures the direct connectivity while excluding the volume conduction effects.

4.3 Overview of PDC using Simulated Data

To evaluate the performance of the PDC, the simulated data was formulated based on the equations 4.8. The parameters of the equations were taken from [7].

$$\begin{aligned}x_1(i) &= 0.95\sqrt{2}x_1(i-1) - 0.9025x_1(i-2) + e_1(i) \\x_2(i) &= -0.5x_1(i-1) + e_2(i) \\x_3(i) &= 0.4x_2(i-2) + e_3(i) \\x_4(i) &= -0.5x_3(i-1) + 0.25\sqrt{2}x_4(i-1) + 0.25\sqrt{2}x_5(i-1) + e_4(i) \\x_5(i) &= -0.25\sqrt{2}x_4(i-1) + 0.25\sqrt{2}x_5(i-1) + e_5(i)\end{aligned}\tag{4.8}$$

To generate the simulated MVAR model using Python programming language, code listing 4.1 allows us to specify the MVAR coefficients according to the equations presented in 4.8.

```
1 import numpy as np
2 import connectivipy as cp
3 from connectivipy import mvar_gen
4 import matplotlib.pyplot as plt
5
6 # Specifying A coefficients
7 A = np.zeros((2, 5, 5))
8 A[0, 0, 0] = 0.95 * 2**0.5
9 A[1, 0, 0] = -0.9025
10 A[0, 1, 0] = -0.5
11 A[1, 2, 1] = 0.4
12 A[0, 3, 2] = -0.5
13 A[0, 3, 3] = 0.25 * 2**0.5
14 A[0, 3, 4] = 0.25 * 2**0.5
15 A[0, 4, 3] = -0.25 * 2**0.5
16 A[0, 4, 4] = 0.25 * 2**0.5
```

Listing 4.1: Configuration of MVAR coefficients

From the simulated MVAR coefficients, we can generate the MVAR model by using code listing 4.2.

```

1 | # generate 5-channel signal with 1000 data points
2 | ysig = np.zeros((5, 1000, 5))
3 | ysig[:, :, 0] = mvar_gen(A, 1000)
4 | ysig[:, :, 1] = mvar_gen(A, 1000)
5 | ysig[:, :, 2] = mvar_gen(A, 1000)
6 | ysig[:, :, 3] = mvar_gen(A, 1000)
7 | ysig[:, :, 4] = mvar_gen(A, 1000)

```

Listing 4.2: Generating MVAR data using the simulated coefficients

From the equations given in 4.8, $x_k(i)$ represents the channel k_{th} of the EEG data and $e_k(i)$ is the white noise in the corresponding channel. The data from equations 4.8 with 1000 data points are generated by using code listing 4.3. The simulated data are shown in figure 4.3 and the interconnection structure is summarized in figure 4.2.

```

1 | data = cp.Data(ysig, 128, ["Channel1",
2 |     "Channel2", "Channel3", "Channel4", "Channel5"])
3 |
4 | # Plot data
5 | %matplotlib inline
6 | plt.rcParams['figure.figsize'] = (10, 8)
7 | data.plot_data()

```

Listing 4.3: Plotting MVAR data

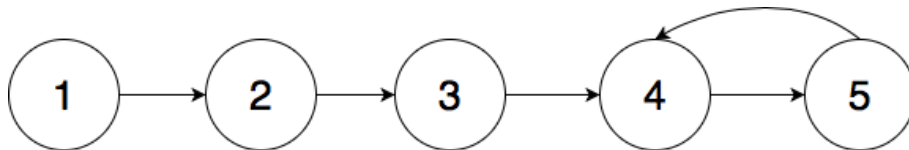


Figure 4.2: Flow of information based on simulated data

Figure 4.4 shows the PDC computed from the simulated data, which can be generated by using code listing 4.4. From the result, if there is no direct connection between channels, $|\bar{\pi}_{ij}(f)|$ will be equal to 0. From the results, the signal propagates from the source $x_1(i)$ sequentially to $x_2(i)$ and $x_3(i)$. The the signal then propagates from $x_3(i)$ into another structure comprises of $x_4(i)$ and $x_5(i)$. This interpretation

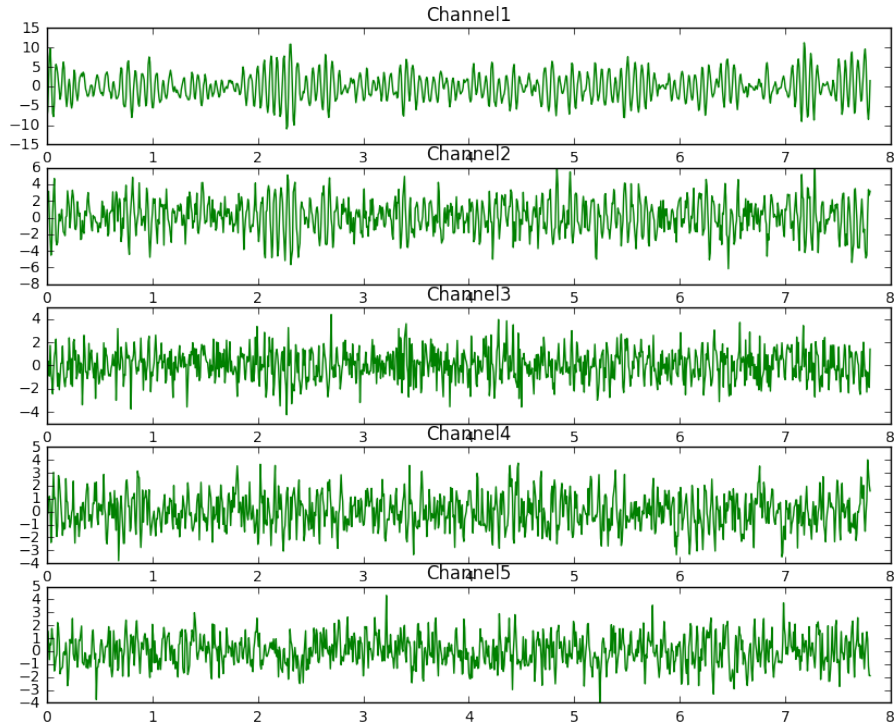


Figure 4.3: Simulated data with 5 channels

of PDC values validates the condition of the network structure based on the defined equations in 4.8.

```

1  # Fitting MVAR model
2  data.fit_mvar(2, 'vm')
3  ar, vr = data.mvar_coefficients
4
5  # Calculating PDC values
6  pdc_values = data.conn('pdc')
7  plt.rcParams['figure.figsize'] = (10, 8)
8  data.plot_conn('PDC', signi=False)

```

Listing 4.4: Calculating PDC values from the simulated signals

4.4 Intensity of Information Flow

The neuron connections in the brain cortex can be represented as a network of directionally connected nodes, where the connectivity can be estimated by using

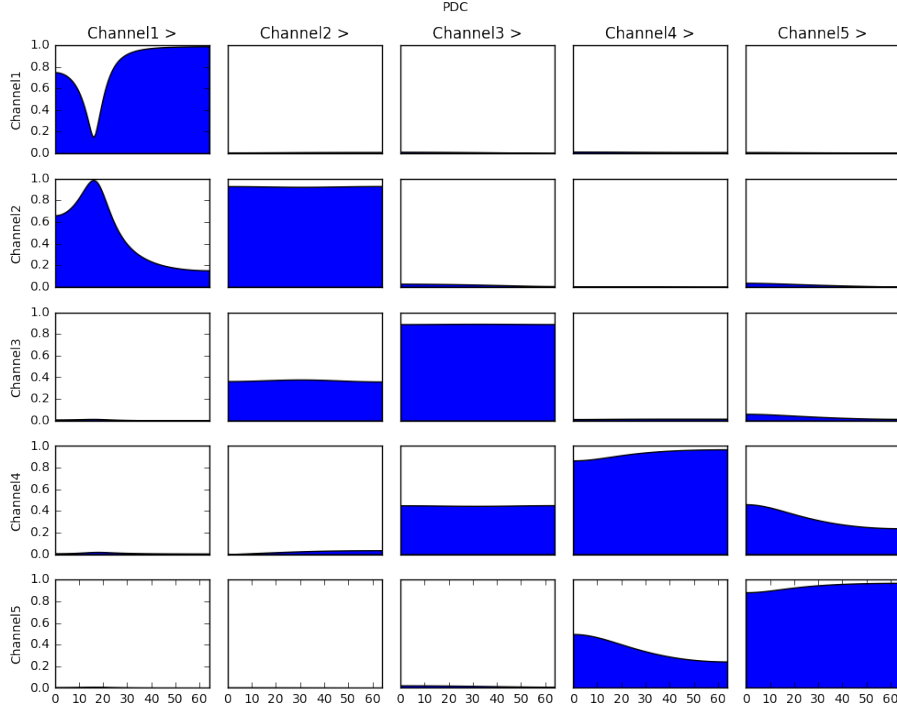


Figure 4.4: PDC calculation of the simulated data

PDC as presented in the previous section. This study proposes using the concept of intensity of information flow, which can be divided into two parts, *Inflow* and *Outflow*. The inflow is a measurement that represents the intensity of information flow from all other nodes to a specific node, while outflow represents an intensity emanating from a given node and spreading onto all other nodes. The intensity of PDC value of channel i to channel j within a given frequency range of (f_1, f_2) in Hz can be defined as:

$$ePDC_{ji}(f_1, f_2) = \int_{f_1}^{f_2} \pi_{ji}^2(f) df \quad (4.9)$$

Inflow can be calculated by adding all the total incoming information intensities from other channels. The inflow at channel i is the sum of the intensities of infor-

mation flow from the rest of the channels $j = 1, 2, \dots, k$ where $j \neq i$ can be defined as shown:

$$flow_{in} = \sum_{j=1, j \neq i}^k ePDC_{ji}(f_1, f_2) \quad (4.10)$$

Similarly, Outflow from channel i represents the sum of all intensities of information flow from channel i to the rest of the channels and it is defined as in:

$$flow_{out} = \sum_{j=1, j \neq i}^k ePDC_{ij}(f_1, f_2) \quad (4.11)$$

The information inflow and outflow, as defined can thus be used to quantify and assess the process of exchanging information from different regions inside the brain. Therefore, by calculating the inflow and outflow of the EEG channels, the underlying patterns of brain activity during the interictal period can be used as essential features for classification, and subsequently could be extended in the case of focal epilepsy as to how such activity patterns are disrupted in the context of a determined 3-D source localization of a seizure onset.

CHAPTER 5
CLASSIFICATION OF INTERICTAL EPILEPTIFORM
DISCHARGES USING PARTIAL DIRECTED COHERENCE

5.1 Introduction

This chapter introduces the classification of patterns extracted from different types of interictal epileptiform discharges (IEDs) that includes interictal spike (IS), spike and slow wave complex (SSC), and repetitive spikes and slow wave complex (RSS)), using the partial directed coherence (PDC) analysis. The PDC analysis estimates the intensity and direction of propagation from neural activities generated in the cerebral cortex, and analyzes the coefficients obtained from employing multivariate autoregressive model (MVAR). Features extracted by using PDC are transformed into adjacency matrices by using surrogate data testing with a 0.05 significance level. The significant propagations are represented as 1 in the adjacency matrix and 0 otherwise. Binary matrices are converted into binary vectors. These vectors are then selected as the inputs of a multilayer Perceptron (MLP) neural network. The trained classifiers were able to detect and classify different types of IEDs when using the features extracted from PDC with a very high performance.

During the epileptic seizures, groups of neurons in the cerebral cortex are being excessively triggered simultaneously resulting in symptoms such as muscle stiffness, muscle spasms and impaired consciousness [20]. The disease is considered a chronic disorder affecting 0.5 - 1% of the entire population. In the United States alone, 1.8% of adults (18 years and older) and 1% of children (aged 0-17), are reported to have epilepsy by the Center for Disease Control and Prevention [21]. Although the symptoms mentioned above are general symptoms, the location, duration and propagation of the seizures vary depending on the individual. Enhancing epilepsy

diagnosis or predicting the occurrence of seizures through recordings, the planning of therapeutic protocols will be improved and lead through the benefits of epileptic patients and society at large.

Among the neurophysiological techniques, electroencephalogram (EEG) remains the most prevalent and reliable modality to examine brain activities as well as using it as the main diagnosis assessment [70]. EEG recording is simple and inexpensive compared to other neuroimaging studies. EEG captures the electrical activities produced by the neurons in the brain including the interictal epileptiform discharges (IEDs). Due to its high temporal resolution, EEG is considered a suitable tool for identifying synchronization between a pair of signals [59]. Substantial amount of epilepsy diagnosis is done by recording and visualizing EEG during seizures and closely monitoring IED in long interictal recordings. Extracting epileptic characteristics of EEG in interictal periods plays a key role in the disease detection. Consequently, extracting the hidden patterns of EEG in the interictal phase may be a beneficial tool to alleviate this complex process of the epilepsy diagnosis.

The analysis of EEG signals with the purpose of helping patients suffering from neurological disorders have been one of the most prominent research fields. Various techniques of computational analysis have been performed to enhance the detection of neurological disease characteristics [62, 33, 34]. However, the characteristics of epilepsy still require an extensive exploration and investigation in order to improve the understanding of the disease [62]. The majority of epilepsy diagnostics are based on the EEG, where epileptic patients will undergo the procedure of EEG recordings for a length of period with an observation from technicians or doctors [56]. One of the key features that can be analyzed by utilizing EEG recordings is the extracted IEDs. IEDs from scalp EEG recording provide important information of lateralization and localization of epileptogenic foci [63] and are the key feature

for classifying types of epilepsy [38].

To extract underlying features of the IEDs, the study of propagation of EEG is introduced where it provides promising results as in [33], and [34]. More recently, the concept of Granger-causality was applied to determine the propagation of EEG activity [25]. The concept of Granger-causality determines the causal influences of variable to another where it is based on the idea that causes precede their effects in time. Granger-causality is evaluated by fitting vector autoregressive models. A method based on the Granger-causality concept, called the partial directed coherence (PDC), is proposed to extract the propagation of the EEG activity [7] where the approach is based on a multivariate autoregressive model (MVAR). Unlike conventional methods such as correlation or coherence, the utilization of MVAR model allows us to examine the interaction between multichannel instead of pair-wise channel resulting in better and more precise results [41].

To the best of our knowledge, this is the first experimental study to incorporate the propagation of information flow to classify the types of IEDs by utilizing machine learning. This study proposes an analysis of classification of IEDs by using the propagation patterns extracted from the EEG data segments and using the PDC methodology. Results obtained from PDC method will be transformed, by using surrogate data testing, into adjacency matrices. The obtained adjacency matrices extracted from each type of IED are used as the main feature in the neural network classifier, where the system will use the tenfold cross validation method to evaluate the performance of the classifier.

5.2 Data Acquisition

In this study, only interictal epileptiform discharges (IED) were used to extract the different characteristics of the 3 types of epileptic biomarkers. To explore synchro-

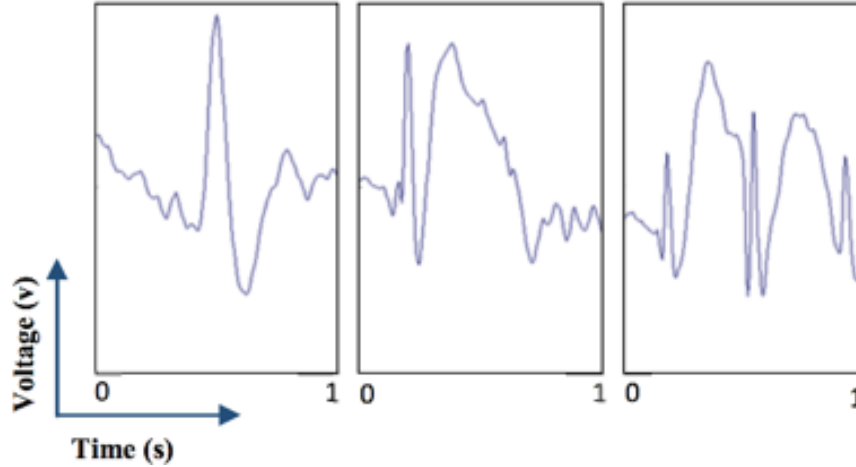


Figure 5.1: Types of interictal epileptiform discharges.(From left to right) interictal spike, spike and slow wave complex, and repetitive spikes and slow wave complex

nization between brain regions in focal and generalized cases, a total of 30 EEG segments from a male patient diagnosed with generalized epilepsy and a female patient diagnosed with focal epilepsy having partial complex seizures were obtained. The research procedure was approved by the Institutional Review Board of Florida International University and received the consents from all subjects. The data were recorded with the 10-20 electrode placement protocol containing the 3 types of IED (IS, SSC, and RSS). An example of these biomarkers is shown in figure 5.1. Recordings are performed containing 19 electrodes (Fp1, F7, T3, T5, O1, F3, C3, P3, Fz, Cz, Pz, Fp2, F8, T4, T6, O2, F4, C4, and P4) using Cz channel as the reference electrode. The data was collected with a sampling rate of 200 Hz.

5.3 Preprocessing

To minimize the effect of undesired noise, The EEG data was preprocessed prior to segmentation. Principle component analysis (PCA) and independent component analysis (ICA) were applied to the data and manually performed an artifact rejection. Eye blinks and muscle movements were removed using ICA components and

the EEG data was reconstructed. The EEG data was divided into 3 groups according to the types of IED. They were segmented into 3-second windows containing a single occurrence of IED in the center of the segment. To focus on the characteristics of IEDs, the peak of the ISs were arranged at the 1.5s of the segment, where the first peak of SSC and RSS were arranged at the 1.2s of the segment due to its longer extent [34]. In total, 10 segments of each type of IEDs were extracted from the original EEG data.

5.4 Feature Extraction

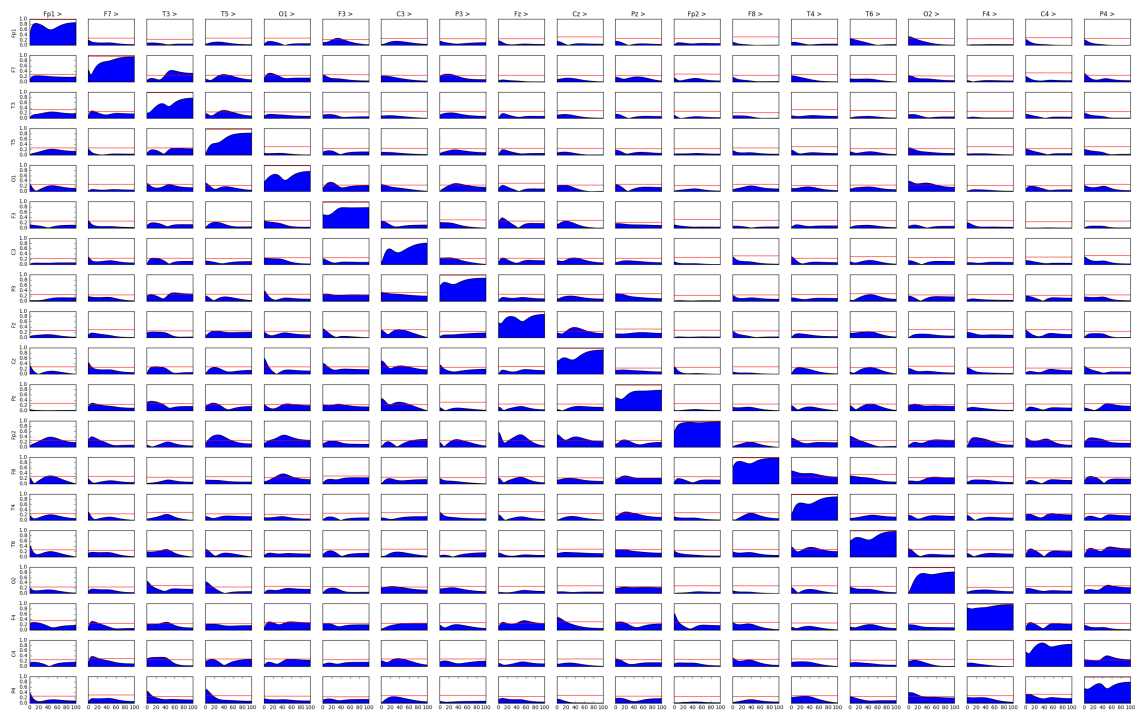
The Partial Directed Coherence (PDC) method based on an estimation of coefficients of a multivariate auto-regressive model (MVAR) would provide a directed network, which reflects the inter-dependence and information flow between EEG channels. By using the PDC concept as explained in chapter 4, the effective connectivity values of the preprocessed EEG segments were extracted. The value of $\pi_{ij}(f)$ ranging from 0 to 1 represents the intensity and direction of information flow from channel j to channel i at frequency f . The significance of every directed connection is evaluated by a statistical test using surrogate data explained in section 2.5. The method is based on the creation of surrogates with basic resemblance to the original data using causal Fourier transform. The procedure includes calculation of a testing matrix (PDC), for both original and surrogate data in order to test the null hypothesis of similarity. Rejection of the null hypothesis results in significance of the causal coupling under test. If the null hypothesis is rejected in more than 95% of tests, the calculated PDC is significant with 95% confidence level. To test the causal coupling between every pairwise electrodes, the multichannel surrogate data is created by preserving all connections except the one currently under test.

Figures 5.2, 5.3, and 5.4 are the samples of PDC values extracted from the IS, SSC, and RSS respectively.

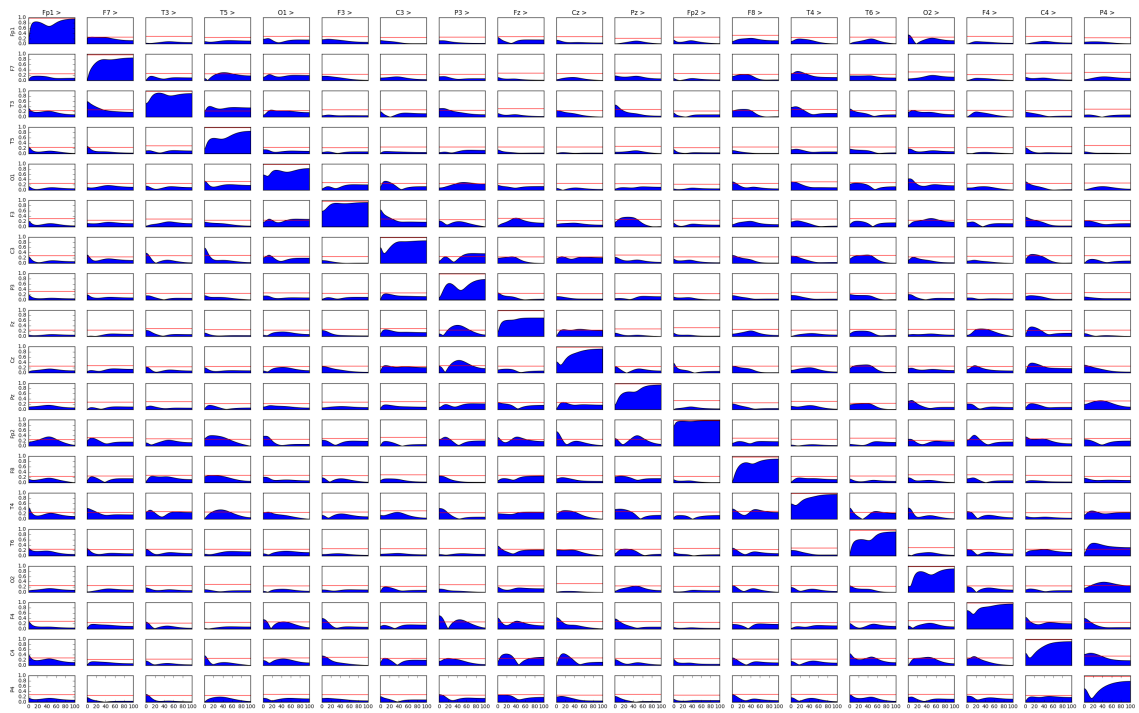
5.5 Feature Transformation

Because the sampling frequency of the EEG data is 200 Hz, the PDC values of every pair-wise channel will fall within the range of 0-100 Hz. After the PDC values were extracted from every EEG segment containing IEDs, the values of the PDC were compared to the significance threshold computed by utilizing surrogate data testing. Figure 5.5 shows the result of PDC extraction from the EEG data. Each of the plots show the values of PDC between the selected channels ranging between 0-100 Hz. The blue area indicates the PDC values within each frequency, where the horizontal red line indicates the values generated from the surrogate data testing. The PDC values at the given frequency are considered significant when the PDC values exceed the red line. The surrogate data testing was set to have a 100 number of repetitions with the level of significance of $\alpha = 0.05$.

To reduce the dimensionality and prepare the data for the neural network classifier, the PDC values of every EEG segment were applied with the threshold obtained from the surrogate data testing. If the value of the PDC surpasses the significance line, the entire segment is represented as 1 and 0 otherwise, creating a 19×19 adjacency matrix as shown in figure 5.6. The eye of the matrix containing the values between the channel and itself will be removed and converted into a vector containing $(19 \times 19 - 19) = 342$ elements. These binary vectors extracted from every EEG segment containing 3 types of IEDs will be used as inputs for the classifier to discriminate between different types of IEDs.

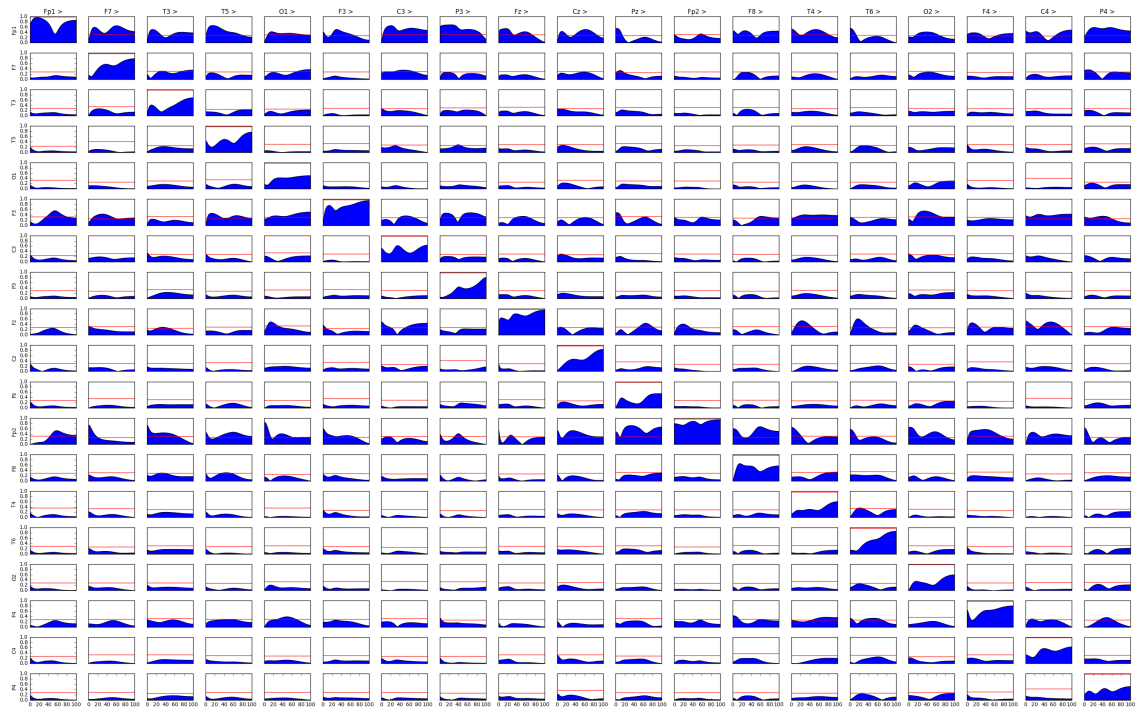


(a)

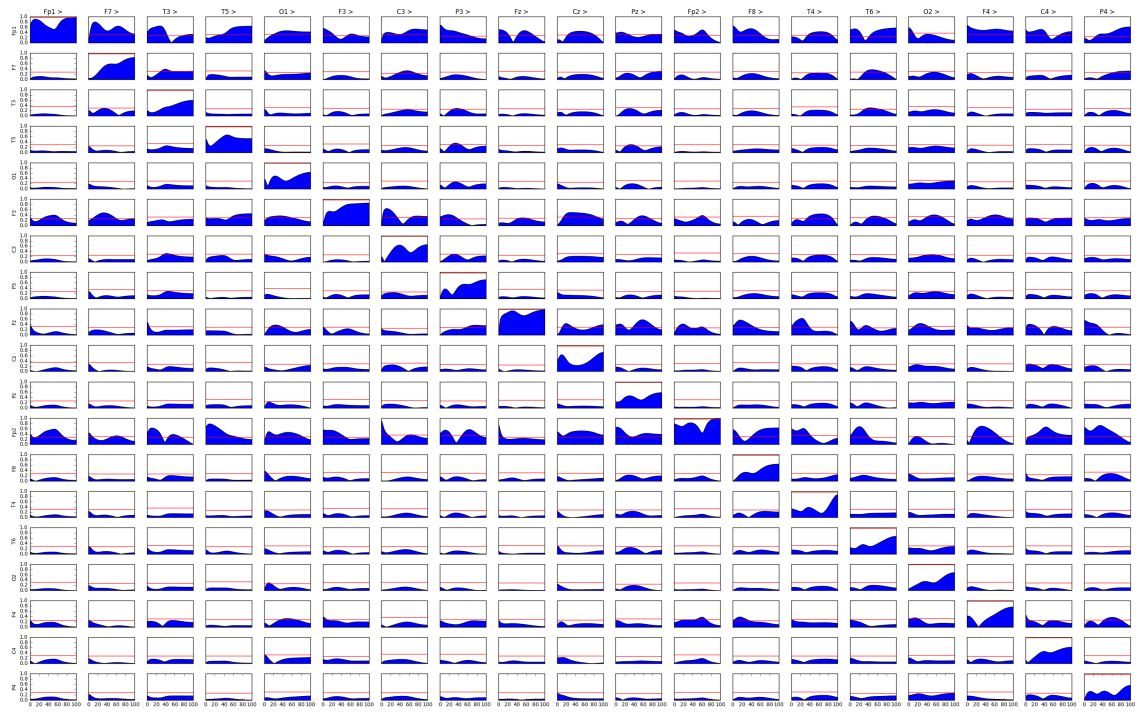


(b)

Figure 5.2: Random samples of PDC values extracted from interictal spike

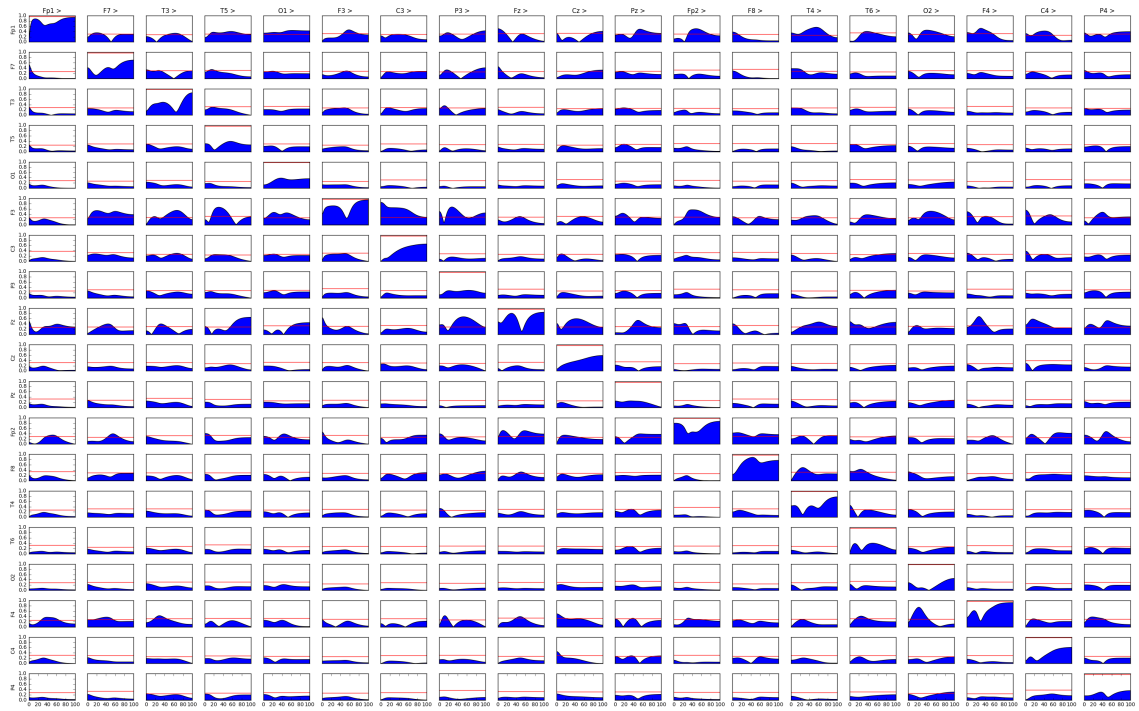


(a)

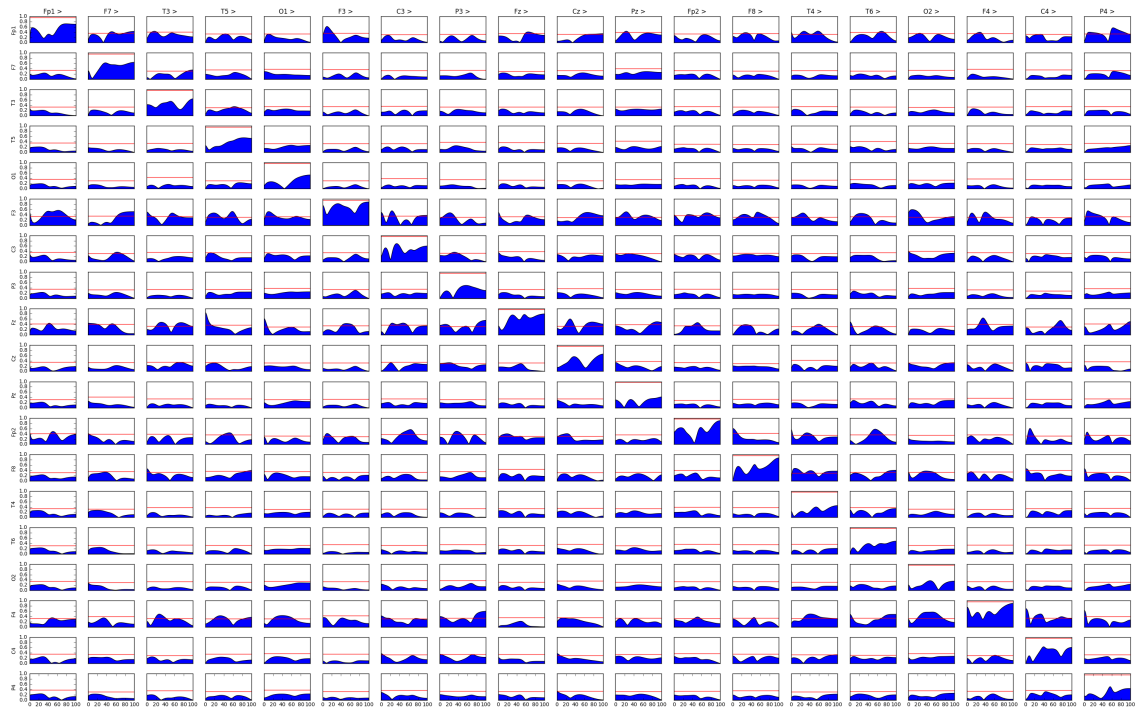


(b)

Figure 5.3: Random samples of PDC values extracted from spike and slow wave complex



(a)



(b)

Figure 5.4: Random samples of PDC values extracted from repetitive spikes and slow wave complex

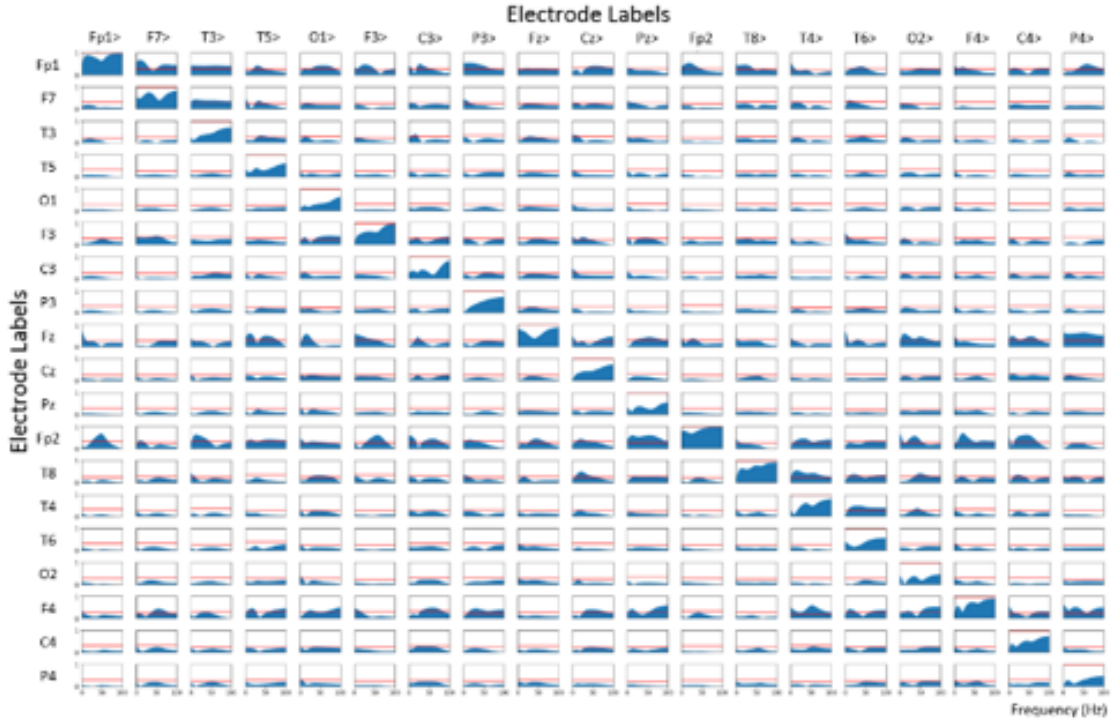


Figure 5.5: Computed partial directed coherence

5.6 Multilayer Perceptron Neural Network

After the feature transformation process, the 3 types of IEDs (IS, SSC, and RSS), were classified using the aforementioned 19×19 adjacency matrices (or 1×342 binary vectors) as inputs for a multilayer Perceptron (MLP) neural network that uses the back-propagation algorithm. To improve the speed of learning, the Nguyen-Widrow initialization method was performed for generating the initial weights. One hidden layer was applied to implement non-linear decision boundaries, where the size of the hidden layer was the same as the number of inputs, i.e., 342, and a bias unit was added to both: input layer and hidden layer. A momentum term was included into the weight upgrade, which could minimize the disruption of convergence caused by some abnormal patterns. These patterns can usually set the convergence towards the minimum, defined by the majority of the patterns. The flowchart of the MLP

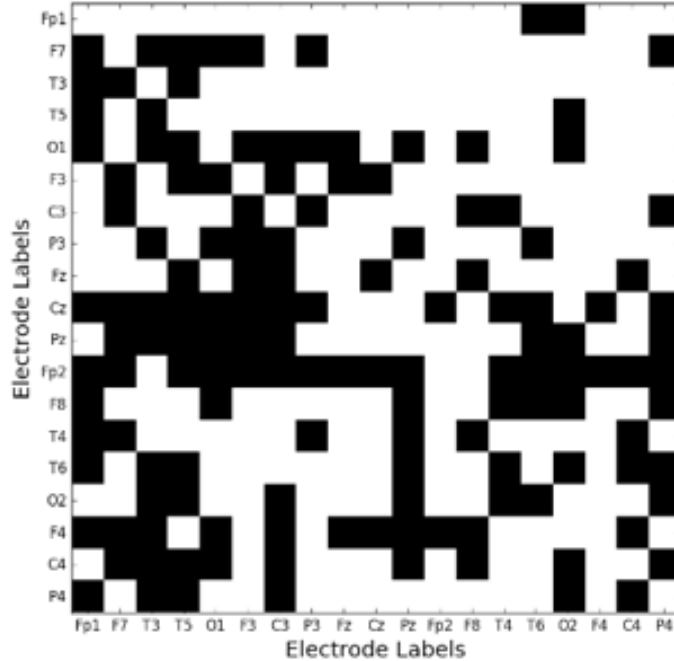


Figure 5.6: Adjacency matrix from the computed PDC

algorithm used in this study is presented in Figure 5.7 After obtaining the final weights and biases of the MLP, then given a new EEG segment, the MLP was able to classify it to a certain type of IEDs precisely.

5.7 Classification Experiment: Tenfold Cross Validation

The classification performance of the MLP was measured by using the F1 score, accuracy, sensitivity, specificity, and precision based on tenfold cross validation process. Both binary classifications (i.e., IS vs. SSC, IS vs. RSS, and SSC vs. RSS) and 3-types classification (i.e., IS vs. SSC vs. RSS) experiments were carried out for estimating our proposed method. In the tenfold cross validation process, the segments were randomly assigned to 10 sets d_0, d_1, \dots, d_9 , so that all sets were equal size. Therefore, the data used in the binary classification experiment should include 20 binary vectors transformed from the corresponding EEG segments, and all 30

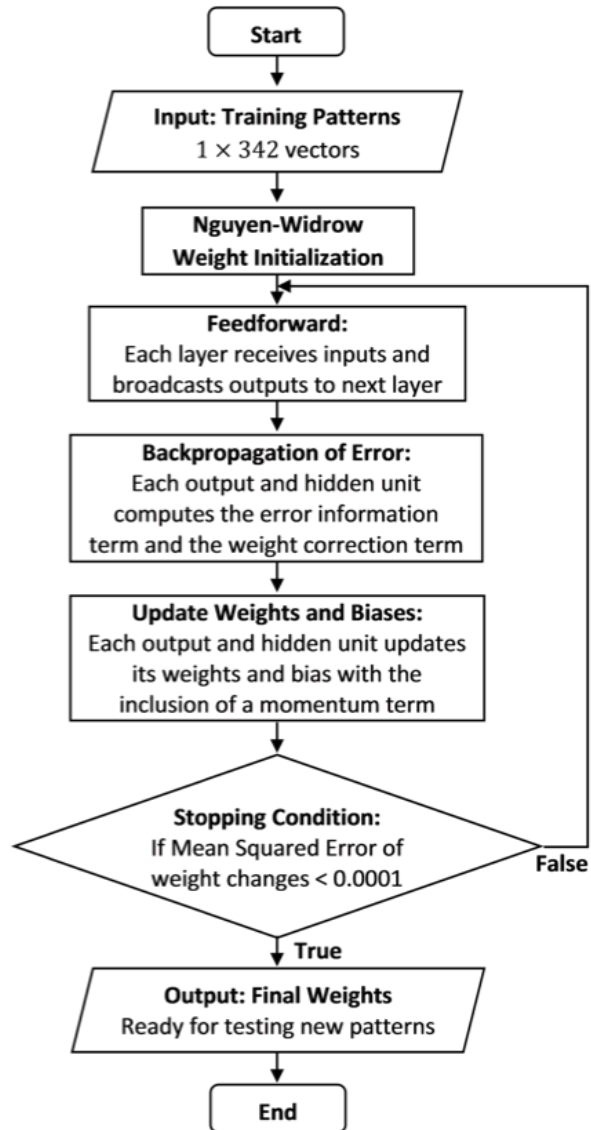


Figure 5.7: Flowchart of the multilayer Perceptron algorithm

vectors need to be involved in the 3-types classification experiment. Then each one of the 10 sets were retained as the validation data while the remaining 9 sets were used for training, thus, every data point was used for both training and validation on each fold. In every single validation performed, the MLP neural network was trained separately and started with a new set of initial weights to ensure the reliability of the experiment results.

5.8 Results

The EEG data was separated by the types of IEDs contained in the data including interictal spike (IS), spike and slow wave complex (SSC), and repetitive spike and slow wave complex (RSS). Each of the IEDs was selected and verified manually by clinical experts. After the artifacts rejection was performed, the data was segmented into 3-s windows containing only a single occurrence of IED and labeled with its type accordingly. adjacency matrices were implemented from the extracted and transformed features.

Figure 5.8, figure 5.9, and figure 5.10 show the sample of adjacency matrices extracted from 3 different types of IEDs. The plot of adjacency matrix contains 2 values representing the significance of propagation between a pair of electrodes. Black color-coded pixel represents the propagation that passes through the threshold generated by using surrogate data testing, where white color-coded pixel represents otherwise. From the figures, the adjacency matrices of different types of IEDs show different patterns of significance propagation. IS type shows a lack of significance propagation in the upper-right quadrant of the adjacency matrix, where SSC and RSS types show denser patterns of significance propagation. The patterns observed from these adjacency matrices between SSC and RSS are more difficult to distinguish visually.

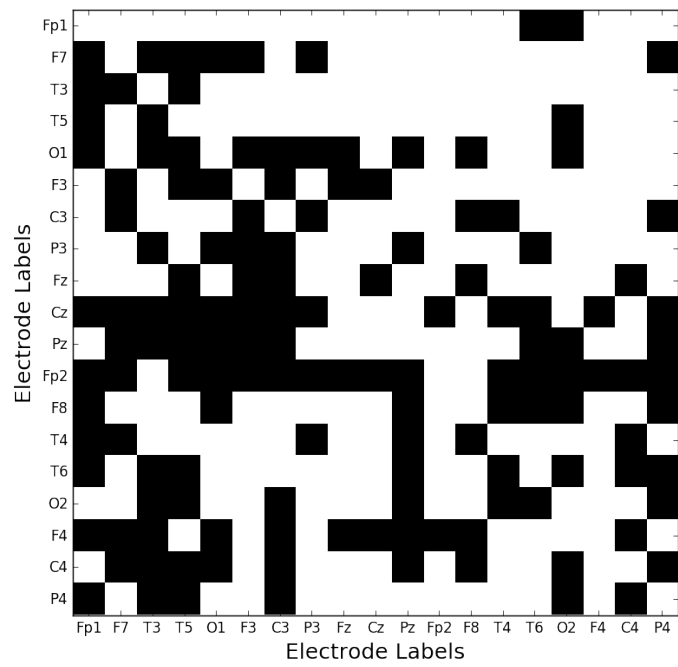


Figure 5.8: Sample of adjacency matrix obtained from interictal spike

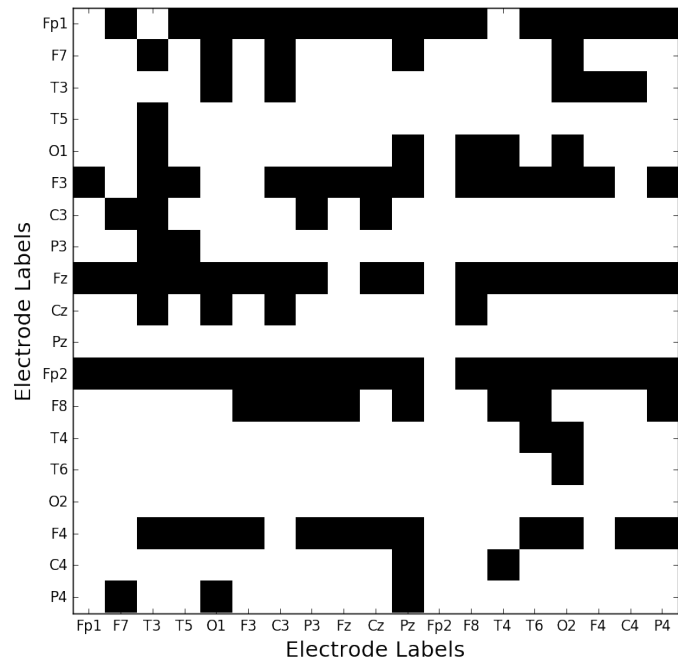


Figure 5.9: Sample of adjacency matrix obtained from spike and slow wave complex

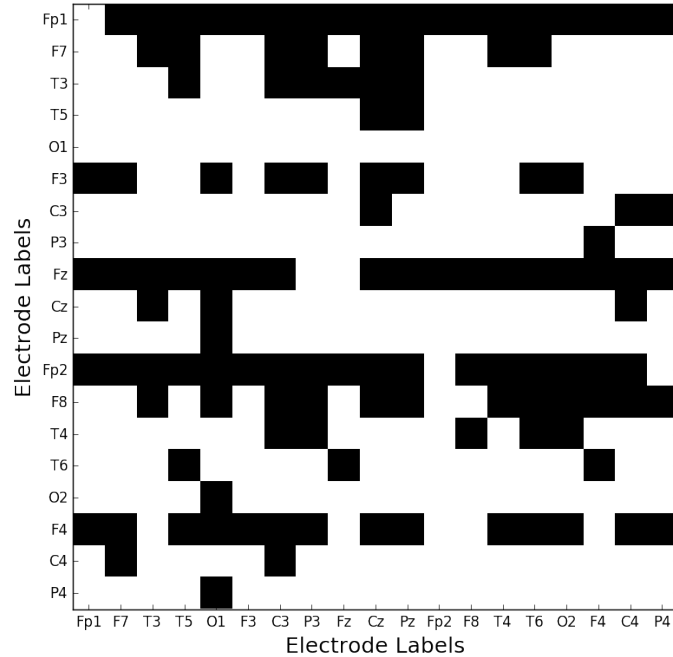


Figure 5.10: Sample of adjacency matrix obtained from repetitive spike and slow wave complex

To perform a classification task, neural network was implemented as a classifier. The obtained adjacency matrices were converted into binary vectors and used as the input, where the results of the classification are divided into two subcategories: 1) a fitted classifier that compares between two types of IEDs and 2) a classifier with all types of IEDs.

5.8.1 Classification between two types of IEDs

Results obtained from the MLP classifier trained to perform a binary classification are summarized in table 5.1. Five indicators were used to evaluate the performance of the classifier namely, F1 score, Accuracy, Sensitivity, Specificity, and Precision by utilizing the tenfold cross validation. Pairwise comparison between types of IEDs (IS vs. SSC, IS vs. RSS, and SSC vs. RSS) was performed. The classifier overall score of 100.00% across every indicator was obtained when classifying between IS

| Classification | F1 (%) | Accuracy (%) | Sensitivity (%) | Specificity (%) | Precision (%) |
|----------------|--------|--------------|-----------------|-----------------|---------------|
| IS vs. SSC | 96.67 | 95.00 | 100.00 | 90.00 | 95.00 |
| IS vs. RSS | 100.00 | 100.00 | 100.00 | 100.00 | 100.00 |
| SSC vs. RSS | 76.67 | 85.00 | 80.00 | 90.00 | 75.00 |
| Average | 91.11 | 93.33 | 93.33 | 93.33 | 90.00 |

Table 5.1: Performance results of binary classification based on neural network classifier with adjacency matrices

vs. RSS. The F1 scores drop when performed on IS vs. SSC with 96.67%, but still provided 100.00% sensitivity. The classifier on SSC vs. RSS performed an F1 score of 76.67%. Overall, the classifier provides a high performance with an average F1 score of 91.11% and 93.33% for all accuracy, sensitivity and specificity.

5.8.2 Classification between all types of IEDs

| Types of IEDs | F1 (%) | Accuracy (%) | Sensitivity (%) | Specificity (%) | Precision (%) |
|------------------|--------|--------------|-----------------|-----------------|---------------|
| IS | 90.00 | 96.67 | 90.00 | 100.00 | 90.00 |
| SSC | 86.67 | 86.67 | 100.00 | 80.00 | 80.00 |
| RSS | 70.00 | 90.00 | 70.00 | 100.00 | 70.00 |
| Overall Accuracy | | | 86.67 | | |

Table 5.2: Performance results of 3-types classification based on neural network classifier with adjacency matrices

Table 5.2 provides a summarization of the performance of the MLP classifier trained to classify between all types of IEDs. Same measurements were obtained to evaluate the performance of the classifier. The results of the classification for IS, SSC, and RSS are 90.00%, 86.67% and 70.00% for F1 scores respectively. The classifier had a drop in performance when used to detect RSS types, but still provides high scores of specificity at 100.00%. The overall accuracy of the classifier was

computed by dividing the total number of correct predictions by the number of data points. The classifier provides a high overall accuracy of 86.87%.

5.9 Discussion

The presented work focused on examining the patterns generated from the extraction of EEG data with the occurrence of IEDs by using PDC analysis. Similar approaches were performed in [36] and [50] by using cross-correlation analysis and a nonlinear analysis, where cross cross-correlation is prone to error induced by volume conduction and the nonlinear analysis is very dependent of the parameters selection. Both [36] and [50] utilized analysis of variance (ANOVA) to analyze the characteristics presented in each IED without implementing any classification algorithm. Our study evaluates the performance of classification by using feature extracted from PDC and by implementing multilayer perceptron neural network to perform IEDs classification. One of the limitations presented in the analysis was the effect of the background activity of the selected segments, where preprocessing had to be done manually to minimize the effect from the artifacts.

5.10 Conclusion

The extraction of propagation information from neural activities by using PDC can generate important features that can be used to distinguish between types of IEDs (interictal spike, spike and slow wave complex, and repetitive spikes and slow wave complex). These features can help characterized the type of epilepsy (focal or generalized) and can provide the information flow between multivariate systems (19 EEG electrodes). By applying surrogate data testing, the significant propagations can be evaluated and transformed into a adjacency matrix. Classification results are promising when implementing a machine learning algorithm (neural network

classifier) that uses features extracted from PDC. Whether the seizure event will be focal or generalized, these distinct features can help to enhanced diagnosis of the disorder.

CHAPTER 6
PARTIAL DIRECTED COHERENCE WITH CONCEPT OF
INFORMATION FLOW

6.1 Introduction

This chapter introduces an approach for the quantification of information flow using brain connectivity analysis and partial directed coherence (PDC). The main objective is to assess the key characteristics that delineate normal controls from patients with epilepsy considering both focal and generalized seizures. The PDC is used here as a feature extraction method for scalp EEG recordings as means to reflect the physiological changes of brain activity during interictal periods. The intensity (or strength) of information flow, including inflow (activity deemed significantly flowing from other regions into a specific region) and outflow (activity emanating from one region and spreading into other regions), were calculated based on the PDC results and are quantified with respect to the defined regions of interest. Three groups were considered for this study, the control population, patients with focalized epilepsy, and patients with generalized epilepsy. A significant difference in inflow and outflow validated by the nonparametric Kruskal-Wallis test was observed for these groups. It is observed that during the interictal phase, with the results obtained, it becomes possible to delineate the distinctive patterns that can be used to classify the two types of epilepsy, focal and generalized. The differences were further examined by applying multiple comparison post-hoc analyses using the same level of significance at 0.05 with multiple comparison corrections.

As mentioned in section 2.3, epilepsy is characterized by the recurrent unprovoked interruption of brain functions, called epileptic seizures. During epileptic seizures, groups of neurons in the cerebral cortex are being excessively triggered

simultaneously resulting in symptoms such as muscle stiffness, muscle spasms and impaired consciousness [20]. Although the symptoms of epileptic seizures are general, the location, duration and propagation of the seizures differ depending on the individual. By enhancing epilepsy diagnosis or predicting the occurrence of seizures through EEG recordings, early intervention and therapeutic protocols could be planned more effectively.

Scalp EEG recording is a noninvasive and highly effective method that is widely used to study and analyze epileptic seizures with high temporal resolution. It is one of the prevalent modalities to examine brain activities[70]. Obtaining EEG recordings is considered a simple procedure and inexpensive compared to other neuroimaging modalities such as MRI, fMRI and PET imaging. Although a multimodal imaging platform is often desired to consolidate temporal and spatial resolutions and to be to validate the onset of a 3D source, EEG on its own captures the electrical activity produced by the neurons in the brain with a high temporal resolution, which makes it a highly suitable tool for identifying such things as synchronization between pairs of signals [1]. A substantial amount of epilepsy diagnosis is performed by visualizing EEG during seizures and long interictal recordings. Extracting epileptic biomarkers of EEG in interictal periods plays a key role for the diagnosis of epilepsy and the planning of clinical treatment. However, the diagnosis from EEG recordings relies heavily on the visual inspection of experienced experts, and the outcome may vary depending on their subjective judgments. Hence, extracting subtle or hidden patterns of EEG in the interictal phase could elicit new findings and new understanding on the complex process of epilepsy diagnosis.

The analysis of EEG signals with the purpose of helping patients suffering from neurological disorders have been one of the most prominent research fields [59]. Several techniques of computational analysis have been performed to enhance the de-

tection of neurological disorders [76, 62, 33]. However, the characteristics of epilepsy still require extensive exploration and investigation in order to improve our understanding of the disease and the myriad of brain activity patterns that characterize the varied manifestations of this neurological disorder [59]. The majority of epilepsy diagnostics are based on the EEG, where epileptic patients will undergo the procedure of EEG recordings with the help of specialized technicians or doctors [34]. One of the key features that can be analyzed by utilizing EEG recordings is to observe the synchronization of neural activities and resulting brain connectivity patterns. The patterns extracted from brain connectivity of scalp EEG recordings can provide important information of lateralization and localization of the epileptogenic foci [51] and could also serve as key features for classifying the different types of epilepsy, namely partial and these could be simple or complex in nature, and generalized where the seizure activity involves the entire brain [56].

Many studies have shown that effective EEG signal analysis can provide key information for effectual diagnosis and classification of epilepsy [63, 38, 73, 35]. To extract underlying features of the interictal period, the propagation of EEG is introduced in several studies where the results seem promising [76, 71]. The concept of extracting brain connectivity information from EEG recordings is not new but it is still relevant as more definite answers are sought [66]. Several connectivity extraction methods are continuously reported and developed [63]. Quantification and assessment of interactions between brain regions can be used to delineate their characteristics and related interactions [42, 66].

Thus, effective connectivity maps on the basis of inflow and outflow information between brain regions will be examined and are the main focus of this study. Effective connectivity refers to the reliable assessment of the intensity measure and direction of information flow between the different neural regions using EEG data.

The aim here is to combine the use of the partial directed coherence (PDC) on the basis of a multivariate autoregressive model (MVAR) model that is designed to extract the needed features that define the propagation flow of interictal EEG activity [7]. Unlike conventional methods, such as correlation or coherence, the utilization of an MVAR model allows us to examine the multichannel interaction instead of limiting the analysis into the pairwise channels, resulting in painting a more cohesive and generalized picture of brain activities, providing as a consequence better and more precise results [41].

To the best of our knowledge, this is the first experimental study that incorporates information flow to extract propagation during interictal periods in epilepsy. This study proposes an analysis of the propagation patterns extracted from randomly selected EEG data segments, and through the use of the PDC methodology combined with the intensity of information flow. Both the inflow and outflow patterns are scrutinized for the different regions of interests..

The flowchart describing the overall structure of the intensity of information flow analysis during a given interictal period is as illustrated in figure 6.1. After the extraction of the partial directed coherence, the intensity of information flow with inflow and outflow directions were quantified by the predefined regions of interest. Statistical analysis was applied to quantify the differences among the 3 groups considered.

6.2 Data Acquisition

With the approval of the Institutional Review Board of Florida International University (protocol number: IRB-150247), 22 subjects (14 epilepsy patients and 8 healthy normal controls) were considered in this study. Of the 14 patients with epilepsy, 8

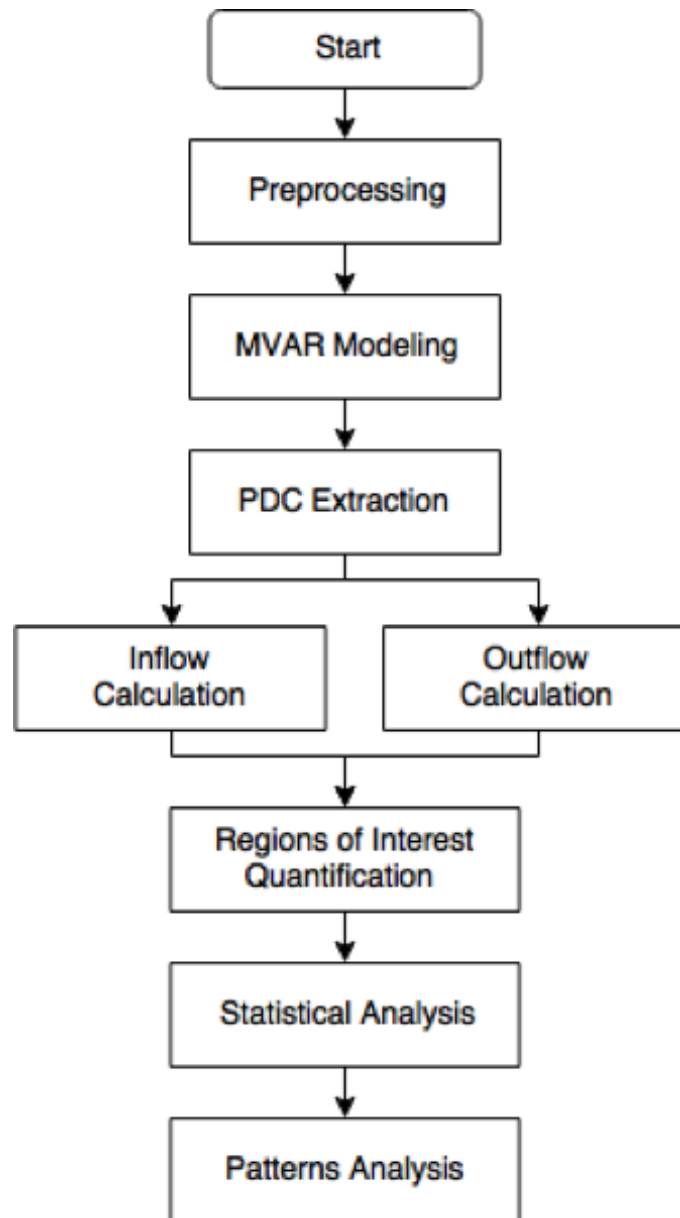


Figure 6.1: Diagram outlining the PDC-based inflow and outflow method of the study

have focal epilepsy and the other 6 patients have generalized epilepsy. The diagnosis of the patients were provided by an expert in the field.

The scalp EEG of all patients were recorded at Baptist Hospital of Miami by using standard international 10-20 electrode placement protocol with 19 electrodes (Fp1, F7, T3, T5, O1, F3, C3, P3, Fz, Cz, Pz, Fp2, F8, T4, T6, O2, F4, C4, and P4). The record of the EEG was done by using a referential montage. During the recording, all patients were asked to relax and minimize any body movement. The EEG signals were digitized by using a sampling frequency of 200 Hz. Interictal and ictal events were both included in all epileptic recordings, but only interictal periods were considered in this study. Table 6.1 summarizes the information of all 22 subjects.

6.3 Preprocessing and Segmentation

To reduce the effect of noise and hence maximize the brain-related activities, the obtained EEG data were inspected by a qualified doctor and only a cleaned portion of EEG data. The EEG data included in this study were cleaned of interictal epileptiform discharge and artifacts such as eye blinks and muscle movements.

In this study, the EEG data was segmented into 3-second windows with 600 data points for each segment. The segments duration ensured that the MVAR model captured important brain-related activities because it was properly fitted [41]. The 3-second non-overlapping windows were randomly selected from the interictal EEG data of epileptic groups and normal EEG data from the control population. Afterwards, the segmented data were normalized by removing the mean waveform across the segment. The total number of segments extracted from different groups are summarized in 6.2.

| Patient | Gender | Condition | Epilepsy Type | Focal Location |
|---------|--------|-----------|---------------|------------------------|
| Pat 1 | M | Normal | - | - |
| Pat 2 | F | Normal | - | - |
| Pat 16 | F | Epileptic | Focal | Right T |
| Pat 17 | M | Epileptic | Generalized | - |
| Pat 19 | M | Normal | - | - |
| Pat 21 | F | Normal | - | - |
| Pat 22 | M | Epileptic | Generalized | - |
| Pat 23 | F | Normal | - | - |
| Pat 25 | F | Epileptic | Focal | Bilateral R-Prominence |
| Pat 26 | M | Epileptic | Focal | Bilateral R-Prominence |
| Pat 27 | F | Normal | - | - |
| Pat 28 | F | Normal | - | - |
| Pat 32 | F | Epileptic | Generalized | - |
| Pat 35 | F | Epileptic | Focal | LFT |
| Pat 36 | F | Epileptic | Focal | LT |
| Pat 40 | F | Epileptic | Focal | RCT |
| Pat 42 | F | Epileptic | Focal | LT |
| Pat 44 | M | Epileptic | Generalized | - |
| Pat 46 | F | Epileptic | Generalized | - |
| Pat 47 | F | Epileptic | Focal | LA/FC |
| Pat 48 | M | Epileptic | Generalized | - |
| Pat 49 | F | Normal | - | - |

Table 6.1: Patients information

| | Control Population | Focal Epilepsy | Generalized Epilepsy | To- tal |
|-----------------------|-----------------------|-------------------|-------------------------|------------|
| Number of Segments | 105 | 118 | 145 | 368 |

Table 6.2: Total number of EEG segmentations per group.

6.4 Connectivity Extraction

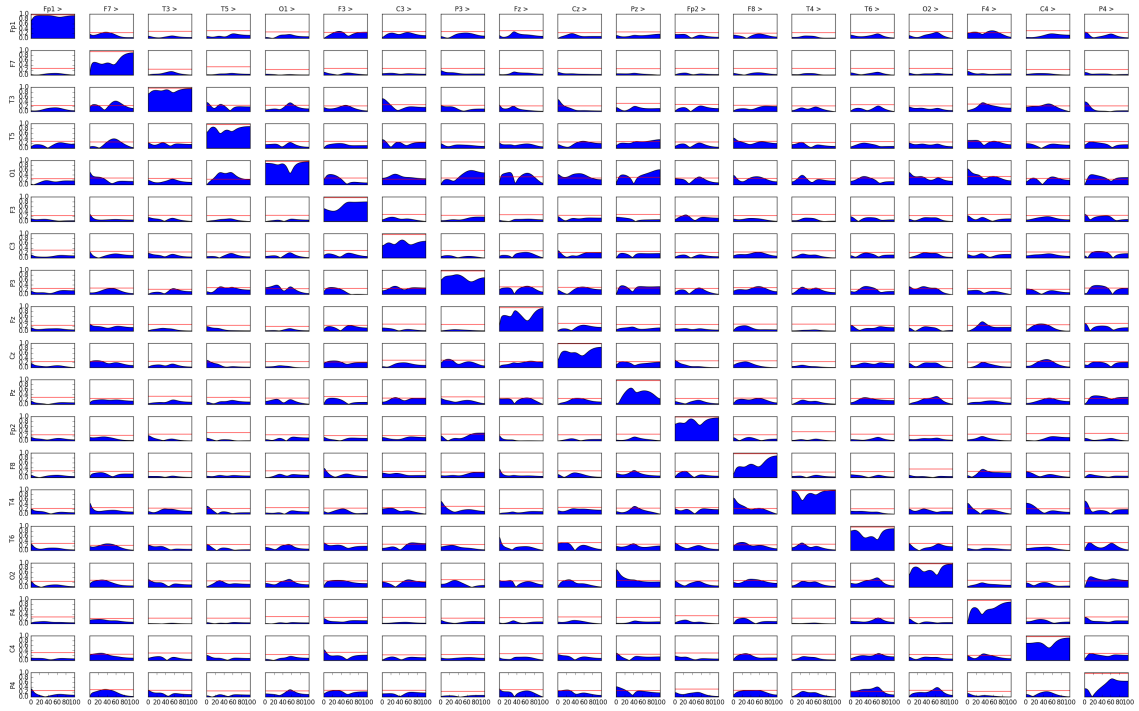
The Partial Directed Coherence (PDC) method based on an estimation of coefficients of a multivariate auto-regressive model (MVAR) provides a directed network, which reflects the inter-dependence and information flow between EEG channels. By using the PDC concept explained in chapter 4, the effective connectivity values of the preprocessed EEG segments were extracted. The value of $\pi_{ij}(f)$ ranging from 0 to 1 represents the intensity and direction of information flow from channel j to channel i at frequency f . The same concept of connectivity extraction from chapter 5 was applied to this experiment. However, instead of applying surrogate data analysis, concept of intensity of information flow was used to analyze the PDC values.

Figures 6.2, 6.3, and 6.4 are the samples of PDC values extracted from the EEG segments of control population, focal epilepsy group, and generalized epilepsy group respectively.

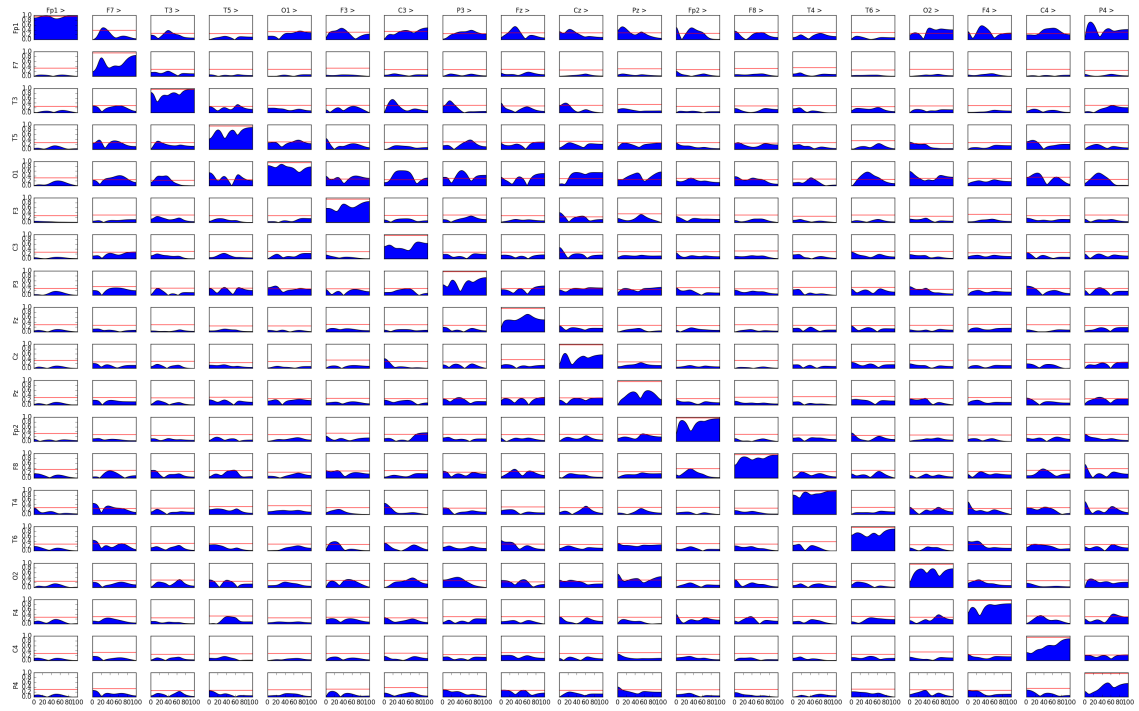
After the data from the PDC extraction were obtained, the concept of intensity of information flow introduced in section 4.4 was applied to the data. The values of inflow and outflow were computed and tabulated to be further quantified and analyzed.

6.5 Quantification of Information Flow by Cortex Regions

In this study, the brain cortex was divided into four different regions of interest. Figure 6.5 illustrates the specified regions that were included in the quantification

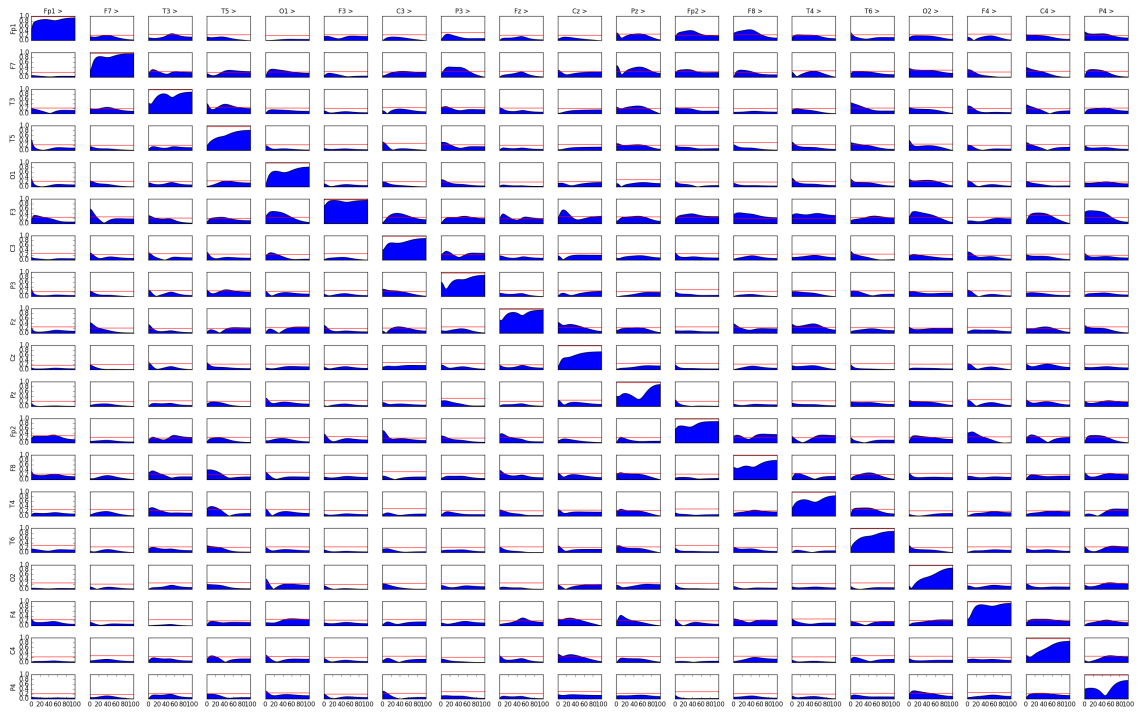


(a)

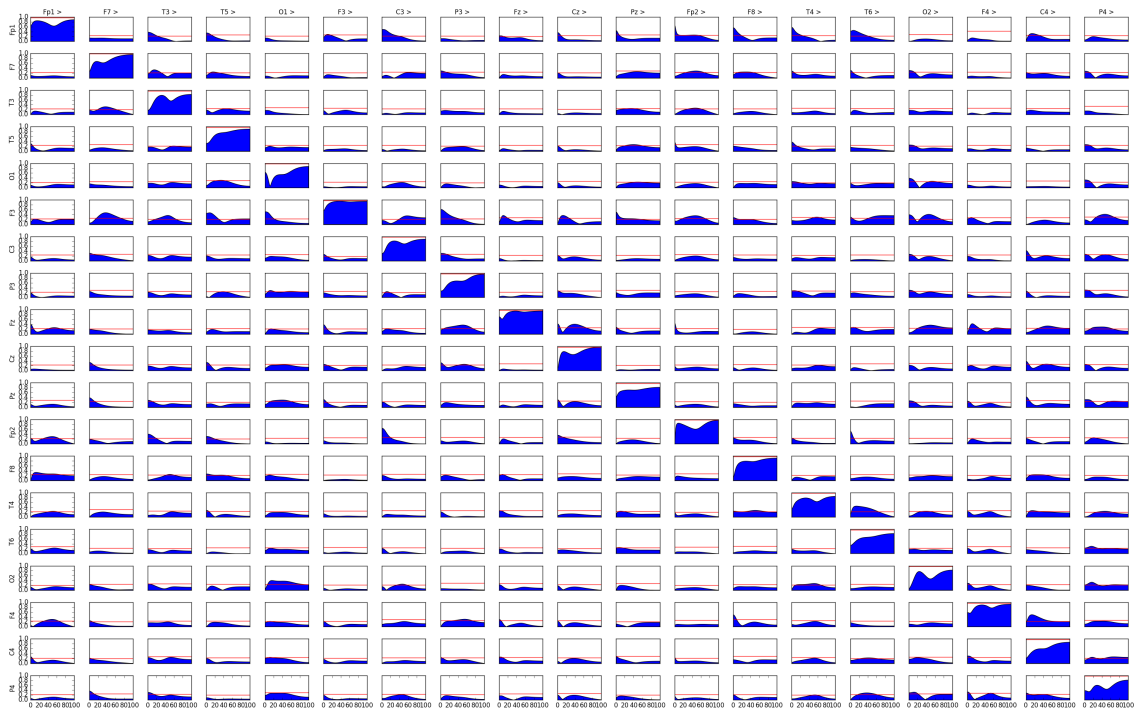


(b)

Figure 6.2: Random samples of PDC values extracted from the EEG segments of control population

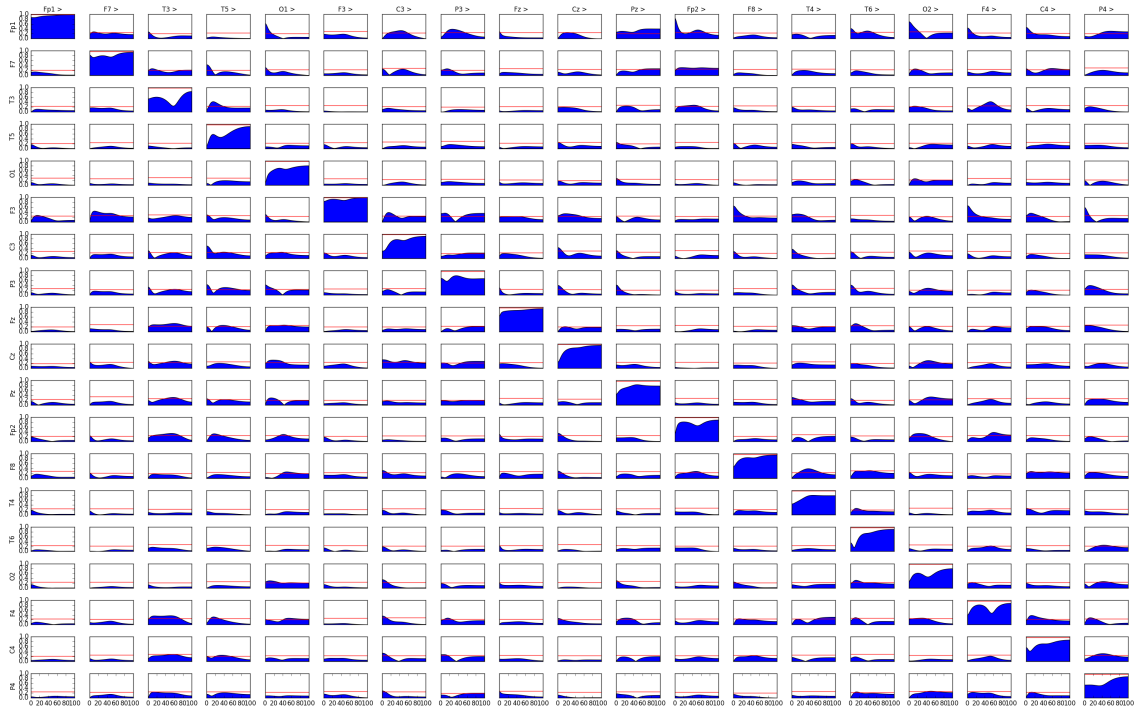


(a)

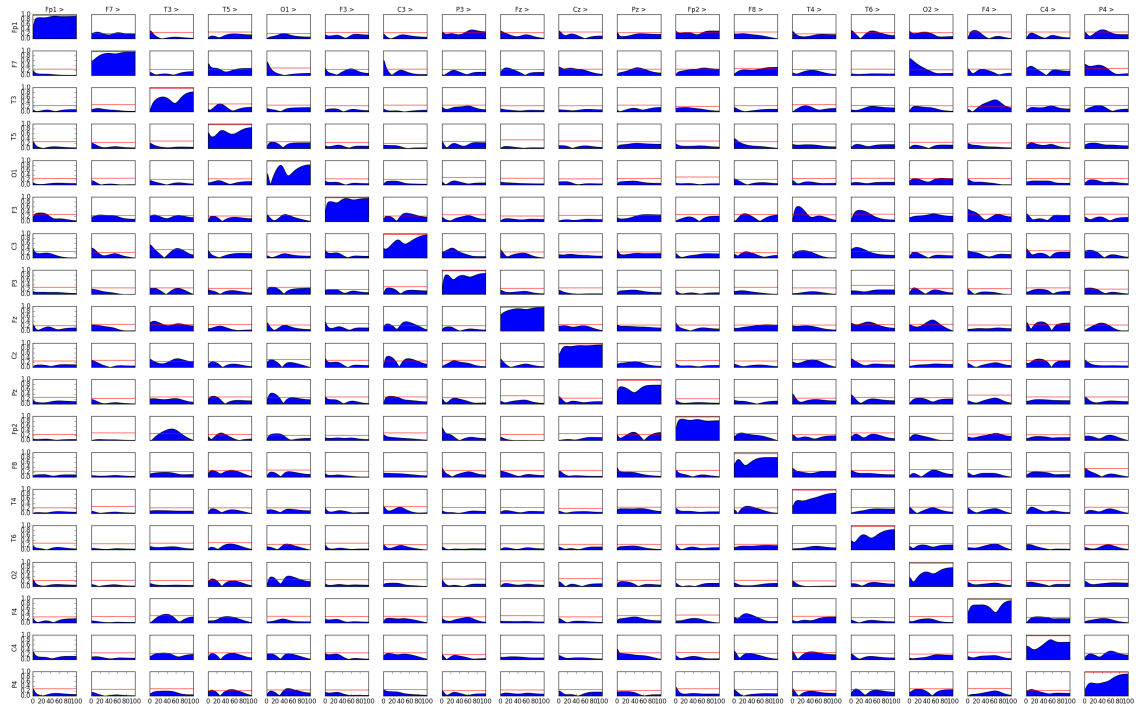


(b)

Figure 6.3: Random samples of PDC values extracted from the EEG segments of focal epilepsy group



(a)



(b)

Figure 6.4: Random samples of PDC values extracted from the EEG segments of generalized epilepsy group

process. The subdivision of the first and second region was done by dividing the cortex based on the left and right hemispheres (LR region). The activities on the left hemispheric region included Fp1, F7, T3, T5, O1, F3, C3, and P3 electrodes and the right hemispheric region contained Fp2, F8, T4, T6, O2, F4, C4, and P4 electrodes. The LR region was separated by the central line, which is a longitudinal fissure that contains Fz, Cz, and Pz electrodes. The subdivision of the third and fourth regions was done based on the anterior-posterior regions (AP region), where the anterior region contained Fp1, Fp2, F7, F3, Fz, F4, and F8 electrodes and the posterior region contained T5, P3, Pz, P4, T6, O1, and O2 electrodes. These regions were separated by the electrodes located along the central sulcus line, which contains T3, C3, Cz, C4, and T4 electrodes.

For each of these regions, the mean value of inflow and outflow was calculated for every 3-second window segment of EEG data. Statistical evaluations were performed to analyze the characteristics of the features for each group of patients.

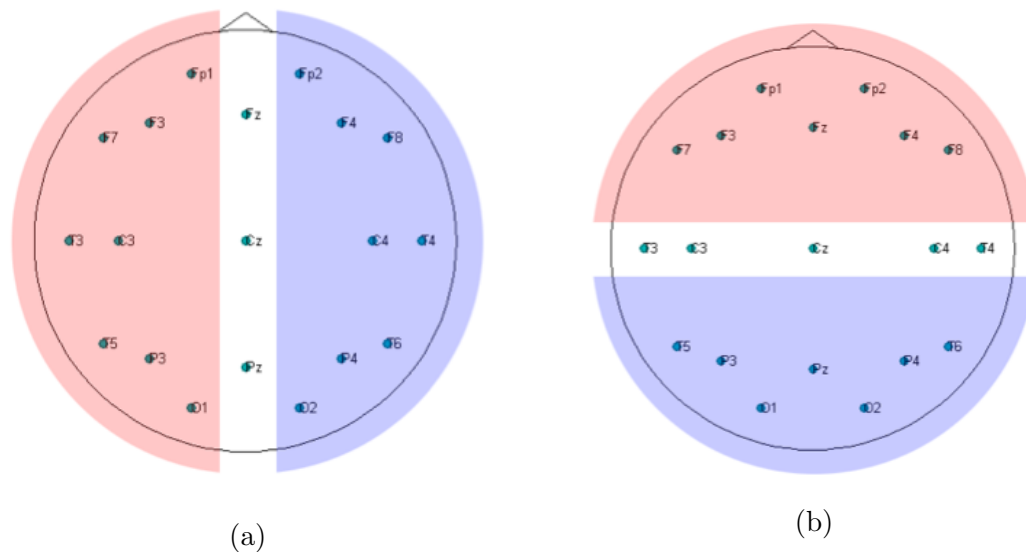


Figure 6.5: Regions of interest, group (a) left-right hemisphere (Left - red, Right - Blue), and (b) anterior-posterior region (Anterior - red, Posterior - blue)

6.6 Exploratory Statistical Analysis

We applied a nonparametric Kruskal-Wallis test to identify the possible differences between the intensity of information flow of control population and epilepsy patients [39]. The multiple comparison post-hoc analysis Conover-Iman [15], with Holm multiple comparison corrections was applied to further investigate the obtained differences.

6.7 Results

Once the data were preprocessed, three-second window segments of EEG were randomly selected from the interictal data and sorted according to their diagnosis. The effective connectivity of every segment was calculated by utilizing PDC method and the model selection of MVAR was performed individually to obtain the optimized model order. The PDC values within the frequency range of [0.5 - 30] Hz were included in this study, where the frequency above 30 Hz was found to have a minimal relationship to epilepsy during the interictal periods [2].

The calculated PDC values of the 368 segments of EEG were averaged according to the groups as shown in figure 6.6. The nodes on the outer layer of the circular connectivity plot are labeled with the 19 channels used in the EEG recordings. The Edges connected to the nodes represent the connection between a particular pair of channels, where the values of the PDC between two channels are represented by color codes. The darker color codes indicate connections with higher PDC values and the lighter color codes indicate connections with lower PDC values. The patterns from Fig. 6.6a show an average connectivity obtained from a control population group. The connections from this group exhibited stronger connections across the cortex, especially between channels T3 - T5, which are not observed in the other two groups.

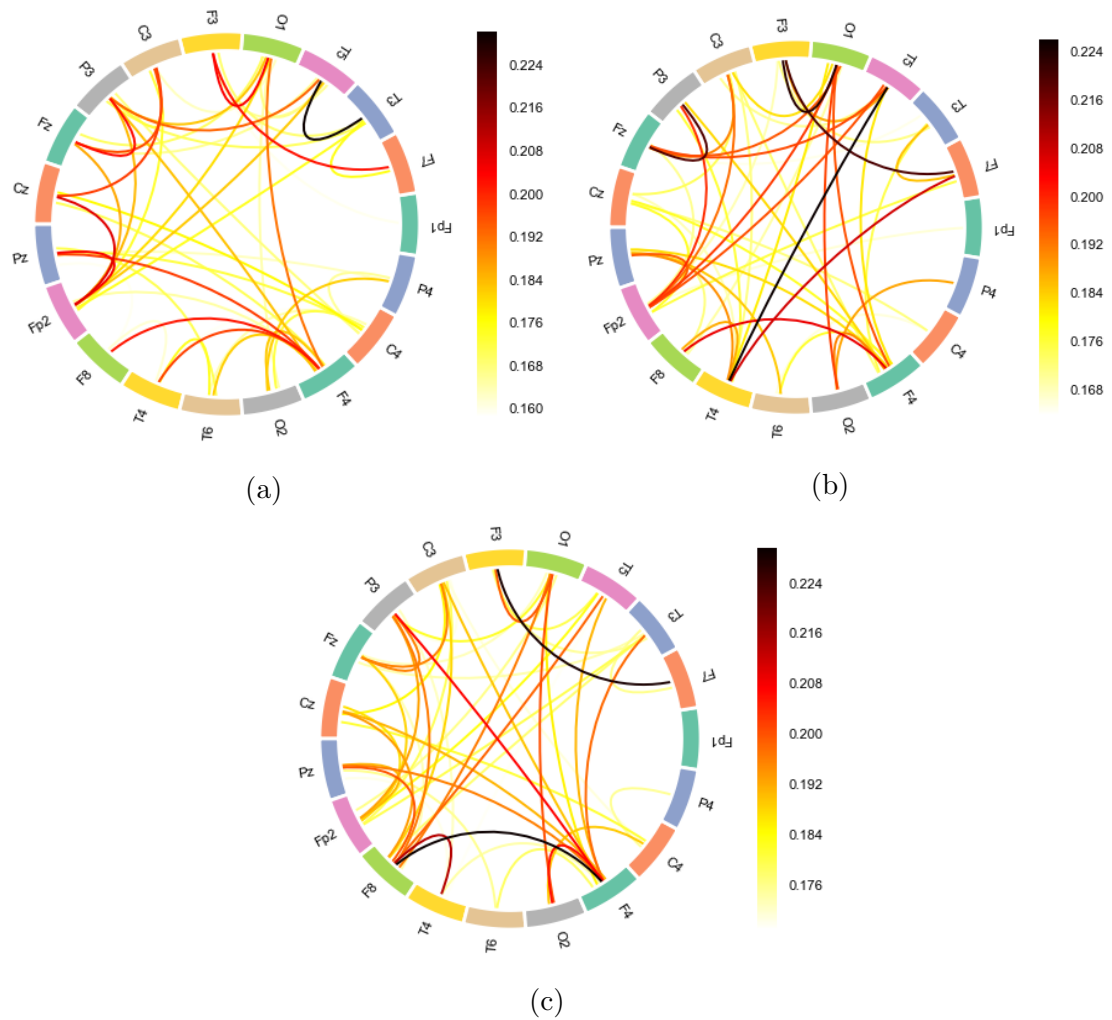


Figure 6.6: Average circular connectivity of (a) control population (b) focal epilepsy (c) generalized epilepsy group.

The connections obtained from the control population group displayed a distinctive pattern compared to the rest of the groups, where the stronger connections are more gathered in the regions between channels T3 T5, and there are fewer connections in channels F8 and T4. For the connections obtained from the epilepsy groups shown in Fig. 6.6b and 6.6c, the overall patterns exhibited a different pattern compared to the control population group, where multiple strong connections occurred across the cortex with less grouped patterns.

6.7.1 Information Inflow and Outflow

To be able to quantify and extract meaningful measurements, the intensity of information flow with inflow and outflow direction for every EEG segment was calculated and separated into the defined regions, which included the left hemisphere, right hemisphere, anterior region, and posterior region. The medians and standard deviations of the inflow and outflow were sorted according to the data groups and categorized into cortex regions as shown in figure 6.7 and figure 6.8. The inflow and outflow calculations can be used to visualize the information flow between different brain regions in the epileptic brain. The outflow patterns in particular are found to be related to the epileptogenic foci.

The summarized distributions of the intensity of information flow with the inflow direction are shown in figure 6.7. The values are separated by the defined regions and categorized by the types of data, which are denoted by color coding. By comparing the data visually, the inflow intensity medians of the control population are higher than the epilepsy group in Left, Anterior, and Posterior regions and lower in the Right region. On the contrary, the inflow intensity extracted from both focal and generalized groups display a similar pattern and behavior. To validate the results, the nonparametric Kruskal-Wallis test was applied with the null hypothesis

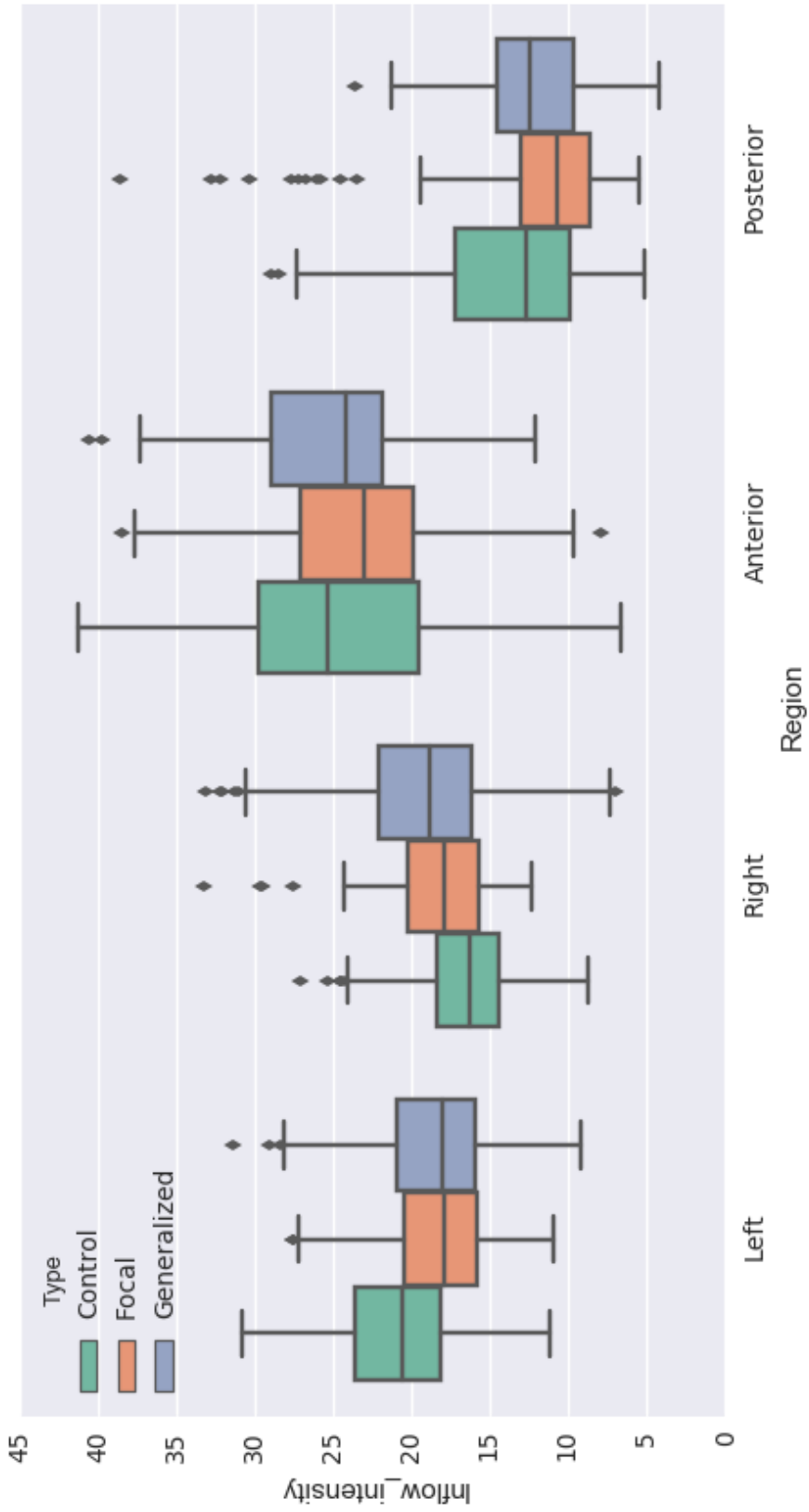


Figure 6.7: The medians and interquartile ranges of the intensity of information flow with inflow direction of the three groups with different regions.

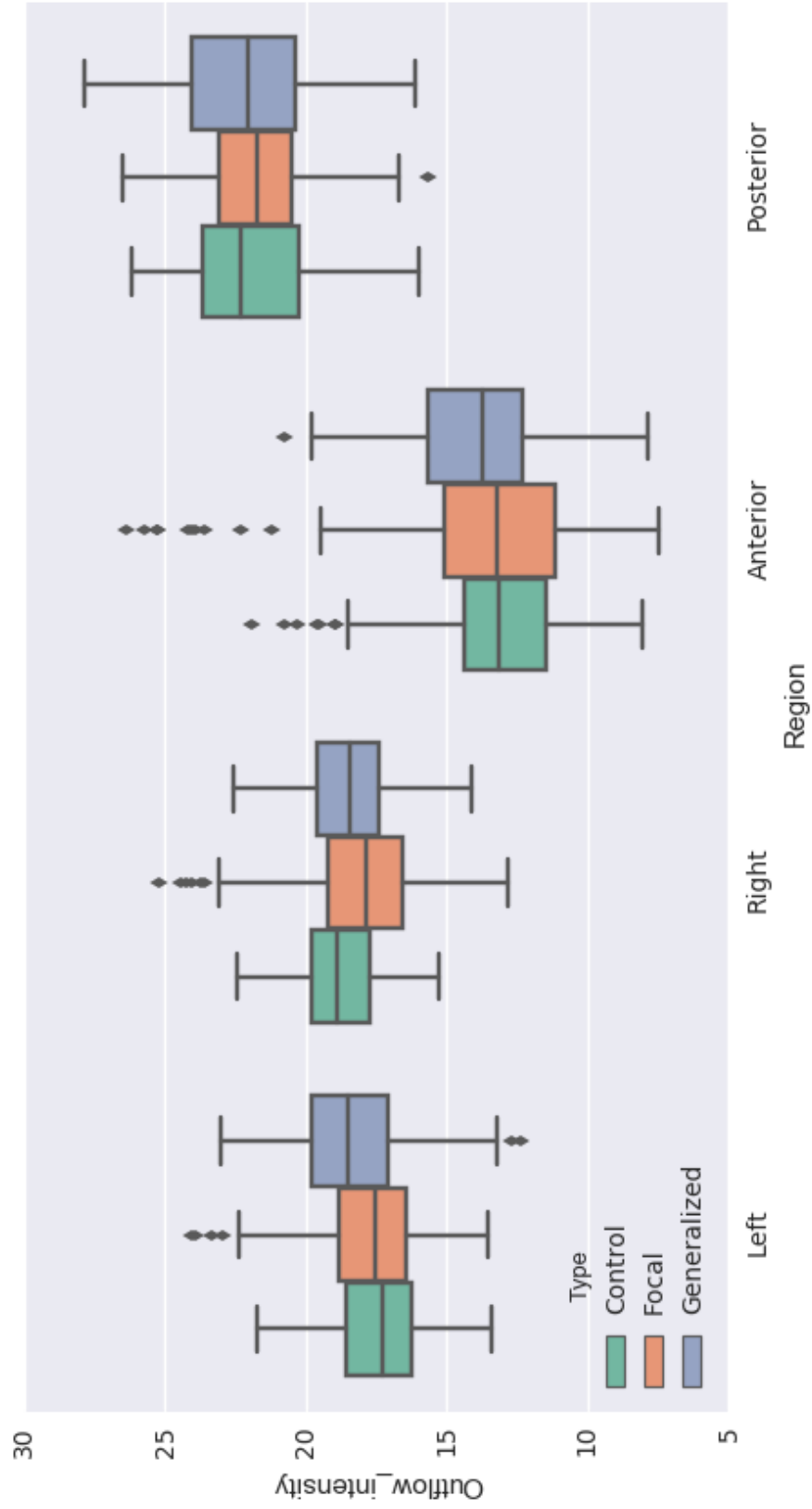


Figure 6.8: The medians and interquartile ranges of the intensity of information flow with outflow direction of the three groups with different regions.

indicating that the distribution of differences in intensity flow between the three groups are identical. The statistical analysis results per region are summarized and displayed in table 6.3 and table 6.4 for both inflow and outflow direction.

The asterisk (*) denotes the region with the significant differences with the rejection of the null hypothesis.

| | Test-Statistics | p-value | Significance Level of 0.05 |
|------------------|-----------------|---------|----------------------------|
| Left Hemisphere | 25.744 | <0.00 | * |
| Right Hemisphere | 31.392 | <0.00 | * |
| Anterior Region | 10.844 | 0.004 | * |
| Posterior Region | 8.591 | 0.013 | * |

Table 6.3: Kruskal-Wallis test of intensity of information flow with inflow direction.

| | Test-Statistics | p-value | Significance Level of 0.05 |
|------------------|-----------------|---------|----------------------------|
| Left Hemisphere | 15.800 | 0.0003 | * |
| Right Hemisphere | 14.640 | 0.0001 | * |
| Anterior Region | 4.003 | 0.135 | |
| Posterior Region | 3.294 | 0.192 | |

Table 6.4: Kruskal-Wallis test of intensity of information flow with outflow direction.

6.7.2 Statistical Differences in Information Inflow and Outflow Directions

From the statistical analysis viewpoint, the null hypothesis of all regions was rejected at the significance level of 0.05. Accordingly, the differences found between the groups are significantly different in every region.

The differences were further examined by applying Conover-Iman multiple comparison post-hoc analysis. The same level of significance at 0.05 with Holm multiple comparison corrections was applied as well. From the post-hoc analysis with the null hypothesis, the differences between the inflow intensity obtained from control population compare to both types of epilepsy (focal and generalized) of Left, Right,

and Posterior regions, were rejected with a $p - value < 0.05$. Thus, the observation was statistically significant. However, the differences of intensity flow between focal and generalized groups were not statistically significant in the Anterior and Posterior regions ($p - value > 0.05$). The results from the multiple comparison analysis are summarized as shown from table 6.5 to table 6.8.

| Group 1 | Group 2 | p-value | Reject H_0 |
|---------|-------------|----------|--------------|
| Control | Focal | 8.289e-5 | True |
| Control | Generalized | 1.727e-6 | True |
| Focal | Generalized | 3.325e-1 | True |

Table 6.5: Multiple comparison of inflow means within the right hemisphere using Conover-Iman test with level of significance = 0.05

| Group 1 | Group 2 | p-value | Reject H_0 |
|---------|-------------|----------|--------------|
| Control | Focal | 5.58e-7 | True |
| Control | Generalized | 7.656e-6 | True |
| Focal | Generalized | 3.325e-1 | True |

Table 6.6: Multiple comparison of inflow means within the left hemisphere using Conover-Iman test with level of significance = 0.05

| Group 1 | Group 2 | p-value | Reject H_0 |
|---------|-------------|----------|--------------|
| Control | Focal | 0.004 | True |
| Control | Generalized | 0.933 | False |
| Focal | Generalized | 4.890e-1 | True |

Table 6.7: Multiple comparison of inflow means within the anterior region using Conover-Iman test with level of significance = 0.05

| Group 1 | Group 2 | p-value | Reject H_0 |
|---------|-------------|---------|--------------|
| Control | Focal | 0.061 | False |
| Control | Generalized | 0.263 | False |
| Focal | Generalized | 0.328 | False |

Table 6.8: Multiple comparison of inflow means within the posterior region using Conover-Iman test with level of significance = 0.05

Same method of analysis was applied to the intensity of information flow with the outflow direction. Figure 6.8 summarizes the medians and standard deviations of the outflow intensity by the defined regions and the data groups. The patterns extracted from the control population, focal and generalized epilepsy groups show a similar trend. The differences of outflow intensity between all the groups seem to be minimal and do not show a significant pattern. By applying Kruskal-Wallis test to the results, only two regions showed significant differences in the outflow intensity. The null hypothesis was rejected for the left hemisphere with a $p - value < 0.05$ and right hemisphere with a $p - value < 0.05$. Thus, the differences found in these regions are significantly different. However, the null hypothesis of anterior and posterior regions was accepted showing no significant difference.

Same multiple comparison post-hoc analysis with the level of significance at 0.05 was applied to the significant regions, left and right hemispheres. In the left hemisphere, the difference between outflow intensity obtained from control population as compared to focal epilepsy group was significant, whereas, the difference found between control population and generalized epilepsy group was found not to be significant. Opposite statistical results were found in the Right region, where the outflow intensity obtained from the control population as compared to the focal epilepsy group was found to be not significant, whereas the difference between the control population and the generalized epilepsy groups was found to be significant. The results from the multiple comparison analysis are summarized as shown from table 6.9 to table 6.12.

6.7.3 Focal Epilepsy and Control Population

To further examine the difference between focal epilepsy group and control population, patients in the focal epilepsy group were divided into two groups according to

| Group 1 | Group 2 | p-value | Reject H_0 |
|---------|-------------|----------|--------------|
| Control | Focal | 7.962e-4 | True |
| Control | Generalized | 0.001 | True |
| Focal | Generalized | 4.378e-2 | True |

Table 6.9: Multiple comparison of outflow means within the right hemisphere using Conover-Iman test with level of significance = 0.05

| Group 1 | Group 2 | p-value | Reject H_0 |
|---------|-------------|----------|--------------|
| Control | Focal | 0.009 | True |
| Control | Generalized | 2.798e-4 | True |
| Focal | Generalized | 0.011 | True |

Table 6.10: Multiple comparison of outflow means within the left hemisphere using Conover-Iman test with level of significance = 0.05

| Group 1 | Group 2 | p-value | Reject H_0 |
|---------|-------------|---------|--------------|
| Control | Focal | 0.486 | False |
| Control | Generalized | 0.149 | False |
| Focal | Generalized | 0.534 | False |

Table 6.11: Multiple comparison of outflow means within the anterior region using Conover-Iman test with level of significance = 0.05

| Group 1 | Group 2 | p-value | Reject H_0 |
|---------|-------------|---------|--------------|
| Control | Focal | 0.405 | False |
| Control | Generalized | 0.738 | False |
| Focal | Generalized | 0.261 | False |

Table 6.12: Multiple comparison of outflow means within the posterior region using Conover-Iman test with level of significance = 0.05

their epileptic focus location. As shown in table 6.13, four patients, Pat 16, Pat 25, Pat 26, and Pat40 were considered to be in the *focal right group* and patients, Pat 35, Pat 36, Pat 42, and Pat 47, were in the *focal left group*. The same concept of information flow was applied to find the difference of the patterns extracted between these groups and the control population.

| Patient | Group | Condition | Epilepsy Type | Focal Location |
|---------|-------|-----------|---------------|------------------------|
| Pat 16 | Right | Epileptic | Focal | Right T |
| Pat 25 | Right | Epileptic | Focal | Bilateral R-Prominence |
| Pat 26 | Right | Epileptic | Focal | Bilateral R-Prominence |
| Pat 35 | Left | Epileptic | Focal | LFT |
| Pat 36 | Left | Epileptic | Focal | LT |
| Pat 40 | Right | Epileptic | Focal | RCT |
| Pat 42 | Left | Epileptic | Focal | LT |
| Pat 47 | Left | Epileptic | Focal | LA/FC |

Table 6.13: Focal epilepsy patients information

The summarized distributions of the intensity of information flow between the focal left group and control population are shown in Figure 6.9 and Figure 6.10. The results as shown in Figure 6.9 provide the medians and interquartile ranges of inflow direction in each of the defined regions and Figure 6.10 shows the outflow direction. To validate the results, the nonparametric Kruskal-Wallis test was applied with the null hypothesis stating that the distribution of differences in intensity flow between the two groups are identical. The statistical analysis results per region are summarized and displayed in table 6.14 and table 6.15 for both inflow and outflow direction respectively.

From the statistical analysis viewpoint, the null hypotheses for the left hemisphere, right hemisphere, and anterior region were rejected at the $p - value$ of 0.05. The inflow values in the left hemisphere appeared to be significantly lower compared to the control population, while the inflow values were higher in the right hemisphere. From the summarized statistics of outflow values shown in table 6.15,

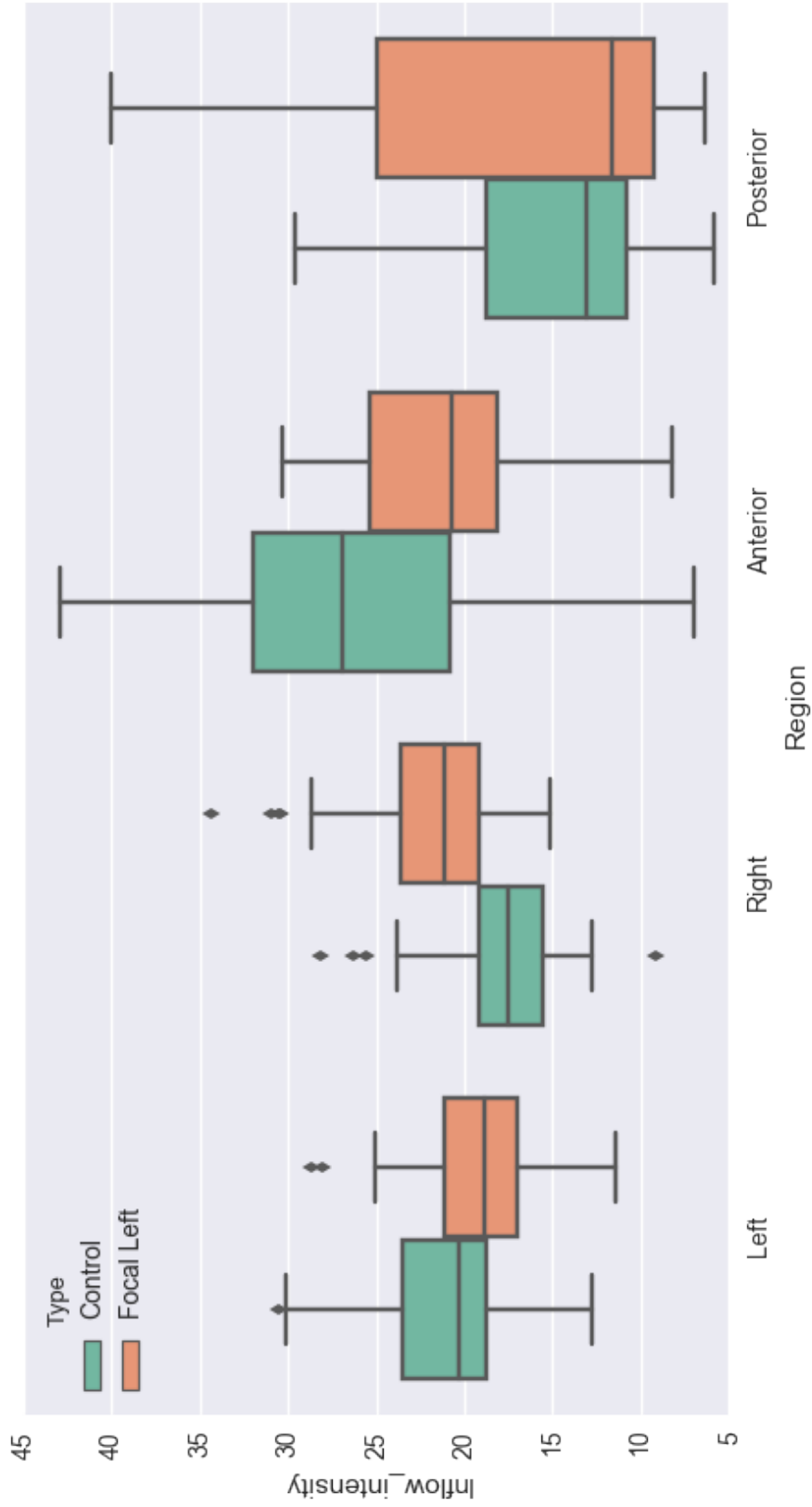


Figure 6.9: The medians and interquartile ranges of the intensity of information flow with inflow direction of the focal left group and control population with different regions.

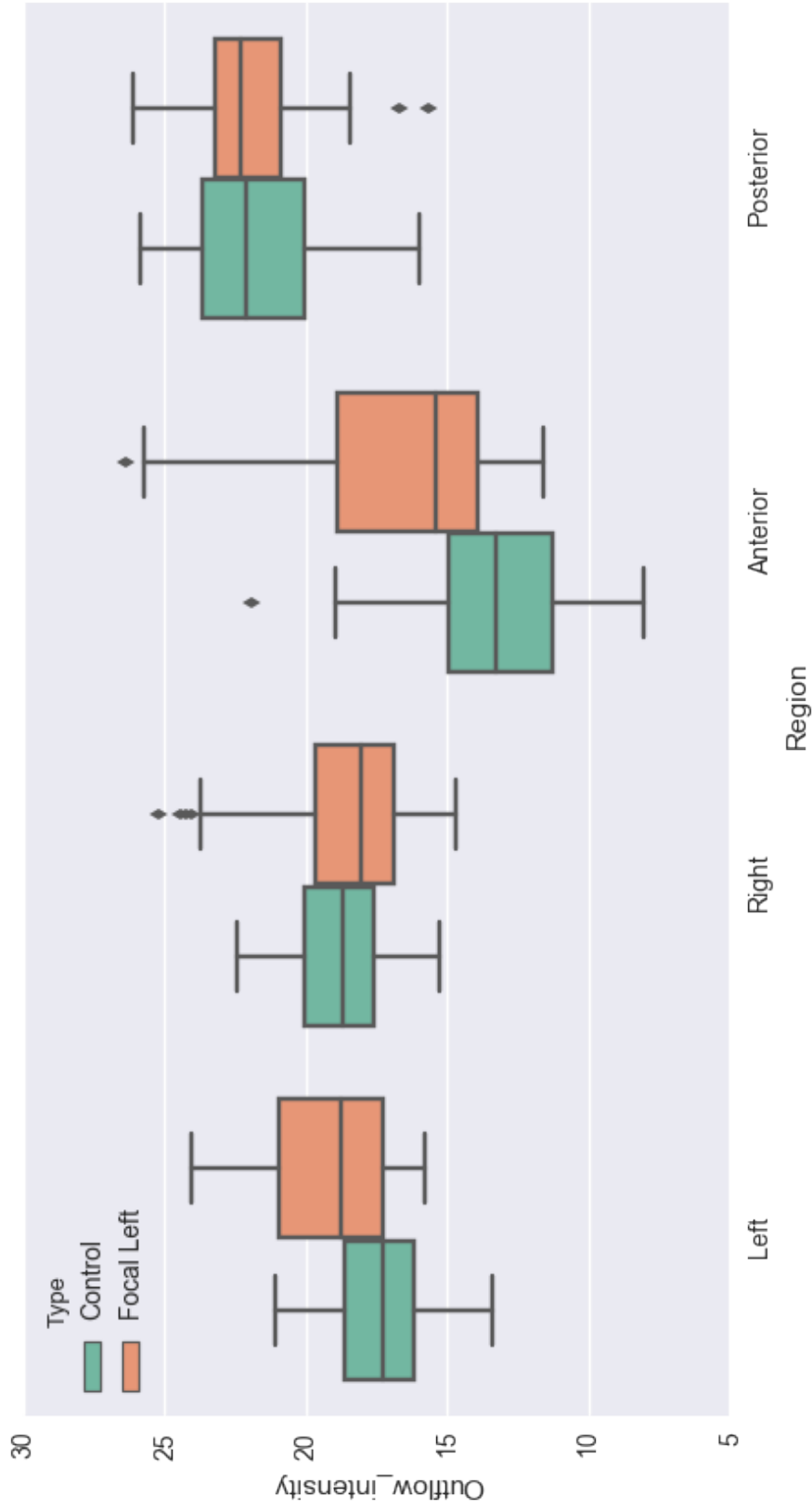


Figure 6.10: The medians and interquartile ranges of the intensity of information flow with outflow direction of the focal left group and control population with different regions.

| | Test-Statistics | p-value | Significance Level of 0.05 |
|------------------|-----------------|---------|----------------------------|
| Left Hemisphere | 6.3795 | 0.0115 | * |
| Right Hemisphere | 28.4675 | 9.5e-8 | * |
| Anterior Region | 14.2070 | 0.0001 | * |
| Posterior Region | 0.1878 | 0.6647 | |

Table 6.14: Kruskal-Wallis test of intensity of information flow with inflow direction between focal left group and control population.

| | Test-Statistics | p-value | Significance Level of 0.05 |
|------------------|-----------------|---------|----------------------------|
| Left Hemisphere | 13.187 | 0.00002 | * |
| Right Hemisphere | 1.7469 | 0.1862 | |
| Anterior Region | 20.056 | 7.5e-6 | * |
| Posterior Region | 0.0871 | 0.767 | |

Table 6.15: Kruskal-Wallis test of intensity of information flow with outflow direction between focal left group and control population.

the null hypotheses for left hemisphere and anterior region were rejected. The outflow values computed in the left hemisphere were found to be significantly higher than those of the control population.

The results of the inflow and outflow for the focal right group comparison are summarized as shown in figure 6.11 and figure 6.12. To validate the results, same Kruskal-Wallis test was applied to the results, where table 6.16 and table 6.17 show the statistical analyses of between the focal right group and the control population.

| | Test-Statistics | p-value | Significance Level of 0.05 |
|------------------|-----------------|---------|----------------------------|
| Left Hemisphere | 13.397 | 0.0002 | * |
| Right Hemisphere | 0.04388 | 0.834 | |
| Anterior Region | 0.51231 | 0.4741 | |
| Posterior Region | 9.6924 | 0.0018 | * |

Table 6.16: Kruskal-Wallis test of intensity of information flow with inflow direction between focal right group and control population.

The results obtained from the comparison between the focal right group and the control population displays a similar pattern to the results obtained from the focal left group. For the intensity of information flow with inflow direction, the inflow

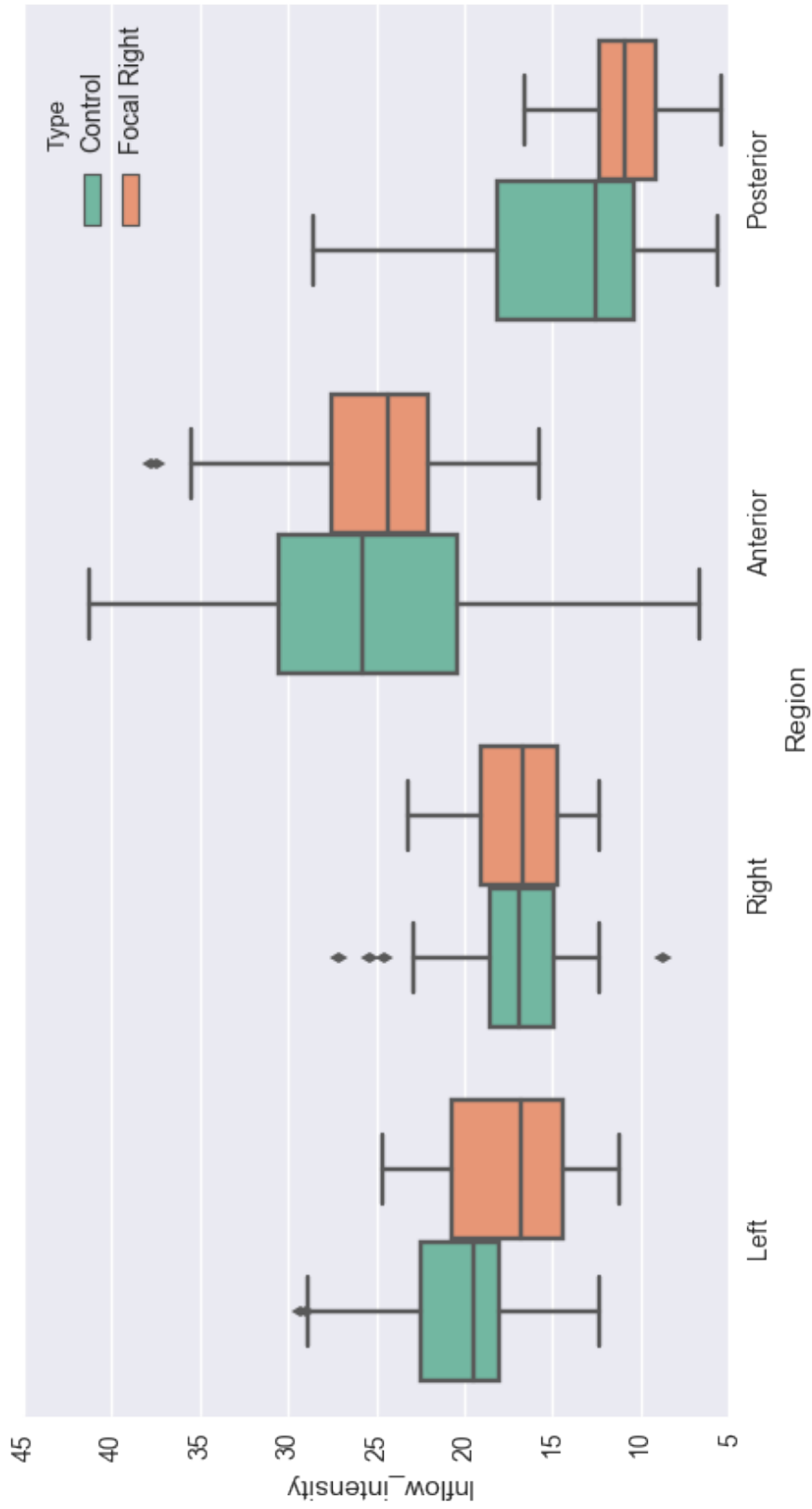


Figure 6.1.1: The medians and interquartile ranges of the intensity of information flow with inflow direction of the focal right group and control population with different regions.

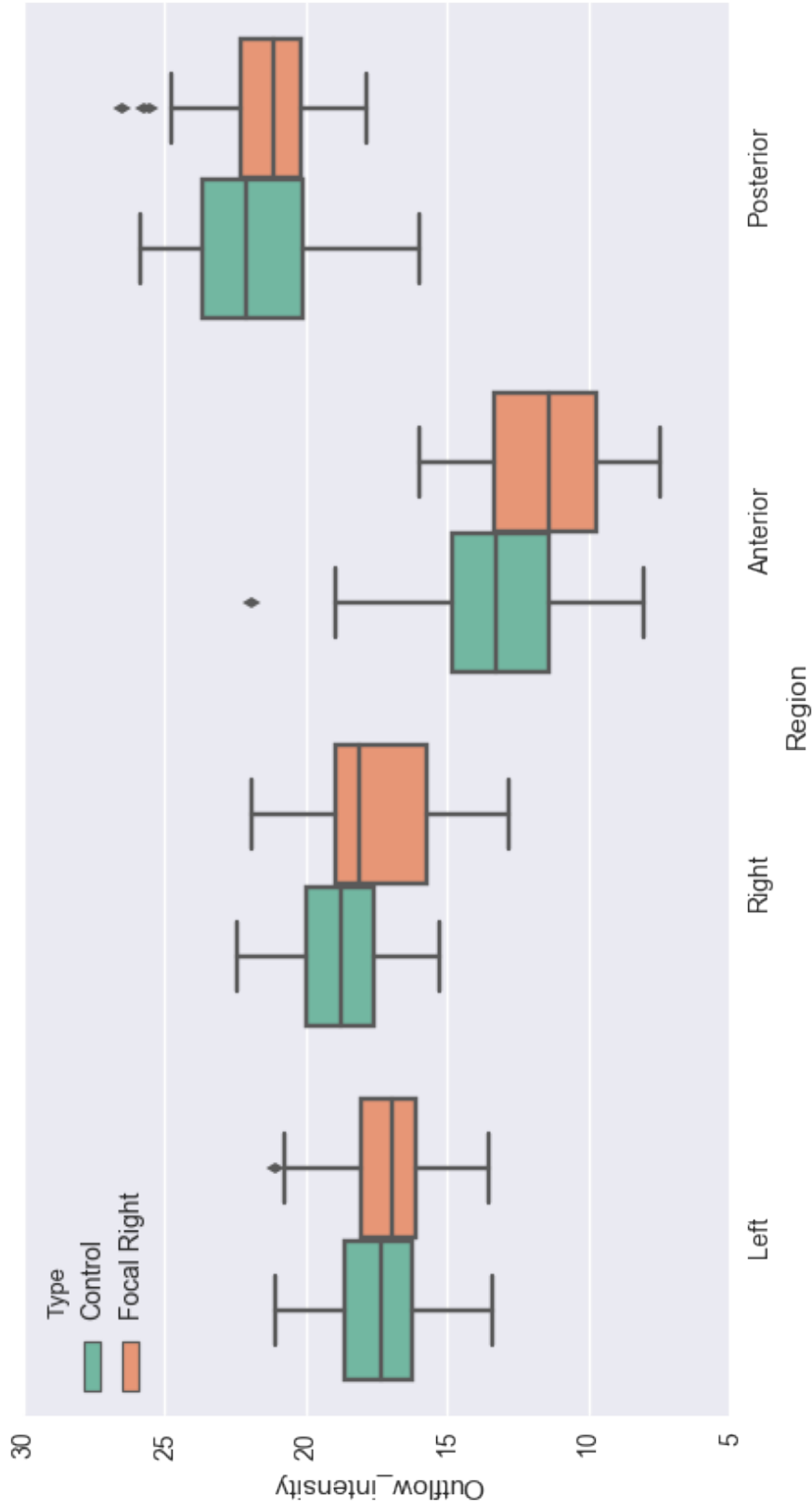


Figure 6.12: The medians and interquartile ranges of the intensity of information flow with outflow direction of the focal right group and control population with different regions.

| | Test-Statistics | p-value | Significance Level of 0.05 |
|------------------|-----------------|---------|----------------------------|
| Left Hemisphere | 1.667 | 0.1966 | |
| Right Hemisphere | 8.9611 | 0.002 | * |
| Anterior Region | 9.8537 | 0.0016 | * |
| Posterior Region | 2.2687 | 0.132 | |

Table 6.17: Kruskal-Wallis test of intensity of information flow with outflow direction between focal right group and control population.

values in the left hemisphere and the posterior region were significantly different at $p - value < 0.05$. For the outflow direction, both right hemisphere and anterior region showed lower outflow values compared to the control population.

6.8 Discussion

To explore the patterns of the cerebral information flow generated during the interictal phase, the intensity of information flow with inflow and outflow directions was extracted from 3-second segments of the EEG data. A total of 22 patients was included in this study, where the obtained EEG data was classified as control population, focal epilepsy, and generalized epilepsy group. Segments of the EEG data were randomly selected. From the epilepsy groups, only the segments extracted from within the interictal phases were included. The concept of partial directed coherence was used to extract meaningful connectivity patterns of each segment, and from them inflow and outflow intensity measures were calculated. From the results of the inflow intensity direction, the average values of inflow intensity across all groups delineated a similar trend, whereas the highest inflow intensity was generated from the anterior region and the lowest inflow intensity was found in the posterior region. Within the epilepsy group, focal and generalized epilepsy, the inflow patterns were observed to be similar in most of the regions indicating that epilepsy group exhibited the same behavior during the interictal phrases, which can be distinguished from the

control population. From the statistical analysis, the differences in inflow intensity found between control population and epilepsy groups were significant, while within the epilepsy groups, the differences were not. By comparing the obtained results between inflow and outflow intensity, we observed that the patterns extracted using inflow intensity provided more significant information. Post-hoc analysis indicated that we could distinguish between controls and epilepsy groups by using inflow intensity, but we were unable to classify these groups by using outflow intensity. In general, focal outflow is larger in the Left region (Focal vs. Control) and anterior regions. These results are in concordance with the epileptic foci locations since most of them are found to be situated to the left temporal and frontal regions. Also, inflow is lower in the left and anterior regions. This is an indication that the left and anterior regions discharged abruptly and the activation propagated from the areas near the epileptic source to other brain regions.

The concept of brain connectivity has been widely used to analyze the patterns generated in the cerebral cortex in multiple neurological diseases. Many studies attempted to investigate the alteration of neural synchrony between epileptic brains and healthy brains [66]. Studies of epilepsy using EEG, intracranial EEG, and MEG recordings revealed an increase of brain connectivity and significant differences in graph theory features [8, 30, 32]. However, conflicting results were reported when features such as raw brain connectivity values, clustering coefficient, average shortest path length were investigated. Some studies reported a decrease in clustering coefficient and average path length of the network [8, 67] where others discovered an increase in clustering coefficient and average path length in patients with focal epilepsy [30]. The contradiction found in these studies could reflect in differences in methodology and the types of disease itself [68]. In addition, these network features might not be sufficient to fully understand the underlying patterns between brain

connectivity and epilepsy. Thus, we propose an alternative approach to investigate the patterns by utilizing intensity of information flow concept. Similar approaches were performed in studies [36] and [50] by using cross-correlation analysis and nonlinear analysis, where cross cross-correlation is prone to error induced by volume conduction and the nonlinear analysis is very dependent on the parameters selection. Also, by utilizing functional connectivity only provide structural connectivity without providing direction of information flow. Using PDC to extract brain connectivity not only provides directional information, but also minimizes the effect of volume conduction on the results as well.

The present study has several limitations. First of all, the limitations presented in the analysis was the effect of the background activity of the selected segments, where preprocessing had to be done manually to minimize the effect of the artifacts. The segments with any artifacts or interictal discharges presented were excluded from the study. Thus, the amount of segments included in this study decreases dramatically. Secondly, the focal epilepsy group in this study is not representative for focal epilepsy in general, where we attempted to generalize the finding by grouping patients in a broader group. However, depending on the foci of epileptic seizures, the patterns of intensity of information flow might vary. This study compensates the following pitfall by including only interictal data without any interictal discharge presented [48]. For further improvement, an increase number of sample and patients in the group of focal epilepsy should be further classified into different group depending on the foci of epileptic seizures. Lastly, we used EEG recordings with 19 electrodes, which provides a low spatial resolution. Thus, the regions of interest are coarsely defined to compensate the low spatial resolution of the recording.

6.9 Conclusion

The extraction of the intensity of information flow of effective connectivity maps from neural activities by using PDC can generate important features that can be used to delineate between the control population and patients with both focal and generalized epilepsy. These features can help in characterizing the underlying patterns that define these two types of epilepsy and can provide the information flow between multivariate systems (which in this case uses 19 EEG electrodes but could be extended to other systems with additional electrodes). By taking advantage of directionality of brain connectivity and extracting the intensity of information flow, it is observed that specific patterns in different regions of interest between each data group can be revealed. This is rather important as researchers could then associate such patterns in context to the 3D source localization where seizures are thought to emanate from for the case of focal epilepsy. This can also serve to identify, on the basis of randomly selected EEG records, other types of neurological and neurodegenerative disorders such as Parkinson, depression, Alzheimers disease, and mental illness.

The obtained results showed that in the absence of ictal events, patterns between control population and patients with epilepsy groups (focal and generalized) exhibited distinct characteristics that were deemed statistically significant. These features of brain connectivity can also be used as key parameters for pattern classification and for enhanced diagnosis on the basis of EEG recordings alone.

CONCLUDING REMARKS AND FUTURE WORK

7.1 Concluding Remarks

This dissertation presented a novel approach for extracting and analyzing patterns of information flow using brain connectivity analysis and partial directed coherence (PDC) in epilepsy. The PDC concept was implemented to measure the effective connectivity or the strength of directional interactions between different cortex regions of patients with epilepsy. The results obtained from the connectivity extraction were quantified by utilizing different approaches, such as surrogate data analysis, intensity of information flow, and graph theory. EEG data of more than 25 patients with epilepsy considering both focal and generalized seizures were included in this unique study. The obtained results showed multiple distinct characteristics presented in different groups of epilepsy, which can be used as key parameters to improve the diagnosis and classification of the disease.

In terms of brain connectivity extraction, the method of PDC is considered as a powerful tool to extract patterns of neural activity. In comparison with conventional methods such as cross-correlation or coherence, PDC provides significantly more accurate and more revealing results. Both cross-correlation and coherence utilize a bivariate approach, which tend to overestimate the strength of the connectivity and are found to be prone to volume conduction problem. On the other hand, PDC utilizes a multivariate approach where the model takes the whole system in consideration producing more accurate and more reliable results. PDC also provides directional information, which leads to multiple approaches of connectivity quantification that reveals more precise neural patterns.

The first experiment, detailed in chapter 5, was performed by using the concept of PDC to analyze the characteristics of interictal epileptiform discharges data, which included the presence of interictal spike (IS), spike and slow wave complex (SSC), and repetitive spikes and slow wave complex (RSS). Adjacency matrices were constructed by applying surrogate data analysis to the extracted connectivity matrices obtained. These adjacency matrices of each IEDs group are found to contain distinct patterns, which were then classified by using the multilayer Perceptron neural network. The results obtained from the classification process are promising and provide high accuracy results. These extracted features can also help characterized the type of epilepsy (focal or generalized) and can provide the information flow between multivariate systems.

The Second experiment, detailed in chapter 6, proposed an approach to the investigation of intensity (or strength) of information flow. The inflow, which measures the significant activity flowing from other regions into a specific region, and outflow, which measures the significant activity emanating from one region and spreading into other regions, were calculated based on the PDC results and are quantified for all the defined regions of interest. Three groups including the control population, patients with focal epilepsy, and patients with generalized epilepsy were included in this experiment. By applying the concept of intensity of information flow to the extracted PDC values, the obtained patterns were used to delineate between the control population and patients with both focal and generalized epilepsy. The results are statistically significant and were validated by applying analysis of variance and multiple comparison tests. The results show that by using only interictal EEG data, patterns of neural activity between control population and patients with epilepsy groups (focal and generalized) exhibited distinct characteristics that were deemed statistically significant, which hence can be used in the classification algorithm.

7.2 Further Research

The interesting construct regarding the concept of brain connectivity relates to the versatility of the concept in extending its use to other neurological and neurodegenerative diseases. Applying changes to a small part of the process will have the potential to produce new results with different application domains. For instance, the selection of the data will change both the focus and interpretation of the analysis. For instance, by applying brain connectivity analysis to ictal periods or interictal periods will provide different features which can be applied in unique classification processes and in direct relation to the patient itself and in the context of the brain dysfunction under consideration. There are thus many key parts that can be explored further in this research.

This research only incorporates EEG data obtained from epileptic patients. To further explore the characteristics presented in epilepsy, combining MRI data with EEG data would provide more insights into the epileptogenic focus and would consolidate the high temporal resolution of EEG with the high spatial resolution of MRI. With these two data combined, the quality of the obtained results will most certainly improve. This method which reveals unique brain connectivity patterns as defined by their inflow and outflow dynamics could lead to new findings and to a better understanding of epilepsy.

We also see the potential of this method, given its generalized construct, that it could extend for the analysis of brain activity patterns in other brain disorders. However, for this EEG-based study, the limitations are seen to be tied to access to data, and where the lack of epileptic EEG data is seen to limit the analysis to a certain degree. To improve this aspect, creating an organized database of epileptic EEG data will bring statistical meaningfulness in analyzing the different types of epilepsy

and their different manifestations. Our research group is beginning to address the data access issue through our collaboration with Nicklaus Children's Hospital and Oregon Health and Science University with whom we just signed memorandum of agreement for consolidating data acquisition from these different institutions to include both EEG and MRI data.

Another aspect that can be further investigated is the incorporation of deep learning techniques such as basic convolution neural network (CNN) [61] or recurrent neural network (RNN) [45]. By combining these techniques into this research, the improvement of application such as epileptic focus localization or seizure prediction could be improved significantly.

BIBLIOGRAPHY

- [1] U. R. Acharya, S. V. Sree, S. Chattopadhyay, W. Yu, and P. C. A. Ang. Application of recurrence quantification analysis for the automated identification of epileptic eeg signals. *International journal of neural systems*, 21(03):199–211, 2011.
- [2] H. Adeli, Z. Zhou, and N. Dadmehr. Analysis of eeg records in an epileptic patient using wavelet transform. *Journal of neuroscience methods*, 123(1):69–87, 2003.
- [3] H. Akaike. A new look at the statistical model identification. *IEEE transactions on automatic control*, 19(6):716–723, 1974.
- [4] L. A. N. Amaral, A. Scala, M. Barthelemy, and H. E. Stanley. Classes of small-world networks. *Proceedings of the national academy of sciences*, 97(21):11149–11152, 2000.
- [5] F. A. Azevedo, L. R. Carvalho, L. T. Grinberg, J. M. Farfel, R. E. Ferretti, R. E. Leite, W. J. Filho, R. Lent, and S. Herculano-Houzel. Equal numbers of neuronal and nonneuronal cells make the human brain an isometrically scaled-up primate brain. *Journal of Comparative Neurology*, 513(5):532–541, 2009.
- [6] L. Baccala, K. Sameshima, G. Ballester, A. Do Valle, and C. Timo-Iaria. Studying the interaction between brain structures via directed coherence and granger causality. *Applied signal processing*, 5(1):40, 1998.
- [7] L. A. Baccalá and K. Sameshima. Partial directed coherence: a new concept in neural structure determination. *Biological cybernetics*, 84(6):463–474, 2001.
- [8] F. Bartolomei, I. Bosma, M. Klein, J. C. Baayen, J. C. Reijneveld, T. J. Postma, J. J. Heimans, B. W. van Dijk, J. C. de Munck, A. de Jongh, et al. Disturbed functional connectivity in brain tumour patients: evaluation by graph analysis of synchronization matrices. *Clinical neurophysiology*, 117(9):2039–2049, 2006.
- [9] K. J. Blinowska and J. Zygierevicz. *Practical Biomedical Signal Analysis Using MATLAB®*. CRC Press, 2011.
- [10] J. W. Britton, L. C. Frey, J. Hopp, P. Korb, M. Koubeissi, W. Lievens, E. Pestana-Knight, and E. L. St. *Electroencephalography (EEG): An introductory text and atlas of normal and abnormal findings in adults, children, and infants*. American Epilepsy Society, Chicago, 2016.

- [11] E. Bullmore and O. Sporns. Complex brain networks: graph theoretical analysis of structural and functional systems. *Nature Reviews Neuroscience*, 10(3):186, 2009.
- [12] S. P. Burns, S. Santaniello, R. B. Yaffe, C. C. Jouny, N. E. Crone, G. K. Bergey, W. S. Anderson, and S. V. Sarma. Network dynamics of the brain and influence of the epileptic seizure onset zone. *Proceedings of the National Academy of Sciences*, 111(49):E5321–E5330, 2014.
- [13] P. Caines and C. Chan. Feedback between stationary stochastic processes. *IEEE Transactions on Automatic Control*, 20(4):498–508, 1975.
- [14] R. Cajal. *Histology of the Nervous System of Man and Vertebrates (History of Neuroscience, No 6)(2 Volume Set)*. Oxford: Oxford University Press, 1995.
- [15] W. Conover and R. L. Iman. On multiple-comparisons procedures. *Los Alamos Sci. Lab. Tech. Rep. LA-7677-MS*, pages 1–14, 1979.
- [16] A. Delorme and S. Makeig. Eeglab: an open source toolbox for analysis of single-trial eeg dynamics including independent component analysis. *Journal of neuroscience methods*, 134(1):9–21, 2004.
- [17] S. Dodel, J. M. Herrmann, and T. Geisel. Functional connectivity by cross-correlation clustering. *Neurocomputing*, 44:1065–1070, 2002.
- [18] O. Faust, U. R. Acharya, H. Adeli, and A. Adeli. Wavelet-based eeg processing for computer-aided seizure detection and epilepsy diagnosis. *Seizure*, 26:56–64, 2015.
- [19] R. S. Fisher, C. Acevedo, A. Arzimanoglou, A. Bogacz, J. H. Cross, C. E. Elger, J. Engel Jr, L. Forsgren, J. A. French, M. Glynn, et al. Ilae official report: a practical clinical definition of epilepsy. *Epilepsia*, 55(4):475–482, 2014.
- [20] R. S. Fisher, W. V. E. Boas, W. Blume, C. Elger, P. Genton, P. Lee, and J. Engel Jr. Epileptic seizures and epilepsy: definitions proposed by the international league against epilepsy (ilae) and the international bureau for epilepsy (ibe). *Epilepsia*, 46(4):470–472, 2005.
- [21] C. for Disease Control, P. (CDC, et al. Epilepsy in adults and access to care—united states, 2010. *MMWR. Morbidity and mortality weekly report*, 61(45):909, 2012.

- [22] P. J. Franaszczuk, K. J. Blinowska, and M. Kowalczyk. The application of parametric multichannel spectral estimates in the study of electrical brain activity. *Biological cybernetics*, 51(4):239–247, 1985.
- [23] K. J. Friston. Functional and effective connectivity: a review. *Brain connectivity*, 1(1):13–36, 2011.
- [24] J. Geweke. Measurement of linear dependence and feedback between multiple time series. *Journal of the American statistical association*, 77(378):304–313, 1982.
- [25] C. W. Granger. Investigating causal relations by econometric models and cross-spectral methods. *Econometrica: Journal of the Econometric Society*, pages 424–438, 1969.
- [26] M. Guye, F. Bartolomei, and J.-P. Ranjeva. Imaging structural and functional connectivity: towards a unified definition of human brain organization? *Current opinion in neurology*, 21(4):393–403, 2008.
- [27] P. Hagmann, L. Cammoun, X. Gigandet, R. Meuli, C. J. Honey, V. J. Wedeen, and O. Sporns. Mapping the structural core of human cerebral cortex. *PLoS biology*, 6(7):e159, 2008.
- [28] Y. He and A. Evans. Graph theoretical modeling of brain connectivity. *Current opinion in neurology*, 23(4):341–350, 2010.
- [29] D. Hirtz, D. Thurman, K. Gwinn-Hardy, M. Mohamed, A. Chaudhuri, and R. Zalutsky. How common are the common neurologic disorders? *Neurology*, 68(5):326–337, 2007.
- [30] M.-T. Horstmann, S. Bialonski, N. Noennig, H. Mai, J. Prusseit, J. Wellmer, H. Hinrichs, and K. Lehnertz. State dependent properties of epileptic brain networks: Comparative graph-theoretical analyses of simultaneously recorded eeg and meg. *Clinical Neurophysiology*, 121(2):172–185, 2010.
- [31] M.-P. Hosseini, H. Soltanian-Zadeh, K. Elisevich, and D. Pompili. Cloud-based deep learning of big eeg data for epileptic seizure prediction. In *Signal and Information Processing (GlobalSIP), 2016 IEEE Global Conference on*, pages 1151–1155. IEEE, 2016.
- [32] D. Huang, A. Ren, J. Shang, Q. Lei, Y. Zhang, Z. Yin, J. Li, K. M. von Deneen, and L. Huang. Combining partial directed coherence and graph theory

- to analyse effective brain networks of different mental tasks. *Frontiers in human neuroscience*, 10:235, 2016.
- [33] IEEE. *Pediatric epilepsy: Clustering by functional connectivity using phase synchronization*, 2015.
- [34] IEEE. *Connectivity patterns of interictal epileptiform discharges using coherence analysis*, 2016.
- [35] P. Janwattanapong, M. Cabrerizo, C. Fang, H. Rajaei, A. Pinzon-Ardila, S. Gonzalez-Arias, and M. Adjouadi. Classification of interictal epileptiform discharges using partial directed coherence. In *2017 IEEE 17th International Conference on Bioinformatics and Bioengineering (BIBE)*, pages 473–478. IEEE, 2017.
- [36] P. Janwattanapong, M. Cabrerizo, H. Rajaei, A. Pinzon-Ardila, S. Gonzalez-Arias, and M. Adjouadi. Epileptogenic brain connectivity patterns using scalp eeg. In *Signal and Information Processing (GlobalSIP), 2016 IEEE Global Conference on*, pages 1161–1165. IEEE, 2016.
- [37] M. Kaminski and K. J. Blinowska. A new method of the description of the information flow in the brain structures. *Biological cybernetics*, 65(3):203–210, 1991.
- [38] K. Krakow, F. Woermann, M. Symms, P. Allen, L. Lemieux, G. Barker, J. Duncan, and D. Fish. Eeg-triggered functional mri of interictal epileptiform activity in patients with partial seizures. *Brain*, 122(9):1679–1688, 1999.
- [39] W. H. Kruskal and W. A. Wallis. Use of ranks in one-criterion variance analysis. *Journal of the American statistical Association*, 47(260):583–621, 1952.
- [40] D. Kugiumtzis. Surrogate data test on time series. In *Modelling and Forecasting Financial Data*, pages 267–282. Springer, 2002.
- [41] R. Kus, M. Kaminski, and K. J. Blinowska. Determination of eeg activity propagation: pair-wise versus multichannel estimate. *IEEE transactions on Biomedical Engineering*, 51(9):1501–1510, 2004.
- [42] R. Li, G.-J. Ji, Y. Yu, Y. Yu, M.-P. Ding, Y.-L. Tang, H. Chen, and W. Liao. Epileptic discharge related functional connectivity within and between networks

- in benign epilepsy with centrotemporal spikes. *International journal of neural systems*, 27(07):1750018, 2017.
- [43] M. Liu, H. Liu, C. Chen, and M. Najafian. Energy-based global ternary image for action recognition using sole depth sequences. In *2016 Fourth International Conference on 3D Vision (3DV)*, pages 47–55. IEEE, 2016.
- [44] S. L. Marple and S. L. Marple. *Digital spectral analysis: with applications*, volume 5. Prentice-Hall Englewood Cliffs, NJ, 1987.
- [45] P. Mirowski, D. Madhavan, Y. LeCun, and R. Kuzniecky. Classification of patterns of eeg synchronization for seizure prediction. *Clinical neurophysiology*, 120(11):1927–1940, 2009.
- [46] R. Nabiei, M. Najafian, M. Parekh, P. Jančovič, and M. Russell. Delay reduction in real-time recognition of human activity for stroke rehabilitation. In *Sensing, Processing and Learning for Intelligent Machines (SPLINE), 2016 First International Workshop on*, pages 1–5. IEEE, 2016.
- [47] P. L. Nunez, R. Srinivasan, et al. *Electric fields of the brain: the neurophysics of EEG*. Oxford University Press, USA, 2006.
- [48] S. Ponten, L. Douw, F. Bartolomei, J. Reijneveld, and C. Stam. Indications for network regularization during absence seizures: weighted and unweighted graph theoretical analyses. *Experimental neurology*, 217(1):197–204, 2009.
- [49] M. A. Quraan, C. McCormick, M. Cohn, T. A. Valiante, and M. P. McAndrews. Altered resting state brain dynamics in temporal lobe epilepsy can be observed in spectral power, functional connectivity and graph theory metrics. *PloS one*, 8(7):e68609, 2013.
- [50] H. Rajaei, M. Cabrerizo, P. Janwattanapong, A. Pinzon-Ardila, S. Gonzalez-Arias, and M. Adjouadi. Connectivity maps of different types of epileptogenic patterns. In *Engineering in Medicine and Biology Society (EMBC), 2016 IEEE 38th Annual International Conference of the*, pages 1018–1021. IEEE, 2016.
- [51] J. C. Robbie, A. R. Clarke, R. J. Barry, F. E. Dupuy, R. McCarthy, and M. Selikowitz. Coherence in children with ad/hd and excess alpha power in their eeg. *Clinical Neurophysiology*, 127(5):2161–2166, 2016.

- [52] Y. Saito, H. Harashima, N. Yamaguchi, and K. Fujisawa. Recent advances in eeg and emg data processing. *Chap. Tracking of information within multichannel EEG record-causal analysis in EEG*, pages 133–146, 1981.
- [53] J. W. Sander. The epidemiology of epilepsy revisited. *Current opinion in neurology*, 16(2):165–170, 2003.
- [54] Y. Schiller and Y. Najjar. Quantifying the response to antiepileptic drugs: effect of past treatment history. *Neurology*, 70(1):54–65, 2008.
- [55] M. M. Shafi, M. B. Westover, L. Oberman, S. S. Cash, and A. Pascual-Leone. Modulation of eeg functional connectivity networks in subjects undergoing repetitive transcranial magnetic stimulation. *Brain topography*, 27(1):172–191, 2014.
- [56] S. Smith. Eeg in the diagnosis, classification, and management of patients with epilepsy. *Journal of Neurology, Neurosurgery & Psychiatry*, 76(suppl 2):ii2–ii7, 2005.
- [57] O. Sporns, G. Tononi, and R. Kötter. The human connectome: a structural description of the human brain. *PLoS computational biology*, 1(4):e42, 2005.
- [58] C. J. Stam. Modern network science of neurological disorders. *Nature Reviews Neuroscience*, 15(10):683, 2014.
- [59] C. J. Stam, G. Nolte, and A. Daffertshofer. Phase lag index: assessment of functional connectivity from multi channel eeg and meg with diminished bias from common sources. *Human brain mapping*, 28(11):1178–1193, 2007.
- [60] H. Su, S. Tian, Y. Cai, Y. Sheng, C. Chen, and M. Najafian. Optimized extreme learning machine for urban land cover classification using hyperspectral imagery. *Frontiers of Earth Science*, 11(4):765–773, 2017.
- [61] Y. R. Tabar and U. Halici. A novel deep learning approach for classification of eeg motor imagery signals. *Journal of neural engineering*, 14(1):016003, 2016.
- [62] M. Takigawa, G. Wang, H. Kawasaki, and H. Fukuzako. Eeg analysis of epilepsy by directed coherence method a data processing approach. *International journal of psychophysiology*, 21(2-3):65–73, 1996.

- [63] J. X. Tao, A. Ray, S. Hawes-Ebersole, and J. S. Ebersole. Intracranial eeg substrates of scalp eeg interictal spikes. *Epilepsia*, 46(5):669–676, 2005.
- [64] J. Theiler, S. Eubank, A. Longtin, B. Galdrikian, and J. D. Farmer. Testing for nonlinearity in time series: the method of surrogate data. *Physica D: Nonlinear Phenomena*, 58(1-4):77–94, 1992.
- [65] G. Tononi and G. M. Edelman. Consciousness and complexity. *science*, 282(5395):1846–1851, 1998.
- [66] P. J. Uhlhaas and W. Singer. Neural synchrony in brain disorders: relevance for cognitive dysfunctions and pathophysiology. *Neuron*, 52(1):155–168, 2006.
- [67] E. van Dellen, L. Douw, A. Hillebrand, I. H. Ris-Hilgersom, M. M. Schoonheim, J. C. Baayen, P. C. D. W. Hamer, D. N. Velis, M. Klein, J. J. Heimans, et al. Meg network differences between low-and high-grade glioma related to epilepsy and cognition. *PloS one*, 7(11):e50122, 2012.
- [68] E. van Diessen, S. J. Diederens, K. P. Braun, F. E. Jansen, and C. J. Stam. Functional and structural brain networks in epilepsy: what have we learned? *Epilepsia*, 54(11):1855–1865, 2013.
- [69] E. Van Diessen, W. M. Otte, K. P. Braun, C. J. Stam, and F. E. Jansen. Improved diagnosis in children with partial epilepsy using a multivariable prediction model based on eeg network characteristics. *PloS one*, 8(4):e59764, 2013.
- [70] P. van Mierlo, M. Papadopoulou, E. Carrette, P. Boon, S. Vandenberghe, K. Vonck, and D. Marinazzo. Functional brain connectivity from eeg in epilepsy: Seizure prediction and epileptogenic focus localization. *Progress in neurobiology*, 121:19–35, 2014.
- [71] L. Wang, J. B. Arends, X. Long, Y. Wu, and P. J. Cluitmans. Seizure detection using dynamic warping for patients with intellectual disability. In *Engineering in Medicine and Biology Society (EMBC), 2016 IEEE 38th Annual International Conference of the*, pages 1010–1013. IEEE, 2016.
- [72] P. Welch. The use of fast fourier transform for the estimation of power spectra: a method based on time averaging over short, modified periodograms. *IEEE Transactions on audio and electroacoustics*, 15(2):70–73, 1967.

- [73] F. Wendling, P. Chauvel, A. Biraben, and F. Bartolomei. From intracerebral eeg signals to brain connectivity: identification of epileptogenic networks in partial epilepsy. *Frontiers in systems neuroscience*, 4:154, 2010.
- [74] C. Wilke, G. A. Worrell, and B. He. Analysis of epileptogenic network properties during ictal activity. In *Engineering in Medicine and Biology Society, 2009. EMBC 2009. Annual International Conference of the IEEE*, pages 2220–2223. IEEE, 2009.
- [75] R. W. Williams and K. Herrup. The control of neuron number. *Annual review of neuroscience*, 11(1):423–453, 1988.
- [76] S. Wostyn, W. Staljanssens, L. De Taeye, G. Strobbe, S. Gadeyne, D. Van Roost, R. Raedt, K. Vonck, and P. van Mierlo. Eeg derived brain activity reflects treatment response from vagus nerve stimulation in patients with epilepsy. *International journal of neural systems*, 27(04):1650048, 2017.

APPENDIX A

This appendix contains the list of source code. For the list of tables and figures, please refer to the beginning of the document.

LIST OF SOURCE CODE LISTING

| LISTING | PAGE |
|---|------|
| 4.1 Configuration of MVAR coefficients | 47 |
| 4.2 Generating MVAR data using the simulated coefficients | 48 |
| 4.3 Plotting MVAR data | 48 |
| 4.4 Calculating PDC values from the simulated signals | 49 |

APPENDIX B

This appendix provides a memorandum from the Office of Research Integrity, sent to the principal investigator, Dr. Malek Adjouadi. For more information, use the IRB protocol approval number (IRB-15-0247) or Topaz reference number (103743). This appendix includes the memorandum issued on August 1, 2016.

MEMORANDUM

To: Dr. Malek Adjouadi
CC: File
From: Maria Melendez-Vargas, MIBA, IRB Coordinator 
Date: September 6, 2016
Protocol Title: "EEG/MRI/fMRI/EKG Brain Research"

The Health Sciences Institutional Review Board of Florida International University has re-approved your study for the use of human subjects via the **Expedited Review** process. Your study was found to be in compliance with this institution's Federal Wide Assurance (00000060).

IRB Protocol Approval #: IRB-15-0247 **IRB Approval Date:** 09/01/16
TOPAZ Reference #: 103743 **IRB Expiration Date:** 07/06/17

As a requirement of IRB Approval you are required to:

- 1) Submit an IRB Amendment Form for all proposed additions or changes in the procedures involving human subjects. All additions and changes must be reviewed and approved by the IRB prior to implementation.
- 2) Promptly submit an IRB Event Report Form for every serious or unusual or unanticipated adverse event, problems with the rights or welfare of the human subjects, and/or deviations from the approved protocol.
- 3) Utilize copies of the date stamped consent document(s) for obtaining consent from subjects (unless waived by the IRB). Signed consent documents must be retained for at least three years after the completion of the study.
- 4) **Receive annual review and re-approval of your study prior to your IRB expiration date.** Submit the IRB Renewal Form at least 30 days in advance of the study's expiration date.
- 5) Submit an IRB Project Completion Report Form when the study is finished or discontinued.

Special Conditions: N/A.

For further information, you may visit the IRB website at <http://research.fiu.edu/irb>.

MMV/em

VITA
PANUWAT JANWATTANAPONG

2012 B.E., Mechatronics Engineering
Assumption University
Bangkok, Thailand

2016 M.S., Electrical and Computer Engineering
Florida International University
Miami, FL

2014 - 2018 Ph.D., Electrical and Computer Engineering
Florida International University
Miami, FL

PUBLICATIONS AND PRESENTATIONS

Fang,C., Janwattanapong, P., Martin,H., Cabrerizo, M., Barreto, A., Loewenstein, A., Duara,R., and Adjouadi, M. “Computerized Neuropsychological Assessment in Mild Cognitive Impairment Based on Natural Language Processing-oriented Feature Extraction”. In IEEE BIBM 2017, November 2017, USA

Fang, C., Janwattanapong, P., Li, C., and Adjouadi, M. (2017). “A global feature extraction model for the effective computer aided diagnosis of mild cognitive impairment using structural MRI images”. arXiv preprint arXiv:1712.00556.

Janwattanapong, P., Cabrerizo, M., Rajaei, H., Ardila, A., Arias, S., Barreto, A., Andrian, J. and Adjouadi, M. “Analysis of Connectivity patterns in epilepsy using the concept of effective information flow and partial directed coherence”, International Journal of Neural System (IJNS) 2018, (under review)

Janwattanapong, P., Cabrerizo, M., Fang, C., Rajaei, H., Ardila, A., Arias, S. and Adjouadi, M. Classification of Interictal Epileptiform Discharges using Partial Directed Coherence. In IEEE BioInformatics and BioEngineering Conference (BIBE) 2017, October 2017, USA

Janwattanapong, P., Cabrerizo, M., Rajaei, H., Ardila, A., Arias, S., Barreto, A., Andrian, J. and Adjouadi, M. “Connectivity Pattern of Interictal Epileptiform Discharges Using Coherence Analysis”. In Signal Processing in Medicine and Biology 2016, December 2016, USA

Janwattanapong, P., Cabrerizo, M., Rajaei, H., Ardila, A., Arias, S. and Adjouadi, M. “Epileptogenic brain connectivity patterns using scalp EEG”. In GlobalSIP 2016, December 2016, USA

Janwattanapong,P., Cabrerizo, M. “Autonomous Bicycle with Gyroscope Sensor” Chapter 25 appears in “Interaction Design for 3D User Interfaces: The World of Modern Input Devices for Research, Applications, and Game Development”, Francisco R. Ortega, Fatemeh Abyarjoo, Armando Barreto, Naphali Rische, Malek Adjouadi . CRC Press, December 2015.

Rajaei, Cabrerizo, M., Janwattanapong, P., H., Ardila, A., Arias, S., Barreto, A. and Adjouadi, M. “Connectivity Dynamics of Interictal Epileptiform Activity”. In IEEE BioInformatics and BioEngineering Conference (BIBE) 2017, October 2017, USA

Rajaei H., Cabrerizo M., Janwattanapong,P., Pinzon A., Gonzalez-Arias S., Barreto A., Andrian, J., Rische, N., and Adjouadi M., “Dynamics and Distant Effects of Temporal Epileptogenic Focus Using Functional Connectivity Maps”, IEEE transactions on Biomedical Engineering 2018, (under review)

Rajaei, H., Cabrerizo, M., Janwattanapong, P., Ardila, A., Arias, S. and Adjouadi, M., “Connectivity Maps of Different Types of Epileptogenic Patterns”. In EMBC 2016, August 2016, USA